AASHTO

Craig Thompson, *President*
Secretary, Wisconsin Department of Transportation
Jim Tymon, *Executive Director*

January 2024 ERRATA for *Mechanistic–Empirical Pavement Design Guide,* 3rd Edition (MEPDG-3)

January 2024

Dear Customer:

AASHTO has issued a third erratum, which includes technical revisions, for the *Mechanistic–Empirical Pavement Design Guide,* 3rd Edition (MEPDG-3).

In the event that you need to download this file again, it can be found on AASHTO's website at:

https://downloads.transportation.org/MEPDG-3-Errata.pdf

This erratum should be applied after the supplement.

The new changes in this erratum are detailed in the table under the "January 2024" heading. No special type style has been used in the text so that the content is easier to read; the "October 2023" changes were extensive. Pages with the new changes have a gray box in the page header reading as follows:

January 2024 Errata

The previous changes are detailed in the table under the "October 2023" and "August 2022" headings. These pages have a gray box in the page header reading that may read one of three ways:

October 2023 Errata	October 2023 Errata August 2022 Errata	August 2022 Errata

AASHTO staff sincerely apologizes for any inconvenience.

555 12th Street NW | Suite 1000 | Washington, DC 20004 | 202-624-5800 Phone | transportation.org

American Association of State Highway and Transportation Officials

This page intentionally left blank.

List of Errata for *AASHTO Mechanistic–Empirical Pavement Design Guide*, 3rd Edition (MEPDG-3)

Original Page	Section	Existing Text	Corrected Text
January 2024			
224	Table 13-3	In row 1, column 2 on this page, the first bullet should be part of the note.	Table reads as follows: *Note*: It is recommended to not use the surface-initiated crack prediction equation as a design criterion until the critical pavement response parameter and prediction methodology has been verified. Refer to Chapter 3. The cumulative damage and longitudinal cracking transfer function (Equations 5-5 and 5-8) should be used with caution when making design decisions (in terms of longitudinal cracking, or top-down cracking) regarding the adequacy of a trial design.
October 2023			
vi	Table P-1	In the Coefficient of Thermal Expansion (CTE) row, AASHTOWare columns, the coefficients both are shown as 5.2.	The coefficients both should be shown as 4.3.
viii		In the Calibration Coefficient in the Rigid Pavement Punchout Prediction Model rows, MEPDG version 1.1 column, the coefficients are shown as APO, αPO, and βPO.	The coefficients should be shown as A_{PO}, α_{PO}, and β_{PO}.
x	Table of Contents	Updated Chapter 5 page numbers to match corrected Chapter 5.	Section 5.3.4 is listed on page 55 and so on through 5.4.6, which is listed on page 84.2.
xiii–xiv	List of Figures	Updated Chapter 5 figure numbers and page numbers to match corrected Chapter 5.	Figures 5-4 through 5-22 object and page numbers are correct.
xvii	List of Tables	Added missing Table 5-7 listing and updated Chapter 5 table page numbers to match corrected Chapter 5.	Table 5-2 is listed on page 54 and so on through Table 5-7, which is listed on page 64.
3	Figure 1-1	Under Inputs for Design, the Traffic Analysis box is missing a vertical connector line.	Figure 1-1 is corrected as shown on the next page.

List of Errata for *AASHTO Mechanistic–Empirical Pavement Design Guide*, 3rd Edition (MEPDG-3)

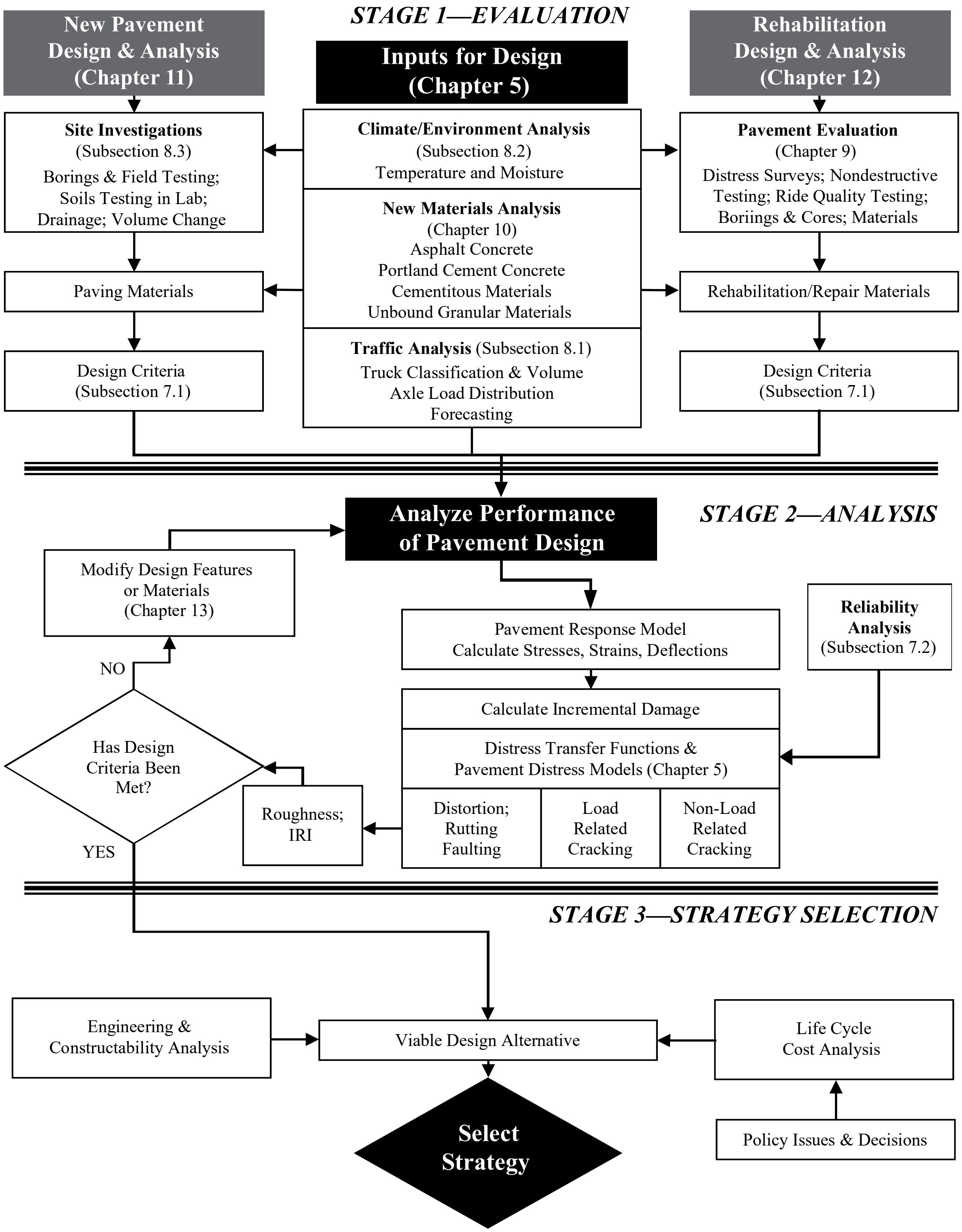

List of Errata for *AASHTO Mechanistic–Empirical Pavement Design Guide*, 3rd Edition (MEPDG-3)

<table>
<tr><th>Original Page</th><th>Section</th><th>Existing Text</th><th>Corrected Text</th></tr>
<tr><td colspan="4">October 2023</td></tr>
<tr><td>6</td><td>1.2</td><td>Step 3 following Figure 1-1 is missing a cautionary statement.</td><td>Step 3 has been revised to end with the following:

A caution to the designer—Some of the input parameters are interrelated; changing one parameter may affect the value of another input parameter. The designer should use caution in making changes in individual parameters.</td></tr>
<tr><td rowspan="3">41</td><td rowspan="3">Table 5-1</td><td>In the Truck Traffic row, most column 1 content should be in column 2 and most column 2 content should be in column 3.</td><td rowspan="3">Table 5-1 has been revised as shown on the next page.</td></tr>
<tr><td>In the All Materials row, most column 1 content should be in column 2 and most column 2 content should be in column 3.</td></tr>
<tr><td>In the All Materials row, “capacitydentifce” should be “capacity, surface”.</td></tr>
</table>

List of Errata for *AASHTO Mechanistic–Empirical Pavement Design Guide*, 3rd Edition (MEPDG-3)

Input Group		Input Parameter	Recalibration Input Level Used
Truck Traffic		Axle load distributions (single, tandem, tridem)	Level 1
		Truck volume distribution	Level 1
		Lane and directional truck distributions	Level 1
		Tire pressure	Level 3, default
		Axle configuration, tire spacing	Level 3, default
		Truck wander	Level 3, default
Climate		Temperature, wind speed, cloud cover, precipitation, relative humidity	Level 1 weather stations
Material Properties	Unbound Layers and Subgrade	Resilient modulus—all unbound layers	Level 1; backcalculation
		Classification and volumetric properties	Level 1
		Moisture-density relationships	Level 1
		Soil-water characteristic relationships	Level 3, defaults
		Saturated hydraulic conductivity	Level 3, defaults
	AC	AC dynamic modulus	Level 3, defaults
		AC creep compliance and indirect tensile strength	Levels 1, 2, and 3
		Volumetric properties	Level 1
		AC coefficient of thermal expansion	Level 3, default
	PCC	PCC elastic modulus	Level 1
		PCC flexural strength	Level 1
		PCC indirect tensile strength (CRCP only)	Level 2
		PCC coefficient of thermal expansion	Level 1
All Materials		Unit weight	Level 1
		Poisson’s ratio	Level 3, default
		Other thermal properties—conductivity, heat capacity, surface absorptivity	Level 3, defaults
Existing Pavement		Condition of existing layers	Levels 1 and 2

List of Errata for *AASHTO Mechanistic–Empirical Pavement Design Guide*, 3rd Edition (MEPDG-3)

Original Page	Section	Existing Text	Corrected Text
		October 2023	
45	Eq. 5-2d	Equation 5-2d wrongly includes "= 0.0075".	The correct equation is as follows: $C_o = Ln\left(\frac{a_1 M_r^{b_1}}{a_9 M_r^{b_9}}\right)$
46–54	5.3.3	The "Asphalt Concrete Layers" subsection has several errors and omissions, detailed below:	
		• The first paragraph under "Asphalt Concrete Layers" is incorrect.	The first paragraph has been revised as follows: Two types of load-related cracks are predicted by the MEPDG: alligator cracking and longitudinal cracking. The MEPDG assumes that alligator, or area cracks, initiate at the bottom of the AC layers and propagate to the surface with continued truck traffic, while longitudinal cracks are assumed to initiate at the surface. *For bottom-up or alligator cracking:* The allowable number of axle load applications needed for the incremental damage index approach to predict bottom-up cracks is shown in Equation 5-4a.
		• Equation 5-4a is incorrect.	The equation reads as follows: $N_{f-AC} = k_{f1}(C)(C_H)\beta_{f1}(\varepsilon_t)^{-k_{f2}\beta_{f2}}(E_{AC})^{-k_{f3}\beta_{f3}}$
		• Following Equation 5-4d, the notation for C_H is incorrect, including row 2 column 2 of the table.	The notation reads as follows: C_H = Thickness correction term … $1/(-0.046908H_{AC}^3 + 0.729644H_{AC}^2 - 0.635578H_{AC} - 1.555892)$
		• Equations 5-4e and 5-4f should not be included.	Equations 5-4e and Equation 5-4f have been deleted. The subheader between them has been moved.
		• In the paragraph before Equation 5-6a, "and length of longitudinal cracking" should not be included.	The first sentence of the paragraph reads as follows: The area of alligator cracking is calculated from the total damage over time (Equation 5-5) using different transfer functions.

List of Errata for *AASHTO Mechanistic–Empirical Pavement Design Guide*, 3rd Edition (MEPDG-3)

Original Page	Section	Existing Text	Corrected Text
October 2023			
46–54, cont'd.		• The content from just below Figure 5-3 to just before the subheader "CTB Layers" is incorrect.	The content from just below Figure 5-3 to just before the subheader "CTB Layers" has been replaced. The new content includes 12 equations, 3 figures, and 2 tables. Note: For easier legibility, content was not bolded.
54–84.4	5.3.3–5.4.6	Equation, figure, and table numbers and their references are incorrect to the end of Chapter 5.	Equation, figure, and table numbers and their references have been corrected to the end of Chapter 5.
57	5.3.4	Equations 5-12b, 5-12d, and 5-12f (now 5-14b, 5-14d, and 5-14f) are incorrect.	The equations read as follows: $S_e\ (Level\ 1; MAAT > 57°F) = 0.14(TC) + 343$ $S_e\ (Level\ 2; MAAT > 57°F) = 0.20(TC) + 343$ $S_e\ (Level\ 3; MAAT > 57°F) = 0.2386(TC) + 343$
63	Table 5-2	Table 5-2 (now Table 5-4) coefficients are incorrect.	Table 5-4 coefficients have been corrected as shown below in red.

Calibration Coefficients	Pavement Type				
	AC over AC	AC over Intact JPCP	AC over Intact CRCP or Fractured JPCP	Semi-Rigid	AC over Semi-Rigid
k_1	0.012	0.012	0.012	0.45	0.012
k_2	0.005	0.005	0.0002	0.05	0.005
k_3	1.00	1.00	0.1	1.0	1.0
C_1	3.22	3.22	3.22	0.1	3.22
C_2	25.7	25.7	25.7	0.9809	25.7
C_3	0.1	0.1	0.1	0.19	0.1
C_4	133.4	133.4	133.4	165.3	133.4
C_5	–72.4	–72.4	–72.4	–5.1048	–72.4

Original Page	Section	Existing Text	Corrected Text
October 2023			
67	5.4.1	The second variable in the where list for Equation 5-20a (now Equation 22a) is incorrect.	The variable reads as follows: $n_{i,j,k,\ \ldots}$

List of Errata for *AASHTO Mechanistic–Empirical Pavement Design Guide*, 3rd Edition (MEPDG-3)

Original Page	Section	Existing Text	Corrected Text
October 2023			
74	5.4.2	In the paragraph before Equations 5-28a and 5-28b (now 5-30a and 5-30b), the variable is incorrect.	The correct variable is Δs.
78	5.4.3	Equation 5-33 (now 5-35) is incorrect.	The equation reads as follows: $cw = Max\left[L\left(\varepsilon_{shr} + \alpha_{PCC}\Delta T_{\varsigma} - \frac{c_2 f_{\sigma long}}{E_{PCC}}\right)(C_c)1000\right]$
81	5.4.4	Equation 5-37 (now 5-39) is incorrect.	The equation reads as follows: $LCRK = \frac{1}{1 + C_4\left(DI_F\right)^{C_5}}$
84	5.4.5	Equation 5-41a (now 5-43a) is incorrect.	The equation reads as follows: $IRI = IRI_I + J1 * CRK + J2 * SPALL + J3 * TFAULT + J4 * SF$
146	Table 10-3	In rows 1 and 2, columns 1 and 2 of Table 10-3, "*EHMA*" and "*EAC*" are incorrect.	The table shows "E_{HMA}" and "E_{AC}".
148		In the embedded table in row 1 of Table 10-3, "µtypical" is incorrect.	The table shows "$\mu_{typical}$"
153	Table 10-5	In Row 1 column 2 of Table 10-5, "*Tz*" is incorrect.	The table shows "T_z".
155	Table 10-7	In Table 10-7, "*E* = 5700(*f′*c)0.5" is incorrect.	The table shows the following: $E = 5700(f'_c)^{0.5}$
157	Table 10-9	In row 1, column 2 of Table 10-9, paragraph breaks are missing between the options.	Table reads as follows: Two Options: Regression coefficients k_1, k_2, k_3 for the generalized constitutive model that defines resilient modulus as a function of stress state and regressed from laboratory resilient modulus tests. Determine the average design resilient modulus for the expected in-place stress state from laboratory resilient modulus tests.
183	12.2.4	In the second to last paragraph of the subsection, the table callout is incorrect.	The callout is as follows: (refer to Table 5-4 in Subsection 5.3.5).
186	12.2.8	In the first paragraph of the subsection, the table callouts are incorrect.	The callouts are as follows: The global calibration model coefficients are included in Tables 5-4 and 5-5.

List of Errata for *AASHTO Mechanistic–Empirical Pavement Design Guide*, 3rd Edition (MEPDG-3)

Original Page	Section	Existing Text	Corrected Text
		October 2023	
211	Table 12-13	In row 1, Faulting, column 2, a bullet point is missing.	The following appears as the fourth of five bullets: • **Decrease joint spacing.** This is applicable to JPCP overlays over existing flexible pavements and unbonded JPCP overlays. Shorter joint spacing generally results in smaller joint openings, making aggregate interlock more effective and increasing joint LTE.
235	Index	Page numbers; based on the original third edition.	Added the following at the top of the first index page: **Note:** Index page numbers are based on the original third edition; they have not been updated to reflect any supplement of errata repagination.
		August 2022	
67	5.4.2	Equation 5-23c is incorrect.	$FAULTMAX_i = FAULTMAX_{i-1} + C_7 \times \frac{\sum_{j=1}^{m} DE_j}{10^6} \times$ $\text{Log}(1 + C_5 \times 5.0^{EROD})^{C_6}$
74	5.4.3	Equation 5-30 is incorrect.	$PO = \frac{C_3}{1 + C_4 \left(DI_{PO}\right)^{C_5}}$
79	5.4.4	The equation and graph in Figure 5-19 are incorrect.	The equation and graph in Figure 5-19 have been revised to match Equation 5-37.
127	9.2.7	At the end of Table 9-8's caption, add "(21)" (citing reference 21 in Chapter 2).	**Table 9-8.** Models Relating Material Index and Strength Properties to M_r (21)
	Table 9-8	In the R-value row of Table 9-8, delete "(22)".	$M_r = 1155 + 555R$ M_r, psi
127	Table 9-8	In the AASHTO layer coefficient row of Table 9-8, change "3000" to "30,000" and delete "(22)".	$M_r = 30{,}000\left(\frac{a_i}{0.14}\right)$ M_r, psi
		In the PI and gradation row of Table 9-8, delete "(See Appendix CC)".	$CBR = \frac{75}{1 + 0.278\left(P_{200}PI\right)}$

<table>
<tr><th>Original Page</th><th>Section</th><th>Existing Text</th><th>Corrected Text</th></tr>
<tr><td colspan="4">August 2022</td></tr>
<tr><td>152</td><td>10.4</td><td>In Table 10-5, the coefficient of thermal expansion values and the default are incorrect.</td><td>
<table>
<tr><th>Aggregates Type</th><th>Coefficient of Thermal Expansion (10^{-6}/°F)</th></tr>
<tr><td>Andesite</td><td>4.3</td></tr>
<tr><td>Basalt</td><td>4.3</td></tr>
<tr><td>Diabase</td><td>4.6</td></tr>
<tr><td>Gabbro</td><td>4.4</td></tr>
<tr><td>Granite</td><td>4.7</td></tr>
<tr><td>Schist</td><td>4.4</td></tr>
<tr><td>Dolomite</td><td>5.0</td></tr>
<tr><td>Limestone</td><td>4.3</td></tr>
<tr><td>Quartzite</td><td>5.2</td></tr>
<tr><td>Sandstone</td><td>5.3</td></tr>
<tr><td>Expanded shale</td><td>4.5</td></tr>
</table>

Where coarse aggregate type is unknown, use MEPDG default value of $4.4*10^{-6}$/°F.</td></tr>
<tr><td>207</td><td>12.3.4</td><td>Performance Prediction Models
The globally calibrated performance models for new pavements apply to rehabilitation design, but with one exception—the JPCP CPR faulting prediction model has slightly different coefficients than the corresponding one for new or reconstructed JPCP.</td><td>Performance Prediction Models
The globally calibrated performance models for new pavements apply to rehabilitation design.</td></tr>
</table>

List of Errata for *AASHTO Mechanistic–Empirical Pavement Design Guide*, 3rd Edition (MEPDG-3)

Original Page	Section	Existing Text	Corrected Text
August 2022			
209	12.3.4	In the JPCP overlay over existing flexible pavement row of Table 12-12, the recommendations read as follows: Selection of design features for the JPCP overlay (including shoulder type and slab width) is similar to that outlined for new or reconstructed design in Chapter 10. Condition of existing flexible pavement is rated as Excellent, Good, Fair, Poor, or Very Poor, as defined in Table 12-10. These ratings will result in adjustments to the dynamic modulus, EHMA, of the existing AC layer that now becomes the base course. Full friction should be input over the full design life of the concrete overlay.	The corrected recommendations read as follows: Selection of design features for the JPCP overlay (including shoulder type and slab width) is similar to that outlined for new or reconstructed design in Chapter 10. Condition of existing flexible pavement is characterized using one of the three hierarchical input levels: • Level 1 rehabilitation calculates the existing damage based on the FWD back-calculated modulus. • Level 2 calculates the damage based on the existing fatigue cracking from a visual distress survey. • Level 3 calculates the damage based on a condition rating as Excellent, Good, Fair, Poor, or Very Poor, as defined in Table 12-10. For all rehabilitation levels, the dynamic modulus, E_{HMS}, is adjusted to reflect the magnitude of damage within the existing asphalt layers. The existing AC layer now becomes the base course in the analysis mod. Full friction should be input over the full design life of the concrete overlay.

Preface

This document or manual of practice describes a pavement design methodology that is based on engineering mechanics and has been validated with extensive road test performance data. This methodology is termed mechanistic-empirical (ME) pavement design, and it represents a major change from the pavement design methods in practice today.

Interested agencies have already begun implementation activities through staff training, collection of input data (materials library, traffic library, etc.), acquiring of test equipment, and preparation of field sections for local calibration. This manual, referred to as the Mechanistic-Empirical Pavement Design Guide (MEPDG), presents the information necessary for pavement design engineers to start using the ME-based design and analysis method. The software supporting this method is called Pavement ME Design® and is commercially available through AASHTOWare. The software is referred to in this document as PMED.

Multiple enhancements have been made to the AASHTOWare PMED based on completed research projects sponsored by the National Cooperative Highway Research Program (NCHRP) and the Federal Highway Administration (FHWA). In addition, revisions to the software were based on evaluations performed by State Highway Agencies and others in the Community of Practice. The third edition of the MEPDG Manual of Practice was prepared so the manual was consistent with the enhanced features and models included in the software through 2018.

The following table (Table P-1) summarizes the key differences noted between the format and calibration factors used in the MEPDG version 1.1 software, the AASHTOWare Pavement ME Design software version 2.3.1, and version 2.5.3 software.

Table P-1. Summary of Key Differences in Software Format and Calibration Factors

<table>
<tr><th colspan="2">Format, Transfer Functions, and Calibration Coefficients</th><th>MEPDG version 1.1</th><th>AASHTOWare Pavement ME Design version 2.3.1</th><th>AASHTOWare Pavement ME Design version 2.5.3</th></tr>
<tr><td colspan="2">Output Format</td><td>Excel-based</td><td>PDF- and Excel-based</td><td>PDF- and Excel-based</td></tr>
<tr><td colspan="2">Climatic Input Data and if Included in Output Summary</td><td>Data from Ground-Based Weather Stations; output summary not included</td><td>Data from NARR database for rigid and flexible pavements; output summary included</td><td>Data from NARR database for rigid pavements and MERRA2 database for flexible and semi-rigid pavements; output summary included</td></tr>
<tr><td colspan="2">Axle Configuration Data in Output Summary</td><td>Not included</td><td>Included</td><td>Included</td></tr>
<tr><td colspan="2">Special Axle Load Configuration</td><td>Included</td><td>Not included</td><td>Not included</td></tr>
<tr><td colspan="2">Reflection Cracking Transfer Function</td><td>Empirical regression equation included</td><td>ME-based fracture mechanics model included</td><td>ME-based fracture mechanics model included</td></tr>
<tr><td colspan="2">Coefficient of Thermal Expansion (CTE)</td><td>CTE for Basalt of 4.6</td><td>CTE for Basalt of 4.3</td><td>CTE for Basalt of 4.3</td></tr>
<tr><td colspan="2">PCC Zero Stress Temperature</td><td>PCC Zero Stress Temperature (60°–120°F)</td><td>PCC Set Temperature (70°–212°F)</td><td>PCC Set Temperature (70°–212°F)</td></tr>
<tr><td colspan="2">Heat Capacity of Asphalt Pavement</td><td>Default value of 0.23 BTU/lb-°F</td><td>Default value of 0.28 BTU/lb-°F</td><td>Default value of 0.28 BTU/lb-°F</td></tr>
<tr><td colspan="2">Thermal Conductivity of Asphalt Pavement</td><td>Default value of 0.67 BTU/(ft)(hr)(F)</td><td>Default value of 1.25 BTU/(ft)(hr)(F)</td><td>Default value of 1.25 BTU/(ft)(hr)(F)</td></tr>
<tr><td colspan="2">Surface Shortwave Absorptivity</td><td>Default value of 0.95</td><td>Default value of 0.85</td><td>Default value of 0.85</td></tr>
<tr><td rowspan="4">Global Model Coefficient for Unbound Materials and Soils in Flexible Pavement Subgrade Rutting Model</td><td>Aggregate Base</td><td rowspan="3">k_{s1} of 1.673</td><td rowspan="3">k_{s1} of 2.03</td><td>k_{s1} of 0.965</td></tr>
<tr><td>Coarse-Grained Soil</td><td>k_{s1} of 0.965</td></tr>
<tr><td>Sand Soil</td><td>k_{s1} of 0.635</td></tr>
<tr><td>Fine-Grained Soil</td><td>k_{s1} of 1.35</td><td>k_{s1} of 1.35</td><td>k_{s1} of 0.675</td></tr>
</table>

Continued on next page.

Table P-1. Summary of Key Differences in Software Format and Calibration Factors, *continued*

Format, Transfer Functions, and Calibration Coefficients		MEPDG version 1.1	AASHTOWare Pavement ME Design version 2.3.1	AASHTOWare Pavement ME Design version 2.5.3
Global Local Calibration or Field Adjustment Constant for Unbound Materials and Soils in Flexible Pavement Subgrade Rutting Model	Aggregate Base	1.0	1.0	1.0
	Coarse-Grained Soil			1.0
	Sand Soil			1.0
	Fine-Grained Soil			1.0
Global Laboratory-Derived Model Coefficients in the Fatigue Cracking Prediction Model in Flexible Pavement		k_{s1} of 0.007566	k_{s1} of 0.007566	k_{s1} of 3.75
		k_{s2} of -3.9492	k_{s2} of 3.9492	k_{s2} of 2.87
		k_{s3} of -1.281	k_{s3} of 1.281	k_{s3} of 1.46
Global Local Calibration or Field-Adjustment Constants for Fatigue Cracking Prediction Model in Flexible Pavement		β_1 of 1.0	β_1 of 1.0	AC thickness dependent; see Chapter 5
		β_2 of 1.0	β_2 of 1.0	β_2 of 1.38
		β_3 of 1.0	β_3 of 1.0	β_3 of 0.88
Global Bottom-Up Alligator Cracking Transfer Function Coefficients		C_1 of 1.0	C_1 of 1.0	1.31
		C_2 of 1.0	C_2 of 1.0	AC thickness dependent; see Chapter 5
Global Calibration or Field-Adjustment Coefficient in the Transverse Cracking Model for AC		k_t (Level 1) of 5.0	k_t (Level 1) of 1.5	k_s (Level 1) is Mean Annual Air Temperature (MAAT) dependent; see Chapter 5.
		k_t (Level 2) of 1.5	k_t (Level 2) of 0.5	k_s (Level 2) is MAAT dependent; see Chapter 5.
		k_t (Level 3) of 3.0	k_t (Level 3) of 1.5	k_s (Level 3) is MAAT dependent; see Chapter 5.
Global Laboratory Derived Model Coefficients in the Rut Depth Prediction Model		k_1 of -3.35412	k_1 of -3.35412	k_1 of -2.45
		k_{2r} of 0.4791	k_2 of 1.5606	k_2 of 3.01
		k_{3r} of 1.5606	k_3 of 0.4791	k_3 of 0.22

Continued on next page.

Table P-1. Summary of Key Differences in Software Format and Calibration Factors, *continued*

Format, Transfer Functions, and Calibration Coefficients	MEPDG version 1.1	AASHTOWare Pavement ME Design version 2.3.1	AASHTOWare Pavement ME Design version 2.5.3
Global Local Calibration or Field Adjustment Coefficients in the Rut Depth Prediction Model	β_1 of 1.0	β_1 of 1.0	β_1 of 0.40
	β_2 of 1.0	β_2 of 1.0	β_2 of 0.52
	β_3 of 1.0	β_3 of 1.0	β_3 of 1.36
Calibration Coefficients in the Rigid Pavement Cracking Prediction Model	C_4 of 1.0	C_4 of 0.52	C_4 of 0.52
	C_5 of -1.98	C_5 of -2.17	C_5 of -2.17
Calibration Coefficients in the Rigid Pavement Faulting Prediction Model	C_1 of 1.29	C_1 of 1.0184	C_1 of 0.595
	C_2 of 1.1	C_2 of 0.91656	C_2 of 1.636
	C_3 of 0.001725	C_3 of 0.0021848	C_3 of 0.00217
	C_4 of 0.0008	C_4 of 0.0008837	C_4 of 0.00444
	C_6 of 0.4	C_6 of 0.47	C_6 of 0.47
	C_7 of 1.2	C_7 of 1.83312	C_7 of 7.3
Calibration Coefficient in the Rigid Pavement Punchout Prediction Model	A_{PO} of 195.789	C_3 of 107.73	C_3 of 107.73
	α_{PO} of 19.8947	C_4 of 2.476	C_4 of 2.475
	β_{PO} of -0.526316	C_5 of -0.785	C_5 of -0.785
Calibration Coefficients in the Short JPCP Overlay Longitudinal Cracking Prediction Model	Excluded	C_4 of 0.4	C_4 of 0.4
		C_5 of -2.21	C_5 of -2.21

Table of Contents

Committee on Materials and Pavement Technical Subcommittee 5d on Pavement Design . . iii
Preface . . . v
List of Figures . . . xiii
List of Tables . . . xvii

1. Introduction . . . 1
1.1 Purpose of Manual . . . 1
1.2 Overview of the Design Procedure . . . 1

2. Referenced Documents and Standards . . . 11
2.1 Test Protocols and Standards . . . 11
2.1.1 Laboratory Materials Characterization . . . 11
2.1.2 In-Place Materials/Pavement Layer Characterization . . . 13
2.2 Material Specifications . . . 13
2.3 Recommended Practices and Terminology . . . 13
2.4 Referenced Documents . . . 14

3. Significance and Use of the MEPDG . . . 17
3.1 MEPDG Performance Indicators . . . 17
3.2 MEPDG General Design Approach . . . 18
3.3 New Flexible Pavement and AC Overlay Design Strategies Applicable to the MEPDG . . . 20
3.4 New Rigid Pavement, PCC Overlay, and Restoration of Rigid Pavement Design Strategies Applicable for Use with the MEPDG . . . 23
3.5 Design Features and Factors Not Included within the MEPDG Process . . . 27

4. Terminology and Definition of Terms . . . 31
4.1 General Terms . . . 31
4.2 Hierarchical Input Levels . . . 33
4.3 Truck Traffic Terms . . . 33
4.4 Smoothness . . . 34
4.5 Distresses or Performance Indicators Terms—AC-Surfaced Pavements . . . 35
4.6 Distress or Performance Indicators Terms—PCC-Surfaced Pavements . . . 36

5. Performance Indicator Prediction Methodologies . . . 39
5.1 Selecting the Input Levels . . . 39
5.2 Calibration Factors . . . 40
5.3 Distress Prediction Equations for Flexible Pavements and AC Overlays . . . 40
5.3.1 Overview of Computational Methodology for Predicting Distress . . . 40
5.3.2 Rut Depth . . . 43
5.3.3 Load-Related Cracking . . . 46

5.3.4 Non-Load Related Cracking—Transverse Cracking 55
5.3.5 Reflection Cracking in AC Overlays and AC Layers of Semi-Rigid Pavements . 59
5.3.6 Smoothness 65
5.4 Distress Prediction Equations for Rigid Pavements and PCC Overlays 67
5.4.1 Transverse Slab Cracking (Bottom-Up and Top-Down)—JPCP 67
5.4.2 Mean Transverse Joint Faulting—JPCP 70
5.4.3 CRCP Punchouts 77
5.4.4 Longitudinal Slab Cracking—SJPCP on Flexible Pavements 80
5.4.5 Smoothness—JPCP 84
5.4.6 Smoothness—CRCP 84.2

6. General Project Information 85
6.1 Design/Analysis Life 85
6.2 Construction and Traffic Opening Dates 85

7. Selecting Design Criteria and Reliability Level 87
7.1 Recommended Design-Performance Criteria 87
7.2 Reliability 88
7.3 Design Reliability Concept for Smoothness (IRI) 90

8. Determining Site Conditions and Factors 93
8.1 Truck Traffic 93
8.1.1 Roadway-Specific Inputs 95
8.1.2 Inputs Extracted from WIM Data 96
8.1.3 Truck Traffic Inputs Not Included in the WIM Data 101
8.2 Climate 102
8.3 Foundation and Subgrade Soils 103
8.3.1 Subsurface Investigations for Pavement Design 103
8.3.2 Laboratory and Field Tests of Soils for Pavement Design 105
8.4 Existing Pavements 105

9. Pavement Evaluation for Rehabilitation Design 109
9.1 Overall Condition Assessment and Problem Definition Categories 109
9.2 Data Collection to Define Condition Assessment 113
9.2.1 Initial Pavement Assessment 117
9.2.2 Prepare Field Evaluation Plan 118
9.2.3 Conduct Condition or Visual Survey 118
9.2.4 Ground Penetrating Radar Survey 122
9.2.5 Refine Field Testing Plan 122
9.2.6 Conduct Deflection Basin Tests 122
9.2.7 Destructive Sampling and Testing—Recover Cores and Boring for the Existing Pavement 124
9.2.8 Laboratory Tests for Materials Characterization of Existing Pavements 128

List of Figures

Figure 1-1. Conceptual Flow Chart of the Three-Stage Design/Analysis Process for AASHTOWare PMED 3

Figure 1-2. Typical Differences between Empirical Design Procedures and an Integrated ME Design System, in Terms of AC Mixture Characterization 4

Figure 1-3. Typical Differences between Empirical Design Procedures and an Integrated ME Design System, in Terms of PCC-Mixture Characterization. 5

Figure 1-4. Flow Chart of the Steps That Are More Policy Decision Related and Needed to Complete an Analysis of a Trial Design Strategy 7

Figure 1-5. Flow Chart of the Steps Needed to Complete an Analysis of a Trial Design Strategy. 8

Figure 3-1. New (Including Lane Reconstruction) Flexible Pavement Design Strategies That Can Be Simulated with the AASHTOWare PMED 21

Figure 3-2. AC Overlay Design Strategies of Flexible, Semi-Rigid, and Rigid Pavements That Can Be Simulated with the AASHTOWare PMED 21

Figure 3-3. New (Including Lane Reconstruction) Rigid Pavement Design Strategies That Can Be Simulated with the AASHTOWare PMED 25

Figure 3-4. PCC Overlay Design Strategies of Flexible, Semi-Rigid, and Rigid Pavements That Can Be Simulated with the AASHTOWare PMED 26

Figure 5-1. Graphical Illustration of the Five Temperature Quintiles Used in the MEPDG to Determine AC Mixture Properties for Load Related Distresses. 42

Figure 5-2. Comparison of Measured and Predicted Total Rutting Resulting from Global Calibration Process 46

Figure 5-3. Comparison of Cumulative Fatigue Damage and Alligator Cracking Resulting from Global Calibration Process. 49

Figure 5-4. Mechanisms of Thermally Induced Reflective Cracks of Asphalt Overlays 50

Figure 5-5a. Measured versus Predicted Number of Days to Crack Initiation 53

Figure 5.5b. Measured versus Predicted Area of Top-Down Cracking. 53

Figure 5-6. Comparison of Measured and Predicted Transverse Cracking Resulting from Global Calibration Process 58

Figure 5-7. Response Mechanisms Used in Reflection Cracking Prediction Methodology 59

Figure 5-8. Mechanisms of Thermally Induced Reflective Cracks of AC Overlays 60

Figure 5-9. Mechanisms of Traffic Induced Reflective Cracks of AC Overlays 60

Figure 5-10. Comparison of Measured and Predicted IRI Values Resulting from Global Calibration Process of Flexible Pavements and AC Overlays of Flexible Pavements 66

Figure 5-11. Comparison of Measured and Predicted IRI Values Resulting from Global Calibration Process of AC Overlays of PCC Pavements and Semi-Rigid Pavements 66

Figure 5-12. Comparison of Measured and Predicted Percentage JPCP Slabs Cracked Resulting from Global Calibration Process 69

Figure 5-13. Comparison of Measured and Predicted Transverse Cracking of Unbounded JPCP Overlays Resulting from Global Calibration Process 69

Figure 5-14. Comparison of Measured and Predicted Transverse Cracking for Restored JPCP Resulting from Global Calibration Process 70

Figure 5-15. Comparison of Measured and Predicted Transverse Joint Faulting for New JPCP Resulting from Global Calibration Process 76

Figure 5-16. Comparison of Measured and Predicted Transverse Joint Faulting for Unbound JPCP Overlays Resulting from Global Calibration Process 76

Figure 5-17. Comparison of Measured and Predicted Transverse Joint Faulting for Restored (Diamond Grinding) JPCP Resulting from Global Calibration Process 77

Figure 5-18. IComparison of Measured and Predicted Punchouts for New CRCP Resulting from Global Calibration Process 80

Figure 5-19. Illustration of Proper Location of Longitudinal Joints to Avoid Overlap with Truck Wheel Paths (to Avoid Corner Cracking) and the Resulting Critical Bending Stresses at Bottom of Slab That Are Considered to Limit Longitudinal Fatigue Cracking 81

Figure 5-20. Measured Longitudinal Fatigue Cracking (LCRK) versus PCC Fatigue Damage (DIF) at Bottom of PCC Slab 83

Figure 5-21. Comparison of Measured and Predicted Percentage SJPCP Overlay Slabs Longitudinally Cracked Resulting from Global Calibration Process 83

Figure 5-22. Comparison of Measured and Predicted IRI Values for New JPCP Resulting from Global Calibration Process 84.2

Figure 7-1. Design Reliability Concept for Smoothness (IRI) 89

Figure 8-1. Comparison of the Five NALS Defaults for Vehicle Class 9 Tandem Axles—Entire Range of Axle Loads 98

Figure 8-2. Comparison of the Five NALS Defaults for Vehicle Class 9 Tandem Axles—Axle Loads between 32,000–50,000 lb 98

Figure 9-1. Steps and Activities for Assessing Condition of Existing Pavements for Rehabilitation Design (Refer to Table 9-2) 114

List of Tables

Table P-1. Summary of Key Differences in Software Format and Calibration Factors vi
Table 5-1. Typical Input Levels Used in the Global Calibration of the AASHTOWare PMED Models and Transfer Functions 41
Table 5-2. Calibration Parameters α_1 and α_2: Global Coefficients 54
Table 5-3. Calibration Parameters for Crack Initiation Time, t_0: Global Coefficients 54
Table 5-4. Global Calibration Coefficients for the Reflection Cracking Transfer Functions for Transverse Cracks 63
Table 5-5. Global Calibration Coefficients for the Reflection Cracking Transfer Functions for Fatigue Cracks 64
Table 5-6. Standard Deviation Equations for the Transverse Cracks 64
Table 5-7. Standard Deviation Equations for the Fatigue Cracks 64
Table 5-8. Assumed Effective Base LTE for Different Base Types 73
Table 7-1. Design Criteria or Threshold Values Recommended for Use in Judging the Acceptability of a Trial Design 88
Table 7-2. Suggested Minimum Levels of Reliability for Different Functional Classifications of the Roadway. 91
Table 8-1. Minimum Sample Size (Number of Days per Year) to Estimate the Normalized Axle Load Distribution—WIM Data.. 94
Table 8-2. Minimum Sample Size (Number of Days per Season) to Estimate the Normalized Truck Traffic Distribution—Automated Vehicle Classifier (AVC) Data 94
Table 8-3. Normalized Axle Load Distribution Included with the AASHTOWare PMED Software 97
Table 8-4. TTC Group Description and Corresponding Truck Class Distribution Default Values Included in the AASHTOWare PMED Software 100
Table 8-5. Definitions and Descriptions for the TTC Groups 101
Table 8-6. Summary of Soil Characteristics as a Pavement Material 106
Table 9-1. Checklist of Factors for Overall Pavement Condition Assessment and Problem Definition. 111
Table 9-2. Hierarchical Input Levels for a Pavement Evaluation Program to Determine Inputs for Existing Pavement Layers for Rehabilitation Design. 115
Table 9-3. Field Data Collection and Evaluation Plan 119

Table 9-4. Guidelines for Obtaining Non-Materials Input Data for Pavement Rehabilitation 120
Table 9-5. Use of Deflection Basin Test Results for Selecting Rehabilitation Strategies and in Estimating Inputs for Rehabilitation Design 123
Table 9-6. Summary of Destructive Tests, Procedures, and Inputs for the MEPDG 125
Table 9-7. Models/Relationships Used for Determining Level 2 E or M_r 126
Table 9-8. Models Relating Material Index and Strength Properties to M_r 127
Table 9-9. Distress Types and Severity Levels Recommended for Assessing Rigid Pavement Structural Adequacy 131
Table 9-10. Distress Types and Levels Recommended for Assessing Current Flexible Pavement Structural Adequacy 132
Table 9-11. LTE Values for Rehabilitation Design 136
Table 9-12. LTE Default Values for Input Level 3 Tied to Crack Severity Level 136
Table 10-1. Major Material Types for the MEPDG 140
Table 10-2. Asphalt Materials and the Test Protocols for Measuring the Material Property Inputs for New and Existing AC Layers, Input Level 1 141
Table 10-3. Recommended Input Parameters and Values; Limited or No Testing Capabilities for AC (Input Levels 2 and/or 3) 146
Table 10-4. PCC Material Input Level 1 Parameters and Test Protocols for New and Existing PCC 150
Table 10-5. Recommended Input Parameters and Values; Limited or No Test Capabilities for PCC Materials (Input Levels 2 or 3) 151
Table 10-6. Chemically Stabilized Materials Input Level 1 Requirements and Test Protocols for New and Existing Chemically Stabilized Materials 154
Table 10-7. Recommended Input Levels 2 and 3 Parameters and Values for Chemically Stabilized Material Properties 155
Table 10-8. C-Values to Convert the Calculated Layer Modulus Values to an Equivalent Resilient Modulus Measured in the Laboratory 156
Table 10-9. Unbound Aggregate Base, Subbase, Embankment, and Subgrade Soil Input Level 1 Material Requirements and Test Protocols for New and Existing Materials 157
Table 10-10. Recommended Levels 2 and 3 Input Parameters and Values for Unbound Aggregate Base, Subbase, Embankment, and Subgrade Soil Material Properties . . . 158
Table 11-1. General IRI Recommendations 167
Table 11-2. Friction Coefficient Values for CRCP Design 172
Table 12-1. Definitions of Surface Condition for Input Level 3 Pavement Condition Ratings and Suggested Rehabilitation Options 180

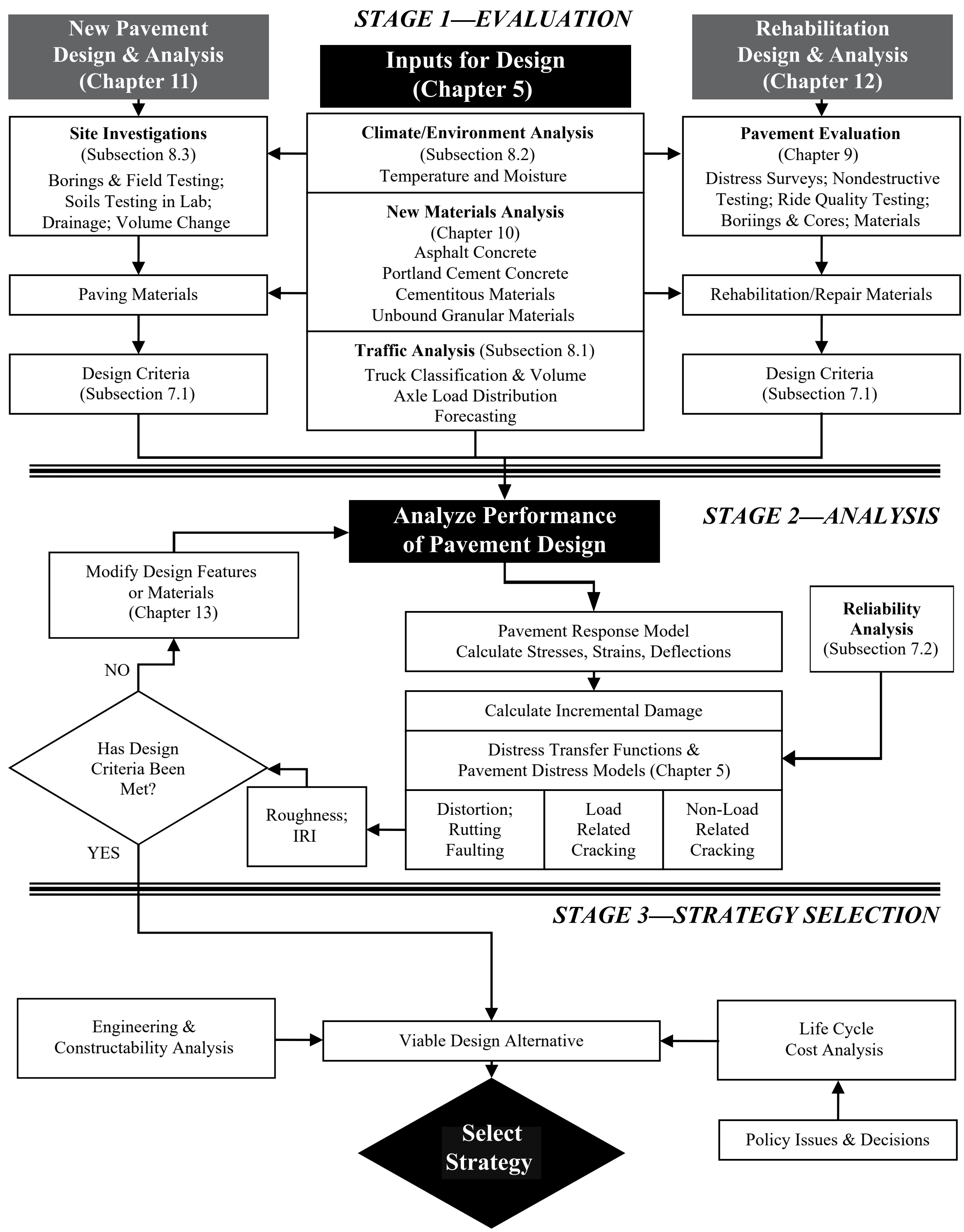

Figure 1-1. Conceptual Flow Chart of the Three-Stage Design/Analysis Process for AASHTOWare PMED

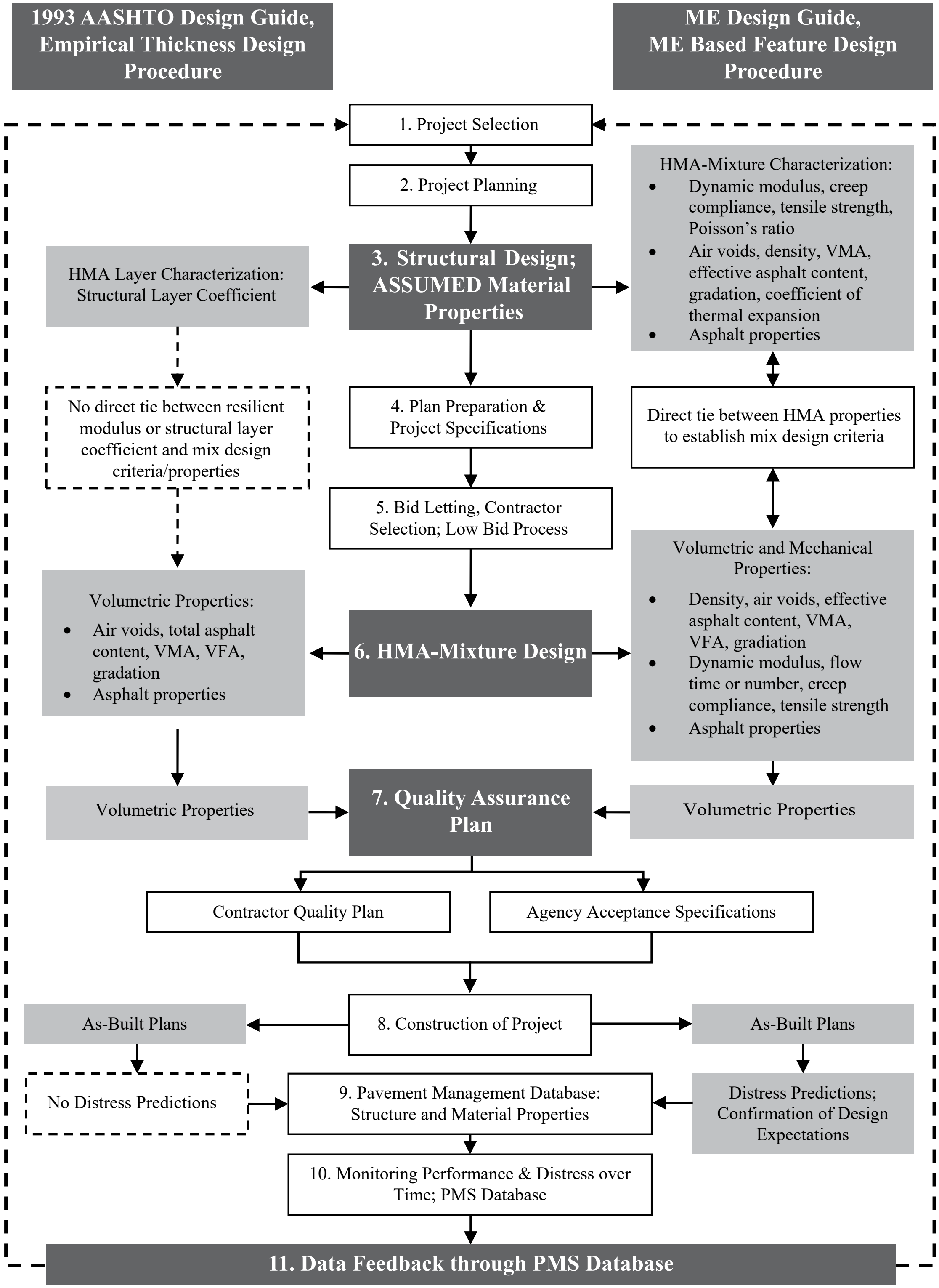

Figure 1-2. Typical Differences between Empirical Design Procedures and an Integrated ME Design System, in Terms of AC Mixture Characterization

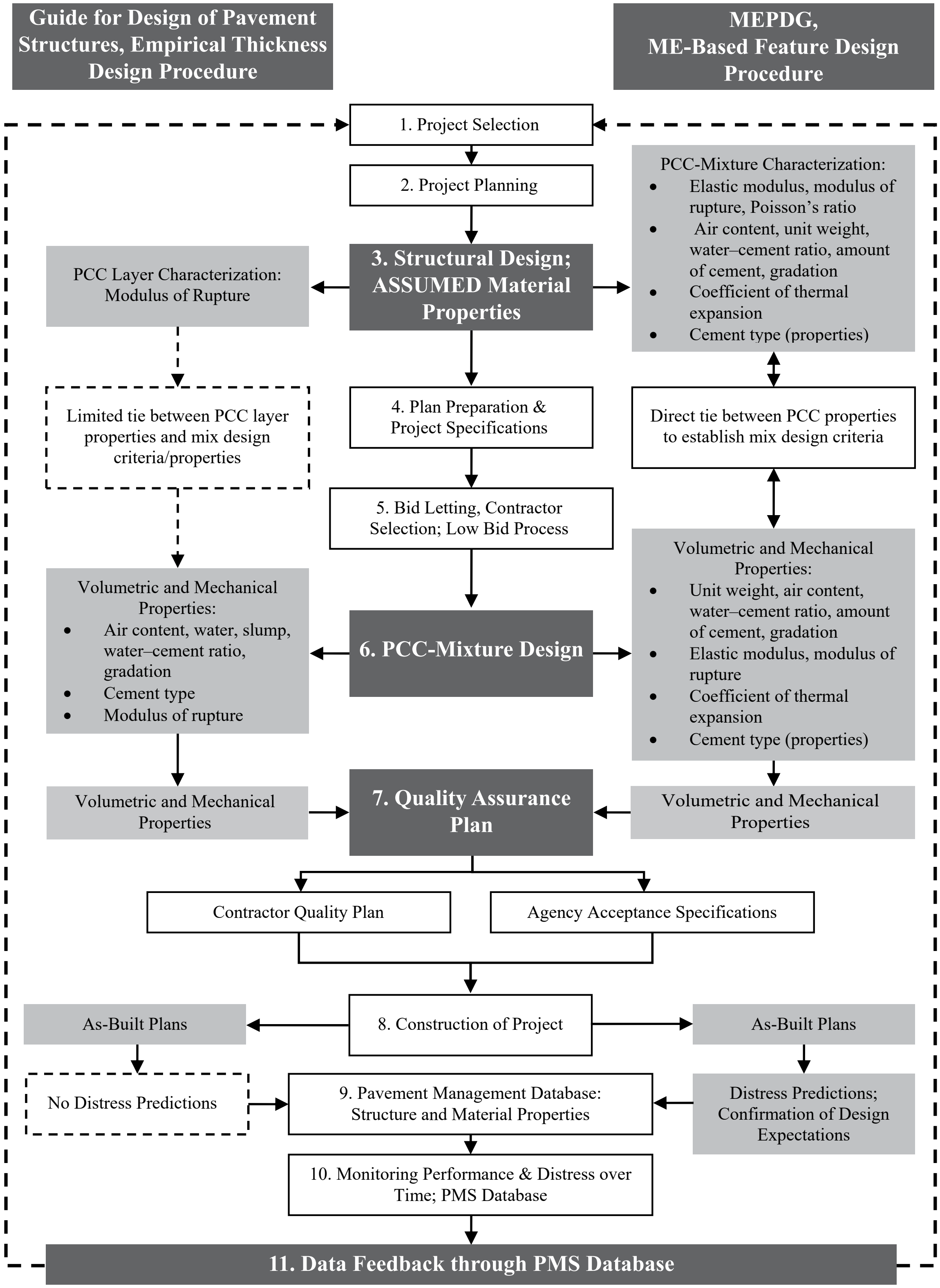

Figure 1-3. Typical Differences between Empirical Design Procedures and an Integrated ME Design System, in Terms of PCC-Mixture Characterization

The ME approach makes it possible to optimize the design and to fully verify that specific distress types will be limited to values less than the failure criteria within the design life of the pavement structure. The basic steps included in the MEPDG are listed below and presented as flow charts in Figures 1-4 and 1-5. The steps shown in Figures 1-4 and 1-5 are referenced to the appropriate sections within this manual of practice.

1. **Select a trial design strategy.** The pavement designer may use an agency-specific procedure to determine the trial design cross section.
2. **Select the appropriate performance indicator criteria (threshold value) and design reliability level for the project.** Design or performance indicator criteria include magnitudes of key pavement distresses and smoothness that may trigger major rehabilitation or reconstruction. These criteria could be a part of an agency's policies for deciding when to rehabilitate or reconstruct. AASHTOWare PMED allows the user to select the performance indicator criteria to be considered. The user can uncheck the box next to the criteria that do not need to be considered. (See Chapter 4.1 for definitions.)
3. **Obtain all inputs for the pavement trial design under consideration.** This step may be a time-consuming effort, but it is what separates the MEPDG from other design procedures. The MEPDG allows the designer to determine inputs using a hierarchical structure in which the effort to quantify a given input is selected based on the importance of the project, importance of the input, and available resources. The required inputs to run the software are obtained using one of three levels of effort that need not be consistent for all of the inputs for a given design. This permits the user to use the "best available" data for all inputs. The hierarchical input levels are defined in Chapters 4 and 5, and are grouped under six broad topics: (1) general project information, (2) design criteria, (3) traffic, (4) climate, (5) structure layering, and (6) material properties (including the design features). *A caution to the designer—Some of the input parameters are interrelated; changing one parameter may affect the value of another input parameter. The designer should use caution in making changes in individual parameters.*
4. **Run AASHTOWare PMED and examine the inputs and outputs for engineering reasonableness.** The software calculates changes in layer properties, damage, key distresses, and the International Roughness Index (IRI) over the design life. The substeps for step 4 include:
   a. Examine the input summary to verify the inputs are correct. This step should be completed after each run, until the designer becomes more familiar with the program and its inputs.
   b. Examine the outputs that comprise the intermediate process—specific parameters (such as climate values), monthly load transfer efficiency (LTE) values for rigid pavement analysis, monthly layer modulus values for flexible and rigid pavement analysis to determine their reasonableness, and calculated performance indicators (pavement distresses and IRI). This step may be completed after each run or

until the designer becomes more familiar with the program. Review of important intermediate processes and steps is presented in Chapter 13.

c. Assess whether the trial design has met each of the performance indicator criteria at the design reliability level chosen for the project. As noted above, IRI is an output parameter predicted over time and a measure of surface smoothness. IRI is calculated from other distress predictions (refer to Figure 1-1), site factors, and initial IRI.
d. If any of the criteria are not met, determine how this deficiency can be remedied by altering the materials used, the layering of materials, layer thickness, or other design features.

5. **Revise the trial design, as needed.** If the trial design has input errors, material output anomalies, or has exceeded the failure criteria at the given level of reliability, revise the inputs/trial design and rerun the program. An automated process to iterate to an optimized thickness is done by AASHTOWare PMED to produce a feasible design.

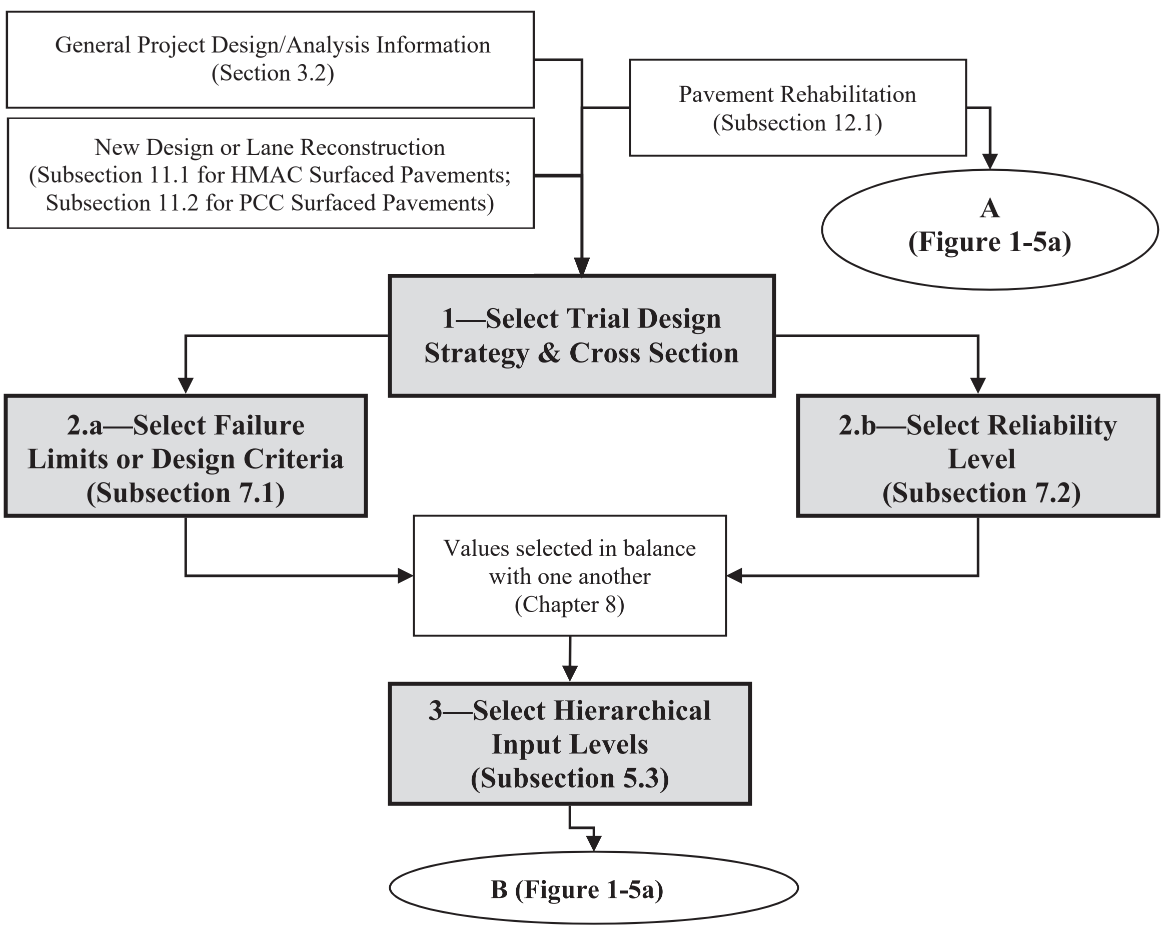

Figure 1-4. Flow Chart of the Steps That Are More Policy Decision Related and Needed to Complete an Analysis of a Trial Design Strategy

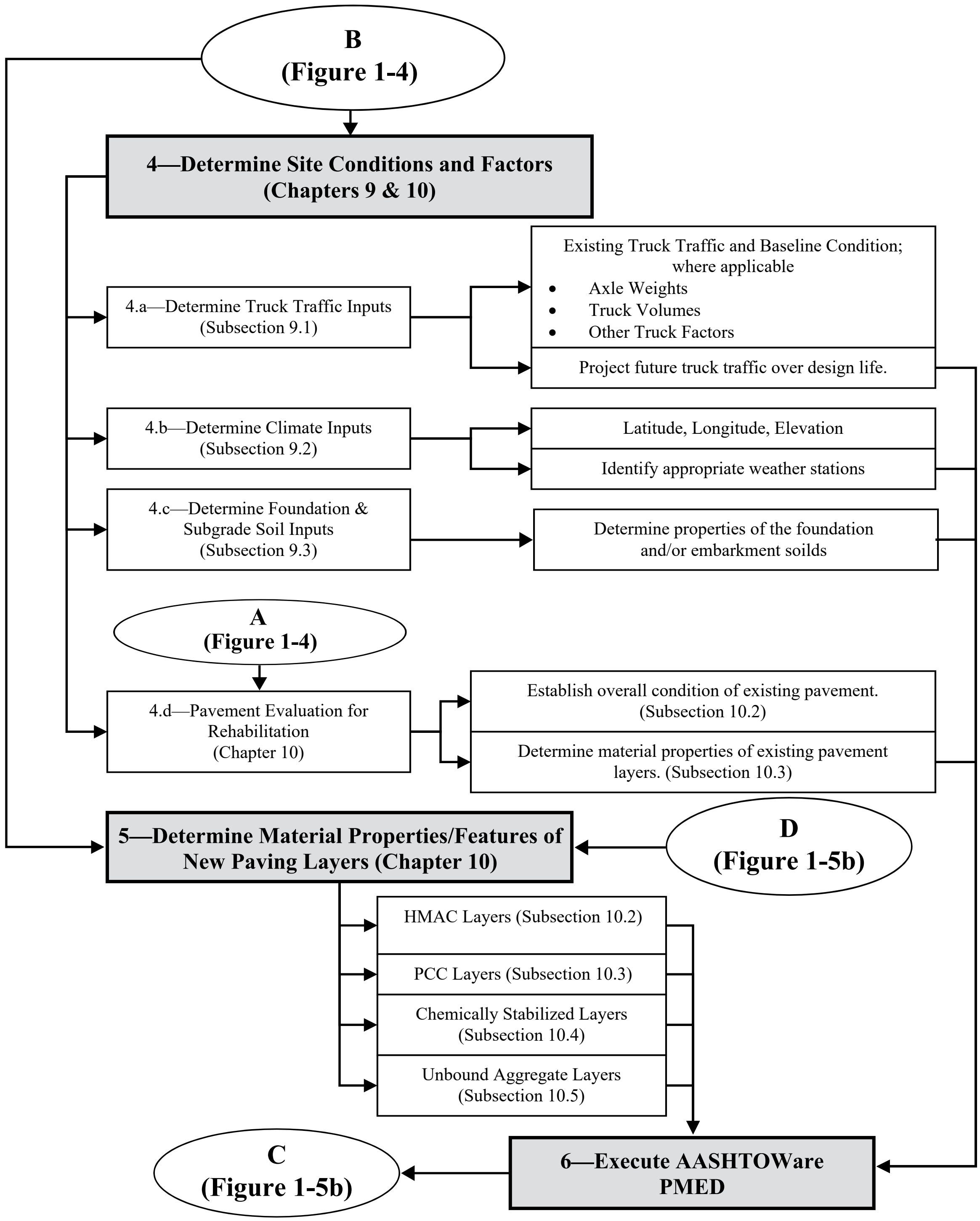

Figure 1-5a. Flow Chart of the Steps Needed to Complete an Analysis of a Trial Design Strategy

Table 5-1. Typical Input Levels Used in the Global Calibration of the AASHTOWare PMED Models and Transfer Functions

Input Group		Input Parameter	Recalibration Input Level Used
Truck Traffic		Axle load distributions (single, tandem, tridem)	Level 1
		Truck volume distribution	Level 1
		Lane and directional truck distributions	Level 1
		Tire pressure	Level 3, default
		Axle configuration, tire spacing	Level 3, default
		Truck wander	Level 3, default
Climate		Temperature, wind speed, cloud cover, precipitation, relative humidity	Level 1 weather stations
Material Properties	Unbound Layers and Subgrade	Resilient modulus—all unbound layers	Level 1; backcalculation
		Classification and volumetric properties	Level 1
		Moisture-density relationships	Level 1
		Soil-water characteristic relationships	Level 3, defaults
		Saturated hydraulic conductivity	Level 3, defaults
	AC	AC dynamic modulus	Level 3, defaults
		AC creep compliance and indirect tensile strength	Levels 1, 2, and 3
		Volumetric properties	Level 1
		AC coefficient of thermal expansion	Level 3, default
	PCC	PCC elastic modulus	Level 1
		PCC flexural strength	Level 1
		PCC indirect tensile strength (CRCP only)	Level 2
		PCC coefficient of thermal expansion	Level 1
All Materials		Unit weight	Level 1
		Poisson's ratio	Level 3, default
		Other thermal properties—conductivity, heat capacity, surface absorptivity	Level 3, defaults
Existing Pavement		Condition of existing layers	Levels 1 and 2

makes extensive use of the EICM for adjusting the pavement layer modulus values with temperature and moisture. The EICM calculates the temperature and moisture conditions throughout the pavement structure on an hourly basis (*16*).

The frequency distribution of AC temperatures using the EICM is assumed to be normally distributed. The temperatures in each AC sublayer are combined into five quintiles. Each quintile represents 20 percent of the frequency distribution for each month of the analysis period for the load related distresses (see Figure 5-1). This is accomplished by computing pavement temperatures corresponding to accumulated frequencies of 10, 30, 50, 70 and 90 percent within a given month. The average temperature within each quintile of a sublayer for each month is used to determine the dynamic modulus of that sublayer. The truck traffic is assumed to be equal within each of the five temperature quintiles. Thus, the flexible pavement procedure does not tie the hourly truck volumes directly to the hourly temperatures.

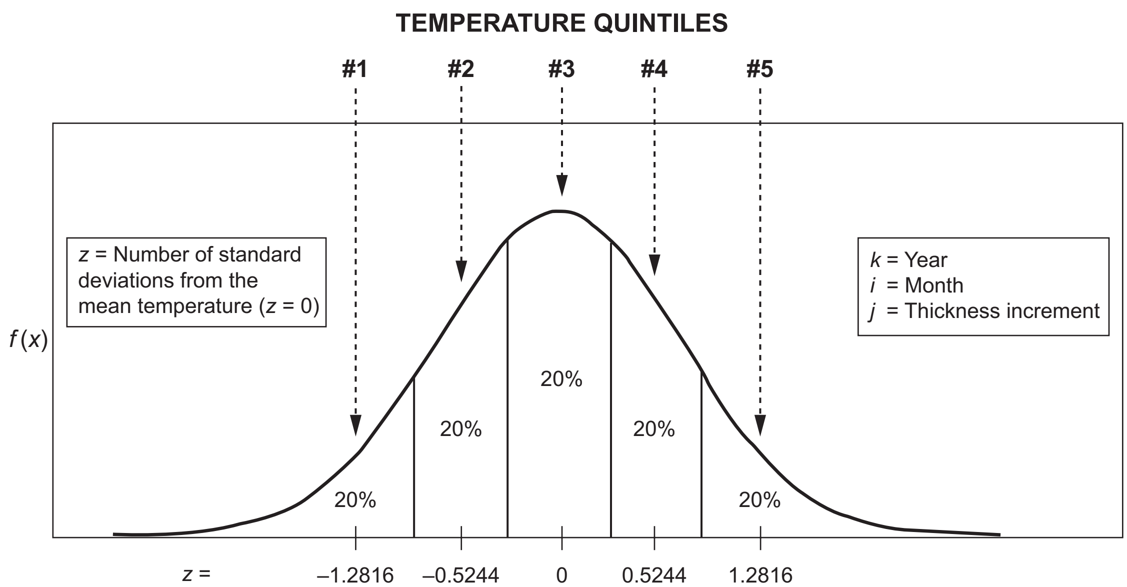

Pavement temperatures within each thickness increment of the AC layers are calculated for each month via the ICM. The pavement temperatures are then combined into five equal groups, as shown above, assuming a normal distribution. The mean pavement temperature within each group for each month for the AC thickness increment is determined for calculating the dynamic modulus as a function of time and depth in the pavement.

Figure 5-1. Graphical Illustration of the Five Temperature Quintiles Used in the MEPDG to Determine AC Mixture Properties for Load Related Distresses

The dynamic modulus is used to compute the horizontal and vertical strains at critical depths on a grid to determine the maximum permanent deformation within each layer and location of the maximum fatigue damage in the asphalt concrete layers. For transverse cracks (non-load related cracks), the EICM calculates the AC temperatures on an hourly basis and uses those hourly temperatures to estimate the AC properties (creep compliance and indirect tensile strength) to calculate the tensile stress throughout the AC surface layer.

The EICM also calculates the temperatures within each unbound sublayer and determines the months when any sublayer is frozen. The resilient modulus of the frozen sublayers is then increased

$$\rho = 10^9 \left\{ \frac{C_o}{\left[1-\left(10^9\right)^{\beta}\right]} \right\}^{\frac{1}{\beta}} \tag{5-2c}$$

$$C_o = Ln\left(\frac{a_1 M_r^{b_1}}{a_9 M_r^{b_9}}\right) \tag{5-2d}$$

where:
W_c = Water content, %
M_r = Resilient modulus of the unbound layer or sublayer, psi
$a_{1,9}$ = Regression constants; a_1 = 0.15 and a_9 = 20.0
$b_{1,9}$ = Regression constants; b_1 = 0.0 and b_9 = 0.0

Figure 5-2 shows a comparison between the measured and predicted total rut depths, including the statistics from the global calibration process. The standard error (s_e) for the total rut depth is the sum of the standard error for the AC and unbound layer rut depths and is a function of the average predicted rut depth. Equations 5-3a–5-3c show the standard error (standard deviation of the residual errors) for the individual layers—AC and unbound layers for coarse and fine-grained materials and soils.

$$s_{e(AC)} = 0.24\left(\Delta_{AC}\right)^{0.8026} + 0.001 \tag{5-3a}$$

$$s_{e(AggrBase)} = 0.1235\left(\Delta_{AggrBase}\right)^{0.5012} + 0.001 \tag{5-3b}$$

$$s_{e(Subgrade)} = 0.1477\left(\Delta_{Subgrade}\right)^{0.6711} + 0.001 \tag{5-3c}$$

where:
Δ_{AC} = Plastic deformation in the AC layers, in.
$\Delta_{AggrBase}$ = Plastic deformation in the aggregate or granular base layers, in.
$\Delta_{Subgrade}$ = Plastic deformation in the subgrade or embankment layers and soils, in.

These equations for the standard errors of the predicted rut depths within each layer were not based on actual measurements of rutting within each layer, because trenches were unavailable for all LTPP test sections used in the global calibration process. The so-called "measured" rut depths within each layer were only estimated by proportioning the total rut depth measured to the different layers using a systematic procedure.

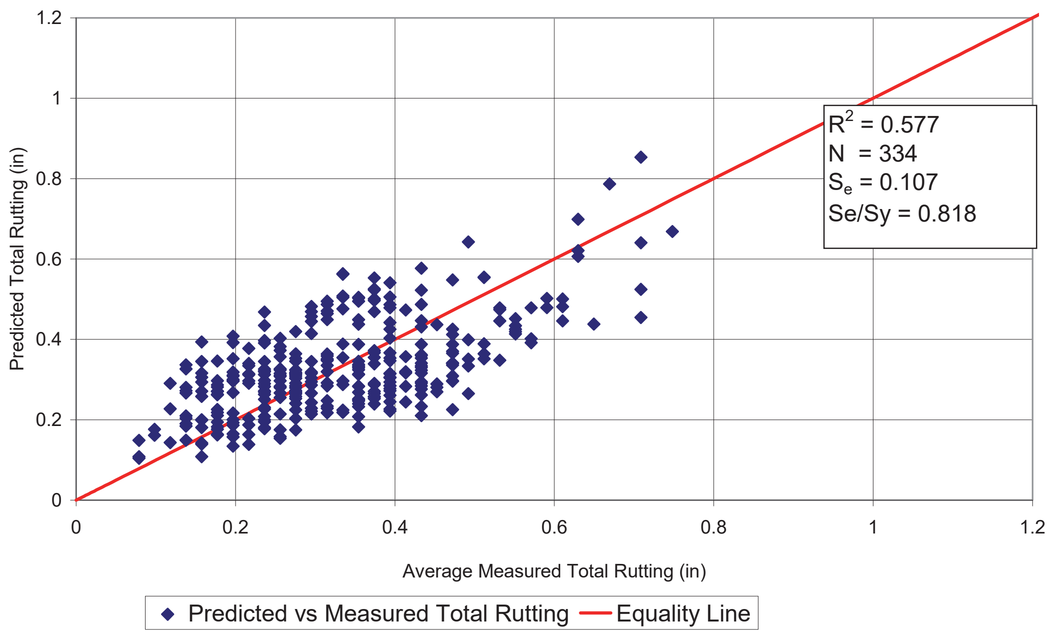

Figure 5-2. Comparison of Measured and Predicted Total Rutting Resulting from Global Calibration Process

5.3.3 *Load-Related Crackinge*

Asphalt Concrete Layers

Two types of load-related cracks are predicted by the MEPDG: alligator cracking and longitudinal cracking. The MEPDG assumes that alligator, or area cracks, initiate at the bottom of the AC layers and propagate to the surface with continued truck traffic, while longitudinal cracks are assumed to initiate at the surface.

For bottom-up or alligator cracking:

The allowable number of axle load applications needed for the incremental damage index approach to predict bottom-up cracks) is shown in Equation 5-4a.

$$N_{f-AC} = k_{f1}(C)(C_H)\beta_{f1}(\varepsilon_t)^{-k_{f2}\beta_{f2}}(E_{AC})^{-k_{f3}\beta_{f3}} \tag{5-4a}$$

where:

$N_{f\text{-}AC}$ = Allowable number of axle load applications for a flexible pavement and AC overlays

ε_t = Tensile strain at critical locations and calculated by the structural response model, in/in.

E_{AC} = Dynamic modulus of the AC measured in compression, psi

k_{f1}, k_{f2}, k_{f3} = Global laboratory-derived model coefficients for dense-graded neat AC mixtures (k_{f1} = 3.75, k_{f2} = 2.87, and k_{f3} = 1.46)

β_{f1}, β_{f2}, β_{f3} = Local or mixture specific field shift or adjustment constants; for the global calibration effort, these constants are: β_{f1} is AC thickness dependent, β_{f2} is 1.38, and β_{f3} is 0.88

For AC thicknesses less than 5 in.: $\beta_{f1} = 0.02054$
For AC thicknesses 5–12 in.: $\beta_{f1} = 5.014(H_{AC})^{-3.416}$ (5-4b)
For AC thicknesses greater than 12 in.: $\beta_{f1} = 0.001032$.

$$C = 10^{M} \tag{5-4c}$$

$$M = 4.84\left(\frac{V_{be}}{V_a + V_{be}} - 0.69\right) \tag{5-4d}$$

where:
H_{AC} = Total thickness of the AC layers, in.
V_{be} = Effective asphalt content by volume, %
V_a = Percent air voids in the AC mixture
C_H = Thickness correction term

C_H =	if $H_{AC} \le 2.5$ in.	$1 / (0.005169 H_{AC}^{2.913059})$
	if 2.5 in < H_{AC} < 14.5 in.	$1/(-0.046908\, H_{AC}^{3} + 0.729644\, H_{AC}^{2} - 0.635578\, H_{AC} - 1.555892)$
	if $H_{AC} \ge 14.5$ in.	4.255

The MEPDG calculates the incremental damage indices on a grid pattern throughout the AC layers at critical depths. The incremental damage index (ΔDI) is calculated by dividing the actual number of axle loads by the allowable number of axle loads (defined by Equation 5-4a, and referred to as Miner's hypothesis) within a specific time increment and axle load interval for each axle type. The cumulative damage index (DI) for each critical location is determined by summing the incremental damage indices over time, as shown in Equation 5-5.

$$DI = \sum (\Delta DI)_{j,m,l,p,T} = \sum \left(\frac{n}{N_{f-HMA}}\right)_{j,m,l,p,T} \tag{5-5}$$

where:
n = Actual number of axle load applications within a specific time period
j = Axle load interval
m = Axle load type (single, tandem, tridem, or quad)
l = Truck type using the truck classification groups included in AASHTOWare Pavement ME Design
p = Month
T = Median temperature for the five temperature intervals or quintiles used to subdivide each month, °F

As noted under Subsection 4.1, General Terms, an endurance limit for AC mixtures can be input into the AASHTOWare PMED, but this concept was excluded from the global calibration process. If the endurance limit concept is selected for use, all tensile strains that are less than the endurance limit input are excluded from calculating the incremental damage index for bottom-up or alligator cracking. The endurance limit concept is not applied in calculating the incremental damage for top-down or longitudinal cracking.

The area of alligator cracking is calculated from the total damage over time (Equation 5-5) using different transfer functions. Equation 5-6a is the relationship used to predict the amount of alligator cracking on an area basis, FC_{Bottom}.

$$FC_{Bottom} = \left(\frac{1}{60}\right)\left\{\frac{C_4}{1+e^{\left[C_1C_1^* + C_2C_2^* \log\left(DI_{Bottom} * 100\right)\right]}}\right\} \tag{5-6a}$$

where:

FC_{Bottom} = Area of alligator cracking that initiates at the bottom of the AC layers, % of total lane area

DI_{Bottom} = Cumulative damage index at the bottom of the AC layers

$C_{1,2,4}$ = Transfer function regression constants; C_4 = 6,000, C_1 = 1.00, and C_2 = 1.00

$$C_1^* = -2C_2^* \tag{5-6b}$$

$$C_2^* = -2.40874 - 39.748\left(1 + H_{AC}\right)^{-2.856} \tag{5-6c}$$

Figure 5-3 shows the comparison of the cumulative fatigue damage and measured alligator cracking, including the statistics from the global calibration process. The standard error, s_e (standard deviation of the residual errors), for the alligator cracking prediction equation is shown in Equation 5-7, and is a function of the average predicted area of alligator cracks.

$$s_{e(Alligator)} = 1.13 + \frac{13}{1+e^{7.57 - 15.5\,Log\left(FC_{Bottom} + 0.0001\right)}} \tag{5-7}$$

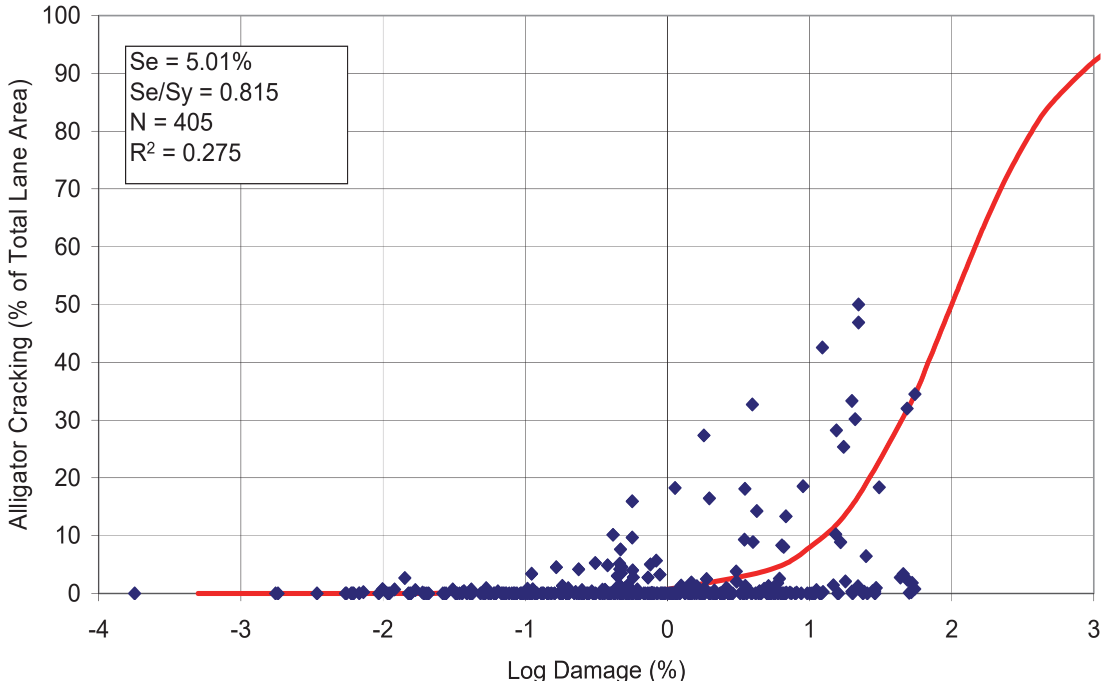

Figure 5-3. Comparison of Cumulative Fatigue Damage and Alligator Cracking Resulting from Global Calibration Process

For top-down cracking:
The fracture mechanics model incorporated into Pavement ME uses the Paris' law of crack propagation to characterize crack growth due to repeated application of traffic loads.

$$\frac{dc}{dN} = A(\Delta K)^n \tag{5-8a}$$

$$\frac{dc}{dT} = A(\Delta K)^n \tag{5-8b}$$

where:
dc = Change or growth in crack length, where c = Crack length
dN = Increase in loading cycles during a time increment, where N = Number of loading cycles
dT = Increase in thermal cycles during a time increment, where T = Temperature
ΔK = Stress intensity amplitude that depends on the stress level, the geometry of the pavement structure, the fracture model, crack length, and load transfer efficiency across the crack or joint
A, n = Fracture properties of asphalt concrete mixture

The NCHRP 1-52 study found that transverse thermal stress does not contribute significantly to the growth of top-down cracking. Therefore, stress intensity at the crack tip due to traffic loading is used to calculate crack length increments. The formation of micro-cracks and subsequent failure of asphalt concrete is modeled using the modified Paris' law shown below in Equation 5-8c.

$$\frac{dc}{dN} = A'\left(J_R\right)^{n'} \tag{5-8c}$$

where:
A', n' = Fracture properties of asphalt concrete mixture
J_R = Pseudo J-integral

The pseudo J-integral used in the modified Paris' law is defined as the increment in dissipated pseudo work per unit crack surface area. The J-integral is related to the stress intensity factors (K, as defined in Equation 5-8a) as shown in Equation 5-9.

$$J_R = \frac{1-\nu^2}{E_R}(K_I^2 + K_{II}^2) + \frac{1+\nu}{E_R}K_{III}^2 \tag{5-9}$$

where:
ν = Poisson's ratio of asphalt concrete
E_R = Representative elastic modulus
K_I = Stress intensity factor in Mode I (opening)
K_{II} = Stress intensity factor in Mode II (in-plane shear)
K_{III} = Stress intensity factor in Mode III (out-of-plane share)

The J-integral is computed from stress intensity factors in all three modes of fracture, which are shown below in Figure 5-4.

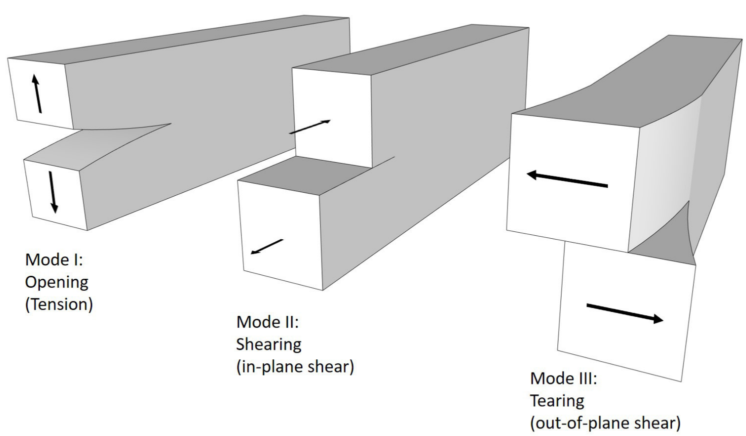

Figure 5-4. Mechanisms of Thermally Induced Reflective Cracks of Asphalt Overlays

The fracture parameter n' is calculated from asphalt mixture volumetrics and the asphalt's relaxation modulus Power law function parameters (E_1 and m), as shown below in Equation 5-10a. The parameter A' was found to be strongly correlated to n' and is calculated directly using a regression equation, as shown in Equation 5-10b.

$$n' = -9.00498 + 1.0627\psi + \frac{2.8713}{m} - 40.8788\left(\frac{1}{E_1}\right)^m + 18.868\frac{P_b}{V_a + P_b} \quad (5\text{-}10a)$$

$$A' = 10^{-1\times(1.2752n + 1.713)} \quad (5\text{-}10b)$$

where:

Ψ = Shape parameter of the aggregate power law function
m, E_1 = Relaxation modulus Power law function parameters, aged asphalt
P_b = Percent asphalt binder by weight of mix, %
V_a = Air voids in the asphalt layer, %

The pseudo J-integrals were calculated using finite element analysis in ABAQUS using different pavement structures, layer thicknesses, material properties (layer moduli), and crack depths. The analyses were performed by inserting a longitudinal crack of length 39.4 in. in the middle of the pavement lane in the longitudinal direction (along the direction of traffic). Artificial neural networks were developed to compute J-integrals at runtime for each set of inputs, i.e., aged asphalt modulus and crack depth at each monthly interval.

Crack growth is modeled using the modified Paris' law over the pavement's design life as described above. The time to crack initiation, defined as the time to reach a crack length of 0.3 in., is calculated using a regression equation, as shown in Equation 5-10c. The longitudinal and alligator cracking data from the LTPP database was used for calibrating the t_0 and crack area transfer functions.

$$t_0 = \frac{K_{L1}}{1 + e^{K_{L2}\times 100\times\frac{a_0}{2A_0} + K_{L3}\times HT + K_{L4}\times LT + K_{L5}\times\log_{10}\text{AADTT}}} \quad (5\text{-}10c)$$

where:

t_0= Time to crack initiation, days
$K_{L1\ \text{through}\ L5}$ = Calibration coefficients for time to crack initiation
$a_0/2A_0$ = Energy parameter, calculated using Equation 5-10d
HT = Annual number of days above 89.6°F
LT = Annual number of days below 32°F
AADTT = Annual average daily truck traffic (initial year)

$$\frac{a_0}{2A_0} = 0.1796 + 1.5\times10^{-5}E_1 - 0.69m - 7.169\times10^{-4}H_a \quad (5\text{-}10d)$$

where:

H_a = total asphalt thickness
K_{L1} through K_{L5} = calibration coefficients
K_{L1} = 64271618
K_{L2} = 0.2855

$K_{L3} = 0.011$
$K_{L4} = 0.0149$
$K_{L5} = 3.266$

The total percentage lane area of top-down cracks is calculated as a function of the number of months to failure and the maximum allowable area of cracking, L_{MAX}. A value of 58 percent is assumed for L_{MAX} and represents the total area of two wheel paths. According to the NCHRP 1-52 study, the definitions of terms related to crack length prediction are:

- Crack initiation: Crack length (depth of the crack from surface) is equal to 0.3 in.
- Failure: Crack length is equal to 1.575 in.
- Months to failure, Month: Number of months required for crack (after initiation) to reach the failure criterion of 1.575 in.

The predicted top-down cracking versus time is an S-shaped curve, and is calculated using the model shown in Equation 5-11a.

$$L(t) = L_{MAX} e^{-\left(\frac{C_1 \rho}{t - C_3 t_0}\right)^{C_2 \beta}} \quad (5\text{-}11a)$$

where:
$L(t)$ = Top-down cracking total lane area (%)
L_{MAX} = Maximum area of top-down cracking (%)
C_1, C_2, C_3 = Calibration coeficcients
ρ = Scale parameter of the top-down cracking curve
t = Analysis month in days
t_0 = Time to crack initiation, days
β = Shape parameter of the top-down cracking curve

The scale and shape parameters ρ and β are calculated as a function of number of months to failure, Month using Equations 5-11b and 5-11c, respectively.

$$\rho = \alpha_1 + \alpha_2 \times \text{Month} \quad (5\text{-}11b)$$

$$\beta = 0.7319 \times \left(\log_{10} \text{Month}\right)^{-1.2801} \quad (5\text{-}11c)$$

α_1 and α_2 are calibration parameters whose values depend on whether the pavement is located in a wet (WF or WNF) or dry (DF or DNF) climatic zone.

The calibration of the top-down cracking model applies to both the cracking prediction model shown in Equation 5-11a as well as the number of days to crack initiation, t_0, as shown in Equation 5-10c. Figure 5-5a includes a comparison of the measured and predicted number of days, t_0, from the LTPP sites included in the study. Figure 5-5b includes a comparison between the measured and predicted area of top-down cracking.

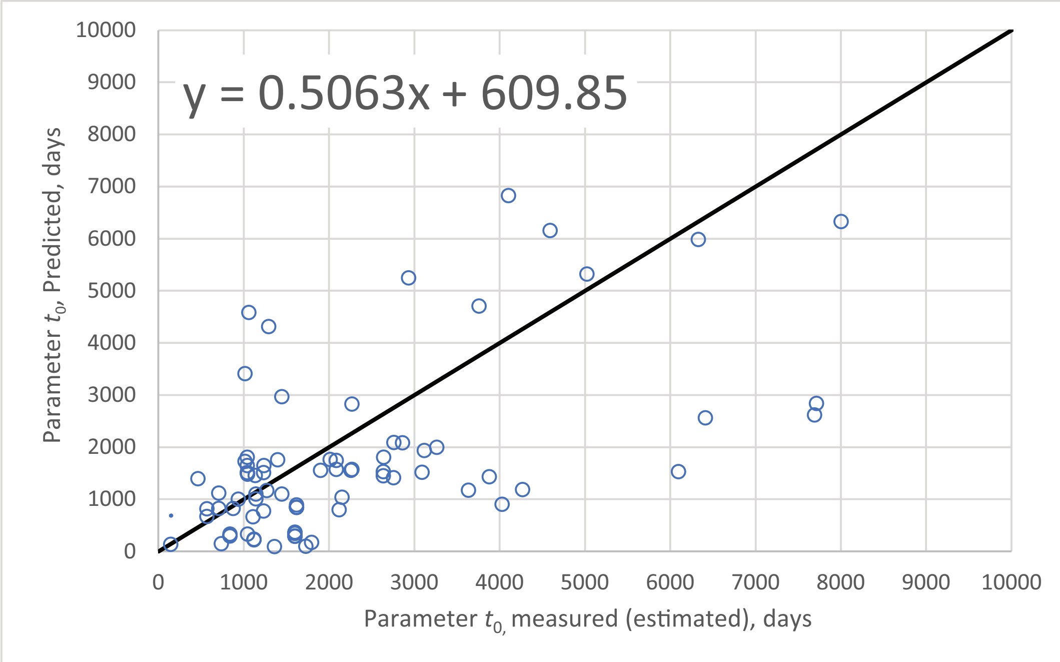

Figure 5-5a. Measured versus Predicted Number of Days to Crack Initiation

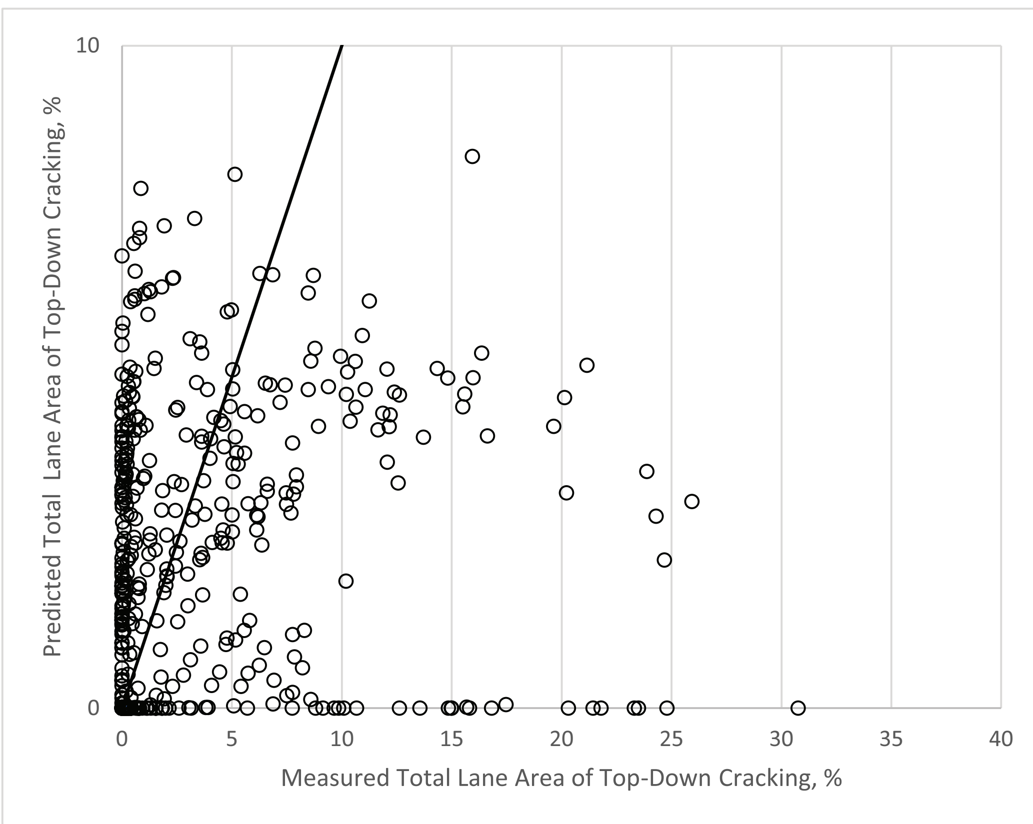

Figure 5-5b. Measured versus Predicted Area of Top-Down Cracking

Table 5-2 shows the values of α_1 and α_2 for the four climatic zones. The calibration parameters for the t_0 values are shown in Table 5-3. Equation 5-11d is the standard deviation of residual errors, σ_{RE}, for determining the reliability of a specific design strategy.

$$\sigma_{RE} = 0.3657(TDC_{Mean}) + 3.6563 \tag{5-11d}$$

where:

TDC_{Mean} = predicted top-down cracking (% total lane area) based on average inputs

Table 5-2. Calibration Parameters α_1 and α_2: Global Coefficients

Climatic Zone	α_1	α_2
Wet Freeze (WF)	631.04	2269.8
Wet Non-Freeze (WNF)	631.04	2269.8
Dry Freeze (DF)	1617.6	–1705.3
Dry Non-Freeze (DNF)	1617.6	–1705.3

Table 5-3. Calibration Parameters for Crack Initiation Time, t_0: Global Coefficients

Calibration Parameter	New Flexible
K_{L1}	64271618
K_{L2}	0.2855
K_{L3}	0.011
K_{L4}	0.0149
K_{L5}	3.266

CTB Layers

For fatigue cracks in CTB layers, the allowable number of load applications, $N_{f\text{-}CTB}$, is determined in accordance with Equation 5-12a, and the amount, or area, of fatigue cracking is calculated in accordance with Equation 5-12b. The global model and calibration coefficients for the CTB base were derived in conjunction with the reflection cracking model coefficients (see Section 5.3.5).

$$\log(N_{f-CTB}) = \frac{k_{c1}\beta_{c1} + \dfrac{\sigma_t}{MR}}{k_{c2}\beta_{c2}} \tag{5-12a}$$

$$FC_{CTB} = C_1 + \frac{C_2}{1 + e^{\left[C_3 - C_4 \log(DI_{CTB})\right]}} \tag{5-12b}$$

where:

$N_{f\text{-}CTB}$ = Allowable number of axle load applications for a semi-rigid pavement

σ_t = Tensile stress at the bottom of the CTB layer, psi. (*Note*: Tensile stress is a negative value computed by the pavement response program in the MEPDG, so the higher the tensile stress, the lower the allowable number of load applications.)
M_R = 28-day modulus of rupture for the CTB layer, psi
DI_{CTB} = Cumulative damage index of the CTB or cementitious layer and determined in accordance with Equation 5-5
$k_{c1,c2}$ = Global model coefficients: k_{c1} = 0.972 and k_{c2} = 0.0825
$\beta_{c1,c2}$ = Global calibration or field-shift adjustment constants: β_{c1} = 1.0, and β_{c2} = 1.0
FC_{CTB} = Area of fatigue cracking, ft^2
$C_{1,2,3,4}$ = Transfer function regression constants: C_1 = 0, C_2 = 75, C_3 = 2.0, and C_4 = 2.0

The computational analysis of incremental fatigue cracking for a semi-rigid pavement uses the damaged modulus approach. In summary, the elastic modulus of the CTB layer decreases as the damage index, DI_{CTB}, increases. Equation 5-12c is used to calculate the damaged elastic modulus within each season or time period for calculating critical pavement responses in the CTB and other pavement layers.

$$E_{CTB}^{D(t)} = E_{CTB}^{Min} + \left\{ \frac{E_{CTB}^{Max} - E_{CTB}^{Min}}{1 + e^{\left[-4+14\left(DI_{CTB}\right)\right]}} \right\} \tag{5-12c}$$

where:
$E_{CTB}^{D(t)}$ = Equivalent damaged elastic modulus at time t for the CTB layer, psi
E_{CTB}^{Min} = Equivalent elastic modulus for total destruction of the CTB layer, psi
E_{CTB}^{Max} = 28-day elastic modulus of the intact CTB layer, no damage, psi

However, the damaged modulus approach was not used to derive the global calibration coefficients. It was assumed that the $E_{CTB}^{D(t)}$ equals E_{CTB}^{Min}, and E_{CTB}^{Max} was equal to the 28-day elastic modulus measured in the laboratory. The reason for making that assumption and not using the damaged modulus approach is that the flexural strength or modulus of rupture used to calculate the allowable number of load applications (see Equation 5-12a) remains constant throughout the design period. As such, the damage index significantly decreases with increasing damage because of the reduction in elastic modulus (see Equation 5-12c), resulting in increasing fatigue cracks at a decreased rate over time. Many of the LTPP semi-rigid pavement sections did not exhibit this characteristic. If the designer selects different values for E_{CTB}^{Min} and E_{CTB}^{Max}, different calibration coefficients need to be used and derived using the damaged modulus approach.

5.3.4 *Non-Load Related Cracking—Transverse Cracking*

The transverse cracking prediction model and transfer function (*19*) is based on fracture mechanics and presented below.

$$\Delta C = A(\Delta K)^n \tag{5-13a}$$

where:

ΔC = Change in the crack depth due to a cooling cycle

ΔK = Change in the stress intensity factor due to a cooling cycle

A, n = Fracture parameters for the AC mixture

Experimental results indicate that reasonable estimates of A and n can be obtained from the indirect tensile creep-compliance and strength of the AC in accordance with Equations 5-13b and 5-13c.

$$A = k_t \beta_t 10^{\left[4.389 - 2.52 \log\left(E_{HMA} \sigma_m n\right)\right]} \tag{5-13b}$$

where:

$$\eta = 0.8\left[1 + \frac{1}{m}\right] \tag{5-13c}$$

k_t = Coefficient determined through global calibration, which was found to be dependent on the MAAT for each input level, as defined below:

MAAT greater than 57°F:

$$k_t = 0.13(MAAT)^2 - 11.68(MAAT) + 244.14 \tag{5-13d}$$

MAAT less than or equal to 57°F:

$$k_t = 3 \times 10^{-7}\left(MAAT\right)^{4.0319} \tag{5-13e}$$

E_{AC} = AC indirect tensile modulus, psi

σ_m = Mixture tensile strength, psi

m = The m-value derived from the indirect tensile creep compliance curve measured in the laboratory

β_t = Local or mixture calibration factor, which were set to unity for the global calibration

The stress intensity factor, K, has been incorporated in the AASHTOWare PMED through the use of a simplified equation developed from theoretical finite element studies (Equation 5-13f).

$$K = \sigma_{tip}\left[0.45 + 1.99\left(C_o\right)^{0.56}\right] \tag{5-13f}$$

where:

σ_{tip} = Far-field stress from pavement response model at depth of crack tip, psi

C_o = Current crack length, ft

The degree of cracking is predicted by the MEPDG using an assumed relationship between the probability distribution of the log of the crack depth to AC layer thickness ratio and the percent of cracking. Equation 5-13g shows the expression used to determine the extent of thermal cracking.

$$TC = \beta_{t1} N \left[\frac{1}{\sigma_d \log\left(\frac{C_d}{H_{AC}}\right)} \right] \quad (5\text{-}13g)$$

where:

TC = Observed amount of thermal cracking, ft/mi

β_{t1} = Regression coefficient determined through global calibration (400)

$N[z]$ = Standard normal distribution evaluated at [z]

σ_d = Standard deviation of the log of the depth of cracks in the pavement (0.769), in.

C_d = Crack depth, in.

H_{AC} = Thickness of AC layers, in.

Figure 5-6 includes a comparison between the measured and predicted cracking and the statistics from the global calibration process for input Levels 1 and 3. The standard error for the transverse cracking prediction equations for the three input levels is shown in Equations 5-14a–5-14f.

$$S_e(Level\ 1;\ MAAT < 57°F) = 0.14(TC) + 168 \quad (5\text{-}14a)$$

$$S_e(Level\ 1;\ MAAT > 57°F) = 0.14(TC) + 343 \quad (5\text{-}14b)$$

$$S_e(Level\ 2;\ MAAT < 57°F) = 0.20(TC) + 168 \quad (5\text{-}14c)$$

$$S_e(Level\ 2;\ MAAT > 57°F) = 0.20(TC) + 343 \quad (5\text{-}14d)$$

$$S_e(Level\ 3;\ MAAT < 57°F) = 0.289(TC) + 168 \quad (5\text{-}14e)$$

$$S_e(Level\ 3;\ MAAT > 57°F) = 0.2386(TC) + 343 \quad (5\text{-}14f)$$

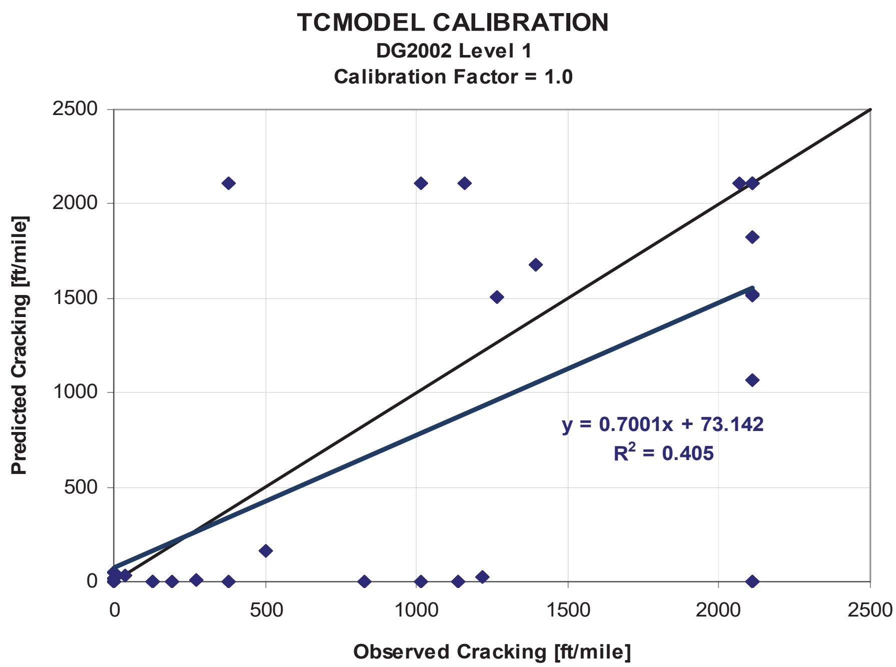

5-6a **Input Level 1 Using the Global Calibration Factor**

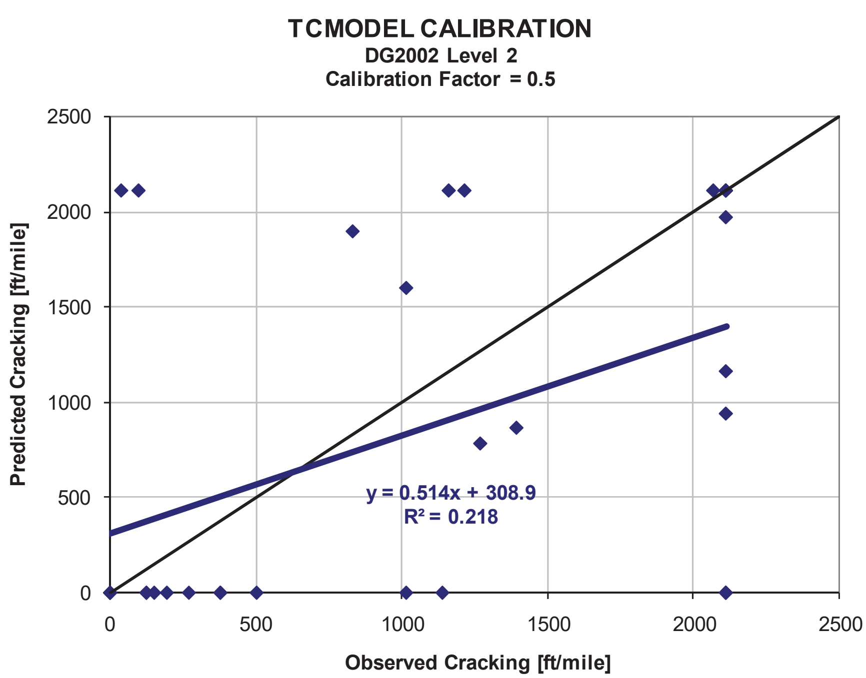

5-6b **Input Level 2 Using the Global Calibration Factor**

Figure 5-6. Comparison of Measured and Predicted Transverse Cracking Resulting from Global Calibration Process

Continued on next page.

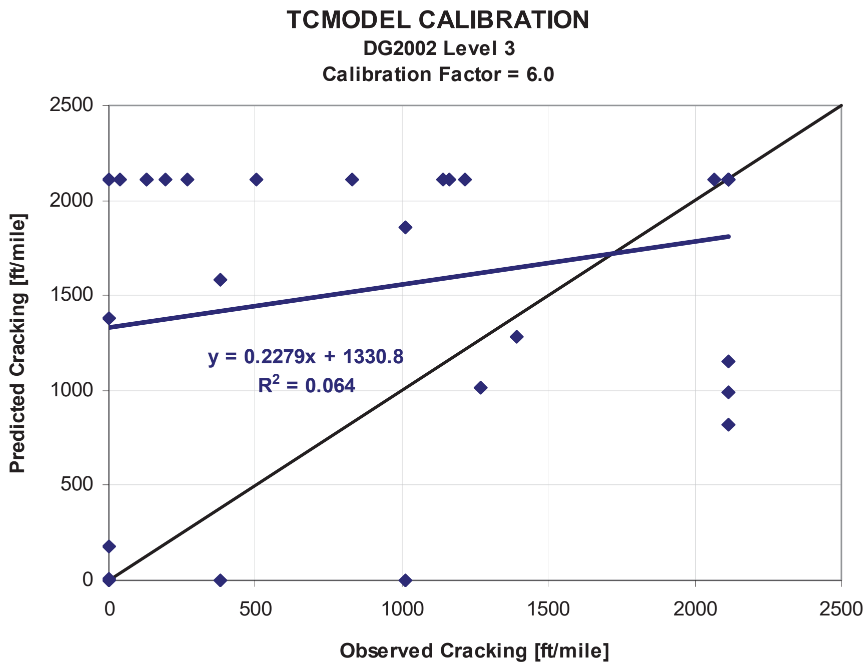

5-6c **Input Level 3 Using the Global Calibration Factor**

Figure 5-6. Comparison of Measured and Predicted Transverse Cracking Resulting from Global Calibration Process, *continued*

5.3.5 *Reflection Cracking in AC Overlays and AC Layers of Semi-Rigid Pavements*

The MEPDG predicts reflection cracks in AC overlays or AC surfaces of semi-rigid pavements using a fracture mechanics-based model based on three response mechanisms: (1) shear, (2) bending, and (3) tension. The three response mechanisms are graphically illustrated in Figure 5-7. The tension related response mechanism is thermally induced (see Figure 5-8), while the bending and shear response mechanisms are traffic induced (see Figure 5-9).

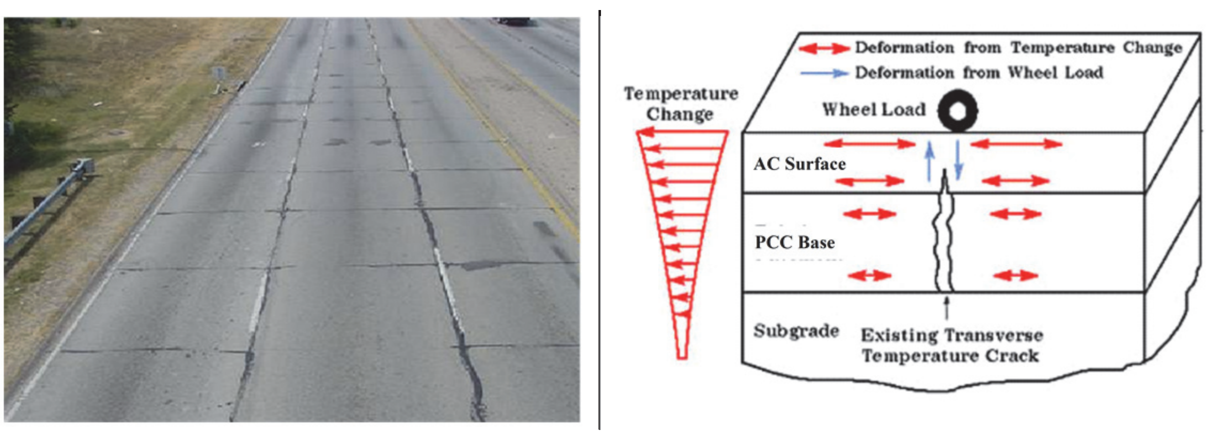

Figure 5-7. Response Mechanisms Used in Reflection Cracking Prediction Methodology

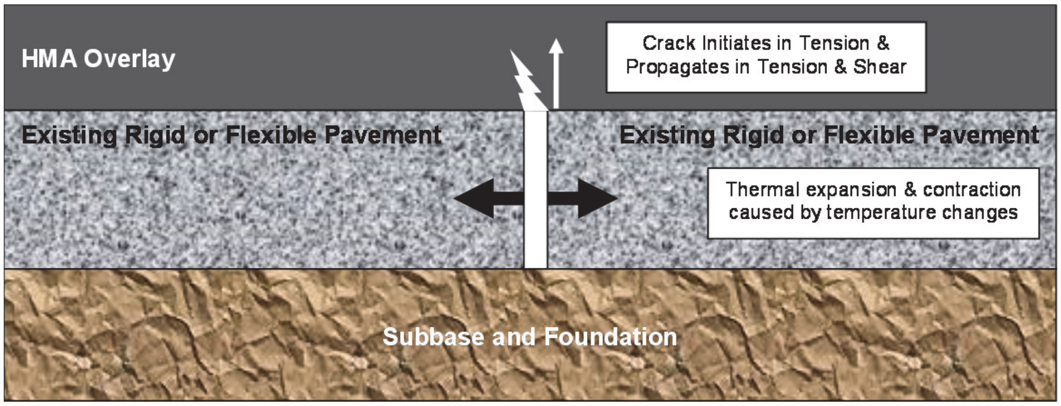

Figure 5-8. Mechanisms of Thermally Induced Reflective Cracks of AC Overlays

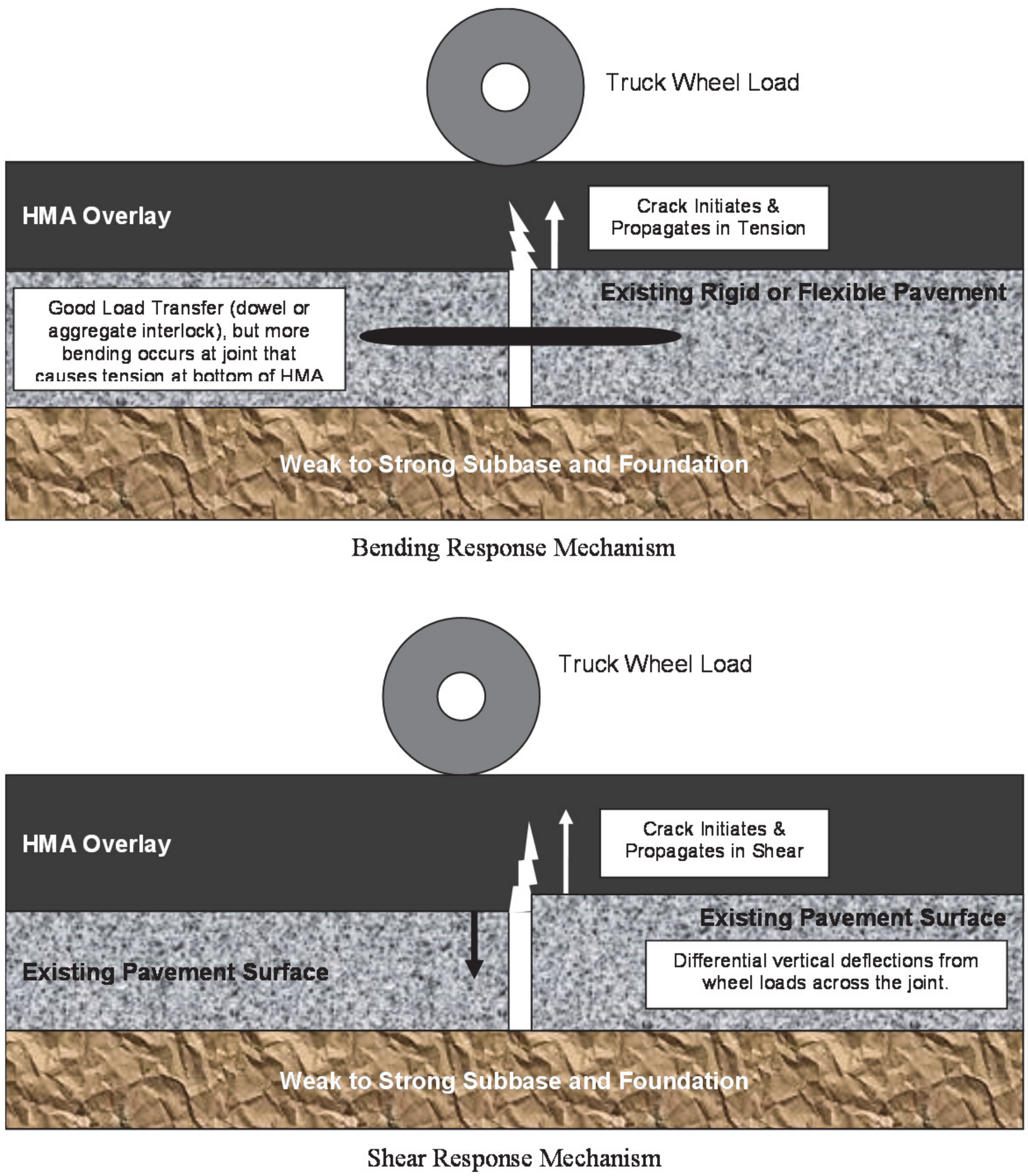

Figure 5-9. Mechanisms of Traffic Induced Reflective Cracks of AC Overlays

Paris-Erdogan's law is used to model crack propagation expressed in Equation 5-15a, and is similar to the one used to predict transverse cracks caused by a low-temperature event. The transfer function is used to estimate the amount of fatigue and transverse cracks exhibited in a non-surface layer that reflect to the AC surface or overlay after a certain period of time. This transfer function predicts the percentage of area of cracks that propagate through the AC as a function of time, as shown in Equation 5-15a due to wheel loads and in Equation 5-15b for temperature changes.

$$\frac{dc}{dN} = A\left(\Delta K\right)^n \tag{5-15a}$$

$$\frac{dc}{dT} = A\left(\Delta K\right)^n \tag{5-15b}$$

where:

c = Crack length and dc is the change or growth in crack length

N = Number of loading cycles and dN is the increase in loading cycles during a time increment

T = Temperature and dT is the increase in thermal cycles during a time increment

ΔK = Stress intensity amplitude that depends on the stress level, the geometry of the pavement structure, the fracture model, crack length, and load transfer efficiency across the crack or joint

A,n = Fracture properties of the asphalt concrete mixture

The fracture properties A and n are calculated from the indirect tensile creep-compliance and strength of the AC mixture in accordance with Equations 5-16a and 5-16b.

$$A = g_2 + \frac{g_3}{m_{mix}}\left(\log D_1\right) + g_4 \log \sigma_t \tag{5-16a}$$

$$n = g_0 + \frac{g_1}{m_{mix}} \tag{5-16b}$$

where:

g_0, g_1, g_2, g_3, g_4 = Mixture regression coefficients

m_{mix} = The log-log slope of the mixture creep compliance versus loading time relationship for the current temperature and loading time

D_1 = Coefficient of the creep compliance expressed in the power law form

σ_t = Tensile strength of the AC mix at the specific temperature

The three response mechanisms are used to estimate the change in crack length over time: bending, shear, and tension. The crack growth or damage increment from each mechanism is provided below.

$$\Delta_{Bend} = A\left(\Delta K_B\right)^n \tag{5-17a}$$

$$\Delta_{Shear} = A\left(\Delta K_S\right)^n \tag{5-17b}$$

$$\Delta_{Tension} = A\left(\Delta K_T\right)^n \tag{5-17c}$$

The loading time for the bending and shear mechanisms (Equations 5-17a and 5-17b) are defined in a similar way to the loading time for the alligator fatigue cracking model, while the loading time for the tensile mechanism (Equation 5-17c) is defined in a similar way to the low temperature cracking model. The stress intensity factors (ΔK) for each mechanism are determined using neural networks, which are similar in concept to those developed for the rigid pavement distress prediction models. The reflection cracking neural network models were developed from finite element analyses for the MEPDG family of pavements: conventional and deep strength flexible pavements, semi-rigid pavements, CRCP, intact JPCP, and fractured JPCP.

The methodology assumes the damage from each mechanism is uncoupled, but additive—similar to Miner's hypothesis for fatigue damage. As such, the following equations are used to estimate the growth of a reflection crack with increasing number of load applications and thermal cycles.

$$\frac{dc}{dN} = A\left[k_1\left(\Delta K_B\right)^n + k_2\left(\Delta K_S\right)^n\right] \tag{5-18a}$$

$$\frac{dc}{dT} = A\left[k_3\left(\Delta K_T\right)^n\right] \tag{5-18b}$$

where:

$k_{1,2,3}$ = Calibration coefficients for reflection cracking

thus:

$$C = \sum_{i=1}^{m}\left(\frac{dc}{dN} + \frac{dc}{dT}\right)_i \tag{5-18c}$$

Equation 5-18c was rewritten in the form of the common fatigue damage index accumulation relationship for AC layers and overlays over chemically stabilized layers, PCC, and existing AC layers with continued truck and temperature loadings. The continual fatigue damage accumulation of these layers is considered in the MEPDG AC overlay analysis procedure in the following form:

$$C = h_{AC} DI_{RC} \tag{5-18d}$$

where:

h_{AC} = Total thickness of the AC layers that the reflection crack will have to propagate through, in.

DI_{RC} = Total damage index for reflection cracks

For any given month, i, the total fracture damage is estimated by Equation 5-18e.

$$DI_{RC} = \sum_{i=1}^{m}\Delta DI_i \tag{5-18e}$$

where:

DI_{RC} = Total damage index for reflection cracks in time increment m

ΔDI_i = Increment of damage index in month i

The incremental damage index within month, i, is defined below.

$$\Delta DI = \Delta DI_N + \Delta DI_T \tag{5-18f}$$

$$\Delta DI_i = \sum_{i=1}^{m} A\left[\left(c_1 k_1 \left(\Delta K_B\right)^n + c_2 k_2 \left(\Delta K_S\right)^n + c_3 k_3 \left(\Delta K_T\right)^n\right)\right] \tag{5-18g}$$

where:

$C_{1,2,3}$ = Calibration coefficients for reflection cracking

As noted above, the k-value, or model coefficients for the reflection cracking transfer functions, are the global calibration factors and defined in Table 5-4 for transverse cracks and in Table 5-5 for fatigue cracks. The area (fatigue cracks) and length (transverse cracks) of reflection cracks from the underlying layer at month or time increment i (RCR_i) are given by Equation 5-19.

$$RCR_i = Ckg\left(\frac{100}{c_4 + e^{c_5 \log DI_i}}\right) \tag{5-19}$$

where:

Ckg = Total area or length of cracks in the existing pavement surface prior to overlay

$C_{4,5}$ = Calibration coefficients for reflection cracking

The reflective fatigue and transverse cracks are calculated separately but based on the same mathematical relationship using the appropriate calibration coefficients for fatigue and transverse cracks. The k- and c-value model coefficients are included in Table 5-4 for transverse cracks and in Table 5-5 for fatigue cracks.

Table 5-4. Global Calibration Coefficients for the Reflection Cracking Transfer Functions for Transverse Cracks

Calibration Coefficients	Pavement Type: AC over AC	AC over Intact JPCP	AC over Intact CRCP or Fractured JPCP	Semi-Rigid	AC over Semi-Rigid
k_1	0.012	0.012	0.012	0.45	0.012
k_2	0.005	0.005	0.0002	0.05	0.005
k_3	1.00	1.00	0.1	1.0	1.0
C_1	3.22	3.22	3.22	0.1	3.22
C_2	25.7	25.7	25.7	0.9809	25.7
C_3	0.1	0.1	0.1	0.19	0.1
C_4	133.4	133.4	133.4	165.3	133.4
C_5	–72.4	–72.4	–72.4	–5.1048	–72.4

Table 5-5. Global Calibration Coefficients for the Reflection Cracking Transfer Functions for Fatigue Cracks

Calibration Coefficients	Pavement Type				
	AC over AC	AC over Intact JPCP	AC over Intact CRCP or Fractured JPCP	Semi-Rigid	AC over Semi-Rigid
k_1	0.012	NA	NA	0.45	0.012
k_2	0.005	NA	NA	0.05	0.005
k_3	1.00	NA	NA	1.00	1.00
C_1	0.38	NA	NA	1.64	0.38
C_2	1.66	NA	NA	1.1	1.66
C_3	2.72	NA	NA	0.19	2.72
C_4	105.4	NA	NA	62.1	105.4
C_5	–7.02	NA	NAA	–404.6	–7.02

For each month, *i*, there will be an increment of damage, ΔDI_i which will cause an increment of cracking area and/or length, CA_i, to the wearing surface or overlay. To estimate the amount of cracking reflected from the non-surface layer to the surface of the pavement for month *m*, the reflective cracking prediction equation is applied incrementally. The standard deviation equations for the standard error are listed in Table 5-6 for transverse cracks and in Table 5-7 for fatigue cracks.

Table 5-6. Standard Deviation Equations for the Transverse Cracks

Pavement Type	Standard Deviation Equation
AC over AC	$70.98(TC)^{0.2994}+30.12$
AC over Intact JPCP	$5.1025(TC)^{0.6513}+30.12$
AC over Intact CRCP or Fractured JPCP	$52.54(TC)^{0.39}+283.3$
Semi-Rigid	$0.000027(TC)^{2.1187}+399.9$
AC over Semi-Rigid	$70.98(TC)^{0.2994}+30.12$

Note: TC = Total length of predicted transverse cracks in ft/mi

Table 5-7. Standard Deviation Equations for the Fatigue Cracks

Pavement Type	Standard Deviation Equation
AC over AC	$1.1097(FC)^{0.6804}+1.23$
AC over Intact JPCP	Not Applicable
AC over Intact CRCP or Fractured JPCP	Not Applicable
Semi-Rigid	$1.3897(FC)^{0.2960}+0.4212$
AC over Semi-Rigid	$1.1097(FC)^{0.6804}+1.23$

Note: FC = Total area of predicted bottom-up fatigue or alligator cracks in percent total lane area.

5.3.6 *Smoothness*

The design premise included in the MEPDG for predicting smoothness degradation is that the occurrence of surface distress will result in increased roughness (increasing IRI value), or, in other words, a reduction in smoothness. Equations 5-20a–5-20c were developed from data collected within the LTPP program and are embedded in the AASHTOWare PMED to predict the IRI over time for AC-surfaced pavements.

IRI Equation for New AC Pavements and AC Overlays of Flexible Pavements:

$$IRI = IRI_o + C_1(RD) + C_2(FC_{Total}) + C_3(TC) + C_4(SF) \tag{5-20a}$$

where:

IRI_o = Initial IRI after construction, in./mi

SF = Site factor (refer to Equation 5-20b)

FC_{Total} = Area of fatigue cracking (combined alligator, longitudinal, and reflection cracking in the wheel path), percent of total lane area. All load related cracks are combined on an area basis—length of cracks is multiplied by 1 ft to convert length into an area basis.

TC = Length of transverse cracking (including the reflection of transverse cracks in existing AC pavements), ft/mi

RD = Average rut depth, in.

$C_{1,2,3,4}$ = Calibration factors: C_1 = 40.0, C_2 = 0.400, C_3 = 0.008, and C_4 = 0.015

The site factor (SF) is calculated in accordance with the following equation:

$$SF = Age^{1.5}[\ln((Precip + 1)(FI + 1)p_{02}) + \ln((Precip + 1)(PI + 1)p_{200})] \tag{5-20b}$$

where:

Age = Pavement age, yr

PI = Plasticity index of the soil, %

FI = Average annual freezing index, °F days

$Precip$ = Average annual precipitation or rainfall, in.

p_{02} = Percent passing the 0.02 mm sieve

p_{200} = Percent passing the 0.075 mm sieve

IRI Equation for AC Overlays of Rigid Pavements and Semi-Rigid Pavements:

$$IRI = IRI_o + PCC\ C_1(RD) + PCC\ C_2(FC_{Total}) + PCC\ C_3(TC) + PCC\ C_4(SF) \tag{5-20c}$$

where:

$PCC\ C_{1,2,3,4}$ = Calibration factors; PCC C_1 = 40.8, PCC C_2 = 0.575, PCC C_3 = 0.0014, and PCC C_4 = 0.00825

Figures 5-10 and 5-11 compare the measured and predicted IRI values and include the statistics resulting from the global calibration process for flexible pavements and AC overlays of flexible pavements and C overlays of PCC pavements, respectively. The standard error of the estimate for new flexible pavements and AC overlays of flexible and semi-rigid pavements is 18.9 in./mi, and it is 9.6 in./mi for AC overlays of intact PCC pavements. The MEPDG assumes that the standard error for AC overlays of fractured PCC pavements is the same as for AC overlays of intact PCC pavements.

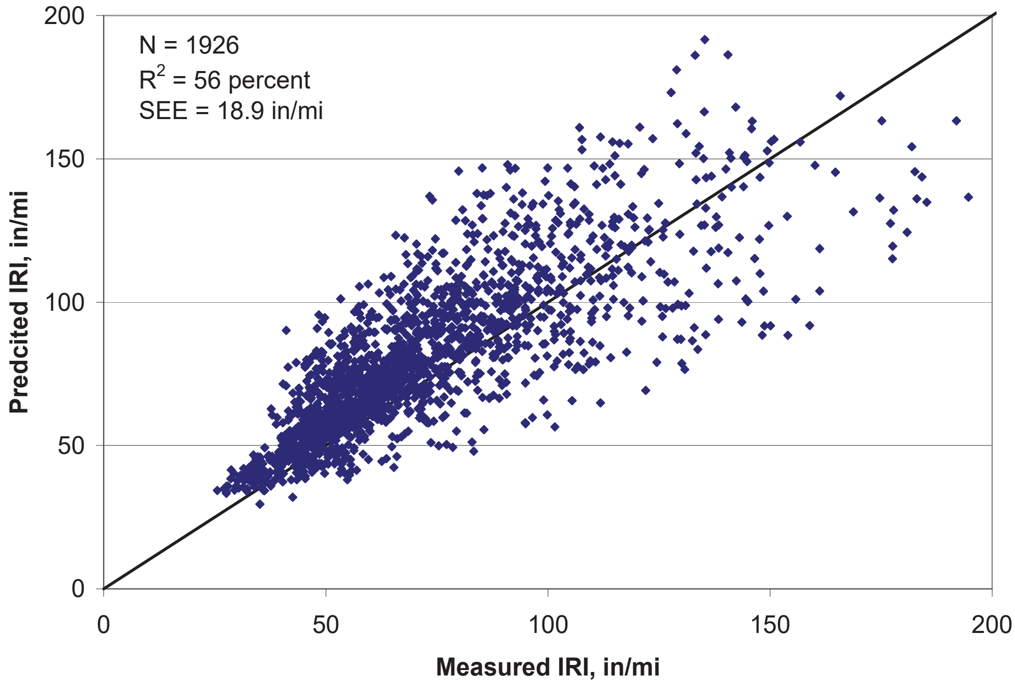

Figure 5-10. Comparison of Measured and Predicted IRI Values Resulting from Global Calibration Process of Flexible Pavements and AC Overlays of Flexible Pavements

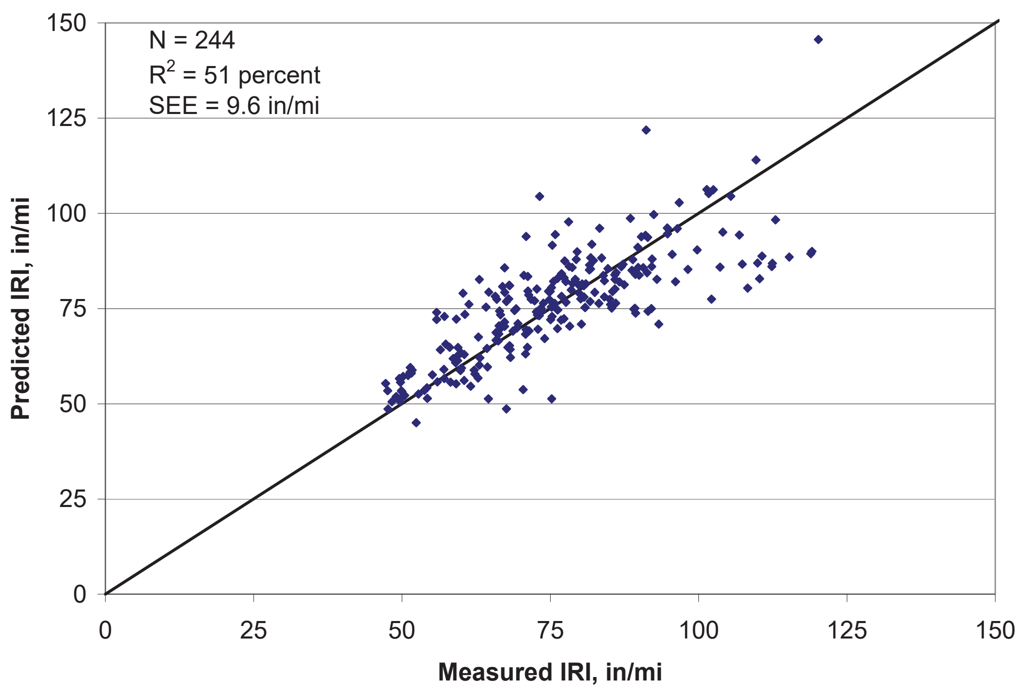

Figure 5-11. Comparison of Measured and Predicted IRI Values Resulting from Global Calibration Process of AC Overlays of PCC Pavements and Semi-Rigid Pavements

5.4 Distress Prediction Equations for Rigid Pavements and PCC Overlays

The following summarizes the methodology and mathematical models used to predict each rigid pavement and PCC overlay performance indicator. The PCC model coefficients were based on the results and findings from NCHRP 20-07, Task 327, and are included in the following sections.

5.4.1 Transverse Slab Cracking (Bottom-Up and Top-Down)—JPCP

As stated earlier for JPCP transverse cracking, both bottom-up and top-down modes of cracking are considered. Under typical service conditions, the potential for either mode of cracking is present in all slabs. Any given slab cracks either from bottom-up or top-down, but not both. Therefore, the predicted bottom-up and top-down cracking are not particularly meaningful by themselves, and combined cracking is reported excluding the possibility of both modes of cracking occurring on the same slab.

The percentage of slabs with transverse cracks (including all severities) in a given traffic lane is used as the measure of transverse cracking, and is predicted using the following global equation for both bottom-up and top-down cracking:

$$CRK = \frac{100}{1 + C_4 (DI_F)^{C_5}} \tag{5-21}$$

where:

CRK = Predicted amount of bottom-up or top-down cracking (fraction)
DI_F = Fatigue damage calculated using the procedure described in this section
$C_{4,5}$ = Calibration coefficients; $C_4 = 0.52$, $C_5 = -2.17$

The general expression for fatigue damage accumulations considering all critical factors for JPCP transverse cracking is known as Miner's hypothesis, and is calculated as follows:

$$DI_F = \sum \frac{n_{i,j,k,l,m,n,o}}{N_{i,j,k,l,m,n,o}} \tag{5-22a}$$

where:

DI_F = Total fatigue damage (top-down or bottom-up)
$n_{i,j,k,\ldots}$ = Applied number of load applications at condition *i, j, k, l, m, n*
$N_{i,j,k,\ldots}$ = Allowable number of load applications at condition *i, j, k, l, m, n*
i = Age (accounts for change in PCC modulus of rupture and elasticity, slab/base contact friction, and deterioration of shoulder LTE)
j = Month (accounts for change in base elastic modulus and effective dynamic modulus of subgrade reaction)
k = Axle type (single, tandem, and tridem for bottom-up cracking; short, medium, and long wheelbase for top-down cracking)
l = Load level (incremental load for each axle type)
m = Equivalent temperature difference between top and bottom PCC surfaces
n = Traffic offset path

o = Hourly truck traffic fraction

The applied number of load applications ($n_{i,j,k,l,m,n}$) is the actual number of axle type, *k*, of load level, *l*, that passed through traffic path, *n*, under each condition *i*, *j*, and *m* (age, season, and temperature difference). The allowable number of load applications is the number of load cycles at which fatigue failure is expected (corresponding to 50 percent slab cracking) and is a function of the applied stress and PCC strength. The allowable number of load applications is determined using the following PCC fatigue equation:

$$\log\left(N_{i,j,k,l,m,n}\right) = C_1 \cdot \left(\frac{MR_i}{\sigma_{i,j,k,l,m,n}}\right)^{C_2} \tag{5-22b}$$

where:

$N_{i,j,k,\ldots}$ = Allowable number of load applications at condition *i*, *j*, *k*, *l*, *m*, *n*
M_{Ri} = PCC modulus of rupture at age *i*, psi
$\sigma_{i,j,k,..}$ = Applied stress at condition *i*, *j*, *k*, *l*, *m*, *n*
C_1 = Calibration constant, 2.0
C_2 = Calibration constant, 1.22

The fatigue damage calculation is a process of summing damage from each damage increment. Once top-down and bottom-up damage are estimated, the corresponding cracking is computed using Equation 5-21 and the total combined cracking is determined using Equation 5-23.

$$TCRACK = \left(CRK_{Bottom-up} + CRK_{Top-down} - CRK_{Bottom-up} \cdot CRK_{Top-down}\right) \cdot 100\% \tag{5-23}$$

where:

$TCRACK$ = Total transverse cracking (percent, all severities)
$CRK_{Bottop\text{-}up}$ = Predicted amount of bottom-up transverse cracking (fraction)and
$CRK_{Top\text{-}down}$ = Predicted amount of top-down transverse cracking (fraction)

It is important to note that Equation 5-23 assumes that a slab cracks from either bottom-up or top-down, but not both. A plot of measured versus predicted transverse cracking and the statistics resulting from the global calibration process is shown in Figures 5-12 through 5-14.

Calculation of critical responses using neural nets (for speed) requires that the slab and base course are combined into an equivalent section based on equivalent stresses (load and temperature/moisture gradients) and contact friction between slab and base. This is done monthly as these parameters change over time.

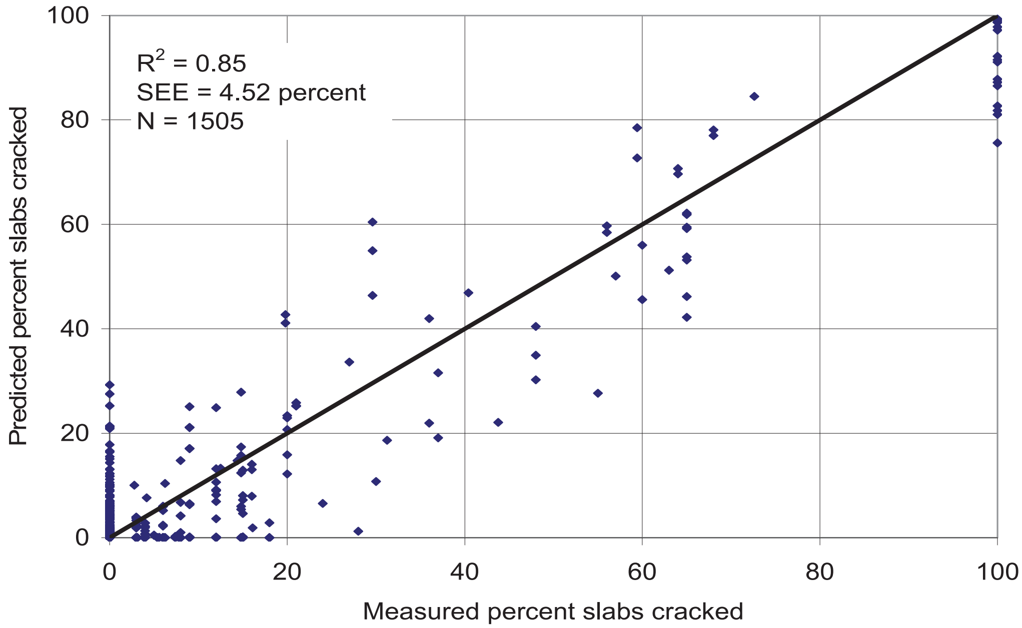

Figure 5-12. Comparison of Measured and Predicted Percentage JPCP Slabs Cracked Resulting from Global Calibration Process

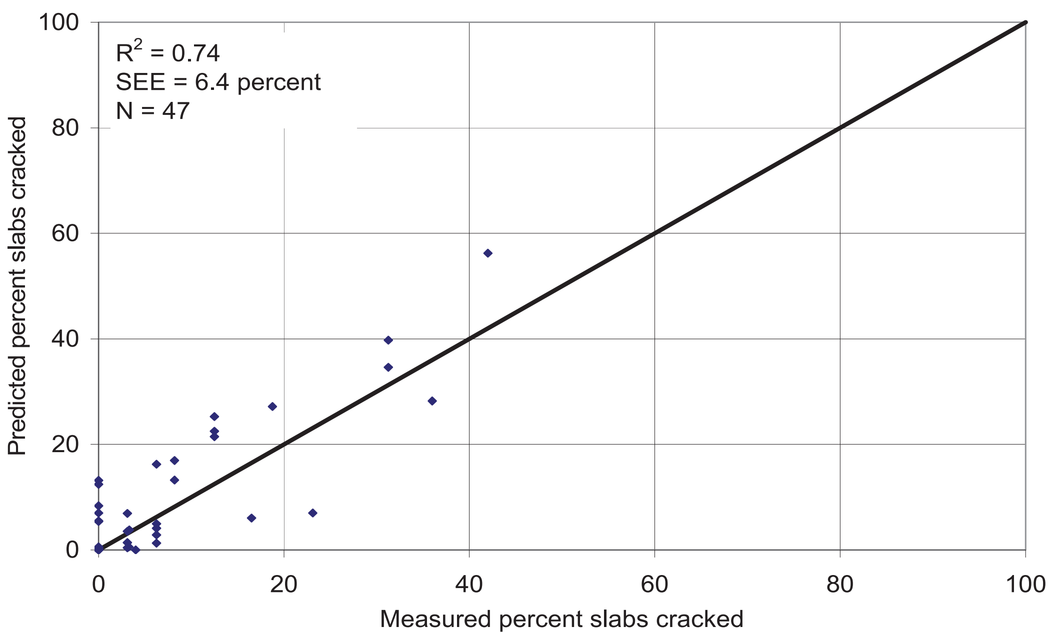

Figure 5-13. Comparison of Measured and Predicted Transverse Cracking of Unbounded JPCP Overlays Resulting from Global Calibration Process

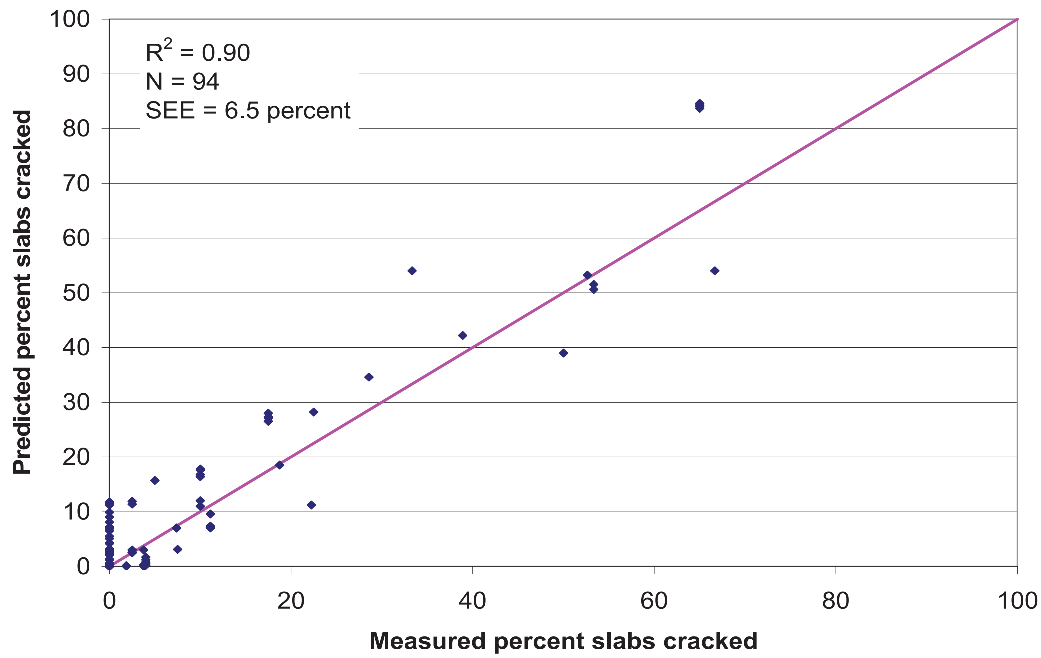

Figure 5-14. Comparison of Measured and Predicted Transverse Cracking for Restored JPCP Resulting from Global Calibration Process

The standard error (or standard deviation of the residual error) for the percentage of slabs cracked prediction global equation is shown in Equation 5-24.

$$s_{e(CR)} = 3.5533(CRACK)^{0.3415} + 0.75 \tag{5-24}$$

where:

$CRACK$ = Predicted transverse cracking based on mean inputs (corresponding to 50% reliability), percentage of slabs

$s_{e(CR)}$ = Standard error of the estimate of transverse cracking at the predicted level of mean cracking

5.4.2 *Mean Transverse Joint Faulting—JPCP*

The mean transverse joint faulting is predicted month by month using an incremental approach. A faulting increment is determined each month and the current faulting level affects the magnitude of increment. The faulting at each month is determined as a sum of the faulting increments from all previous months in the pavement life, starting from the traffic opening date. Use the following equations:

$$Fault_m = \sum_{i=1}^{m} \Delta Fault_i \tag{5-25a}$$

$$\Delta Fault_i = C_{34} \cdot (FAULTMAX_{i-1} - Fault_{i-1})^2 \cdot DE_i \tag{5-25b}$$

$$FAULTMAX_i = FAULTMAX_{i-1} + C_7 \times \frac{\sum_{j=1}^{m} DE_j}{10^6} \times \mathrm{Log}(1 + C_5 \times 5.0^{EROD})^{C_6} \tag{5-25c}$$

$$FAULTMAX_0 = C_{12} \cdot \delta_{curling} \cdot \left[\log\left(1 + C_5 \cdot 5.0^{EROD}\right) \cdot \log\left(\frac{P_{200} \cdot WetDays}{p_s}\right)\right]^{C_6} \quad (5\text{-}25d)$$

where:

$Fault_m$ = Mean joint faulting at the end of month m, in.

$\Delta Fault_i$ = Incremental change (monthly) in mean transverse joint faulting during month i, in.

$FAULTMAX_i$ = Maximum mean transverse joint faulting for month i, in.

$FAULTMAX_0$ = Initial maximum mean transverse joint faulting, in.

DE_i = Differential density of energy of subgrade deformation accumulated during month i (see Equation 5-29a)

$EROD$ = Base/subbase erodibility factor

$\delta_{curling}$ = Maximum mean monthly slab corner upward deflection PCC due to temperature curling and moisture warping

P_S = Overburden on subgrade, lb

P_{200} = Percent subgrade material passing #200 sieve

$WetDays$ = Average annual number of wet days (greater than 0.1-in. rainfall)

$C_{1,2,3,4,5,6,7,12,34}$ = Global calibration constants (C_1 = 0.595, C_2 = 1.636, C_3 = 0.00217, C_4 = 0.00444, C_5 = 250, C_6 = 0.47, C_7 = 7.3, C_8 = 400, and C_{12} and C_{34} are defined by Equations 5-25e and 5-25f). Constants used for restored rigid pavements are: C_1 = 0.6, C_2 = 1.2, C_3 = 0.002125, C_4 = 0.000884, C_5 = 400, C_6 = 0.4, and C_7 = 1.83312)

$$C_{12} = C_1 + C_2 \cdot FR^{0.25} \quad (5\text{-}25e)$$

$$C_{34} = C_3 + C_4 \cdot FR^{0.25} \quad (5\text{-}25f)$$

FR = Base freezing index defined as percentage of time the top base temperature is below freezing (32°F) temperature

For faulting analysis, each passing of an axle causes only one occurrence of critical loading, that is, when DE has the maximum value. Since the maximum faulting development occurs during nighttime when the slab is curled upward, joints are opened, and the load transfer efficiencies are lower, only axle load repetitions applied from 8:00 p.m. to 8:00 a.m. are considered in the faulting analysis.

For faulting analysis, the equivalent linear temperature difference for nighttime is determined for each calendar month as the mean difference between top and bottom PCC surfaces occurring from 8:00 p.m. to 8:00 a.m. The equivalent temperature gradient for each month of the year is then determined as follows:

$$\Delta T_m = \Delta T_{t,m} - \Delta T_{b,m} + \Delta T_{sh,m} + \Delta T_{PCW} \quad (5\text{-}26)$$

where:

ΔT_m = Effective temperature differential for month m

$\Delta T_{t,m}$ = Mean PCC top-surface nighttime temperature (from 8:00 p.m. to 8:00 a.m.) for month m

$\Delta T_{b,m}$ = Mean PCC bottom-surface nighttime temperature (from 8:00 p.m. to 8:00 a.m.) for month m
$\Delta T_{sh,m}$ = For old concrete, equivalent temperature differential due to reversible shrinkage for month m (i.e., shrinkage is fully developed)
ΔT_{PCW} = Equivalent temperature differential due permanent curl/warp

The temperature in the top PCC layer is computed at 11 evenly spaced points through the thickness of the PCC layer at every hour using the available climatic data. These temperature distributions are converted into the equivalent difference of temperatures between the top and bottom PCC surfaces.

The corner deflections due to slab curling and shrinkage warping are determined each month using the effective temperature differential for each calendar month, corresponding effective k-value, and base modulus for the month. The corner deflections are determined using a finite, element-based, neural network, rapid response solution methodology implemented in the AASHTOWare PMED software. The initial maximum faulting is determined using the calculated corner deflections and Equation 5-25d.

Using Equation 5-25c, the maximum faulting is adjusted for the past traffic damage using past cumulative differential energy (i.e., differential energy accumulated from axle-load applications for all months prior to the current month). For each increment and each axle type and axle-load, deflections at the loaded and unloaded corner of the slab are calculated using the neural networks.

The magnitudes of corner deflections of loaded and unloaded slabs are highly affected by the joint LTE. The LTE from aggregate interlock, dowels (if present), and base/subgrade are determined in order to evaluate initial transverse joint LTE. Table 5-8 lists the LTE_{base} values that are included in the AASHTOWare PMED software. The LTE_{agg} and LTE_{dowel} values are explained in latter paragraphs of this section. After the contributions of the aggregate interlock, dowels, and base/subgrade are determined, the total initial joint load transfer efficiency is determined as follows:

$$LTE_{joint} = 100\left[1-(1-LTE_{dowel}/100)(1-LTE_{agg}/100)(1-LTE_{base}/100)\right] \tag{5-27}$$

where:
LTE_{joint} = Total transverse joint LTE, %
LTE_{dowel} = Joint LTE if dowels are the only mechanism of load transfer, %
LTE_{base} = Joint LTE if the base is the only mechanism of load transfer, %
LTE_{agg} = Joint LTE if aggregate interlock is the only mechanism of load transfer, %

The LTE is determined and output for each calendar month can be observed over time to see if it maintains a high level. If the mean nighttime PCC temperature at the mid-depth is below freezing (32°F), then joint LTE for that month is increased. That is done by assigning a 90 percent base LTE for that month. The aggregate interlock and dowel component of LTE are adjusted every month.

Table 5-8. Assumed Effective Base LTE for Different Base Types

Base Type	LTE_{Base}
Aggregate Base	20%
ATB or CTB	30%
Lean Concrete Base	40%

The LTE_{dowel} value (portion of the LTE_{joint} from the mechanism of load transfer from the dowels) is determined in accordance with Equation 5-28a.

$$LTE_{dowel} = \frac{1}{0.01 + 0.012 J_d^{-0.849}} \tag{5-28a}$$

and

$$J_d = J_d^* + (J_o - J_d^*) e^{-DAM_{dowel}} \tag{5-28b}$$

where:

J_d = Non-dimensional dowel stiffness at the time of load application

J_o = Initial non-dimensional dowel stiffness

J^*_d = Critical non-dimensional dowel stiffness

DAM_{dowel} = Damage at the dowel-concrete interface

The dowel damage, DAM_{dowel} is determined as follows:

$$DAM_{dowel} = C_8 \sum_j \frac{J_d(\delta_{loaded} - \delta_{unloaded})(dsp)}{df'_c} \tag{5-28c}$$

where:

C_8 = Coefficient equal to 400

δ_{loaded} = Deflection at the corner of the loaded slab induced by the axle, in.

$\delta_{unloaded}$ = Deflection at the corner of the unloaded slab induced by the axle, in.

dsp = Space between adjacent dowels in the wheel path, in.

f'_c = PCC compressive strength, psi

d = Dowel diameter, in.

Using Equation 5-25c, the maximum faulting is adjusted for the past traffic damage using past cumulative differential energy (i.e., differential energy accumulated from axle load applications for all months prior to the current month). For each increment and for each axle type and axle load, deflections at the loaded and unloaded corner of the slab are calculated using the neural networks. Using these deflections, the differential energy of subgrade deformation, DE, shear stress at the slab corner,τ, and (for doweled joints) maximum dowel bearing stress, σ_b, are calculated:

$$DE = \frac{k}{2}\left(\delta^2_{loaded} - \delta^2_{unloaded}\right) \tag{5-29a}$$

$$\tau = \frac{dsk\left(dsp\right)\left(\delta_{loaded} - \delta_{unloaded}\right)}{h_{PCC}} \tag{5-29b}$$

$$\sigma_b = \frac{\zeta_d\left(\delta_{loaded} - \delta_{unloaded}\right)}{d\left(dsp\right)} \tag{5-29c}$$

$$dsk = k * l * \left[\frac{\left(\dfrac{1}{LTE_{dowel}}\right) - 0.01}{0.012}\right]^{-1.1779} \tag{5-29d}$$

where:

DE = Differential energy, lb/in.

δ_{loaded} = Loaded corner deflection, in.

$\delta_{unloaded}$ = Unloaded corner deflection, in.

AGG = Aggregate interlock stiffness factor

k = Coefficient of subgrade reaction, psi/in.

h_{PCC} = PCC slab thickness, in.

ξ_d = Dowel stiffness factor = $J_d*k*l*dsp$

d = Dowel diameter, in.

dsp = Dowel spacing, in.

J_d = Non-dimensional dowel stiffness at the time of load application

l = Radius of relative stiffness, in.

The incremental loss of shear capacity (Δs)due to repeated wheel load applications within each month is characterized in terms of the width of the transverse joint. This is based on a function derived from the analysis of load transfer test data developed by the Portland Cement Association (PCA). The following loss of shear occurs during the time increment (month):

$$\Delta s = \begin{cases} 0 & \text{If: } jw/h_{PCC} < 0.001 \\ \displaystyle\sum_j \frac{0.005}{1.0 + \left(\dfrac{jw}{h_{PCC}}\right)^{-5.7}} \left(\frac{n_j}{10^6}\right)\left(\frac{\tau_j}{\tau_{ref}}\right) & \text{If: } jw/h_{PCC} < 3.8 \quad (5\text{-}30a) \\ \displaystyle\sum_j \frac{0.068}{1.0 + 6.0 * \left(\dfrac{jw}{h_{PCC}} - 3\right)^{-1.98}} \left(\frac{n_j}{10^6}\right)\left(\frac{\tau_j}{\tau_{ref}}\right) & \text{If: } jw/h_{PCC} > 3.8 \quad (5\text{-}30b) \end{cases}$$

where:

n_j = Number of applied load applications for the current increment by load group j

jw = Joint opening, mils (0.001 in.)

τ_j = Shear stress on the transverse crack from the response model for the load group j, psi, and calculated by Equation 5-30c

$$\tau_j = \frac{AGG*(\delta_{loaded} - \delta_{unloaded})}{h_{PCC}} \tag{5-30c}$$

where:

τ_{ref} = Reference shear stress derived from the PCA test results, psi

$$\tau_{ref} = 111.1* exp\{-exp[0.9988*exp(-0.1089 \log J_{AGG})]\} \tag{5-30d}$$

J_{AGG} = Joint stiffness on the transverse crack computed for the time increment

The total or cumulative loss of shear capacity, S, is determined by Equation 5-30d and based on the total incremental loss of shear capacity, Δs_{total}.

$$S = 0.05(h_{PCC})e^{-0.028\,jw} - \Delta s_{total} \tag{5-30e}$$

The total loss of shear capacity, S, is used to determine the joint stiffness of the transverse crack computed for the time increment, J_{AGG}, in Equation 5-30e.

$$J_{AGG} = 10^{-3.19626 + 16.09737 e^{-e^{-\left(\frac{S-0.35}{0.38}\right)}}} \tag{5-30f}$$

Equation 5-25b determines the faulting increment developed using the current month. The magnitude of the increment depends on the level of maximum faulting, level of faulting at the beginning of the month, and total differential energy, *DE*, accumulated for a month from all axle loads passed from 8:00 p.m. to 8:00 a.m. Using Equation 5-25a, the faulting at the end of the current month is determined. These steps are repeated for the number of months in the pavement design life.

More than one-third of the sections used to calibrate this prediction model were non-doweled. The dowel diameter in the remaining sections varied from 1–1.625 in. A plot of measured versus predicted mean transverse joint faulting based on the global calibration exercise is shown in Figures 5-15 through 5-17. The standard error for the transverse joint faulting global prediction equation is shown in Equation 5-31.

$$s_{e(F)} = 0.07162(Fault)^{0.368} + 0.00806 \tag{5-31}$$

where:

Fault(t) = Predicted mean transverse joint faulting at any given time *t*, in.

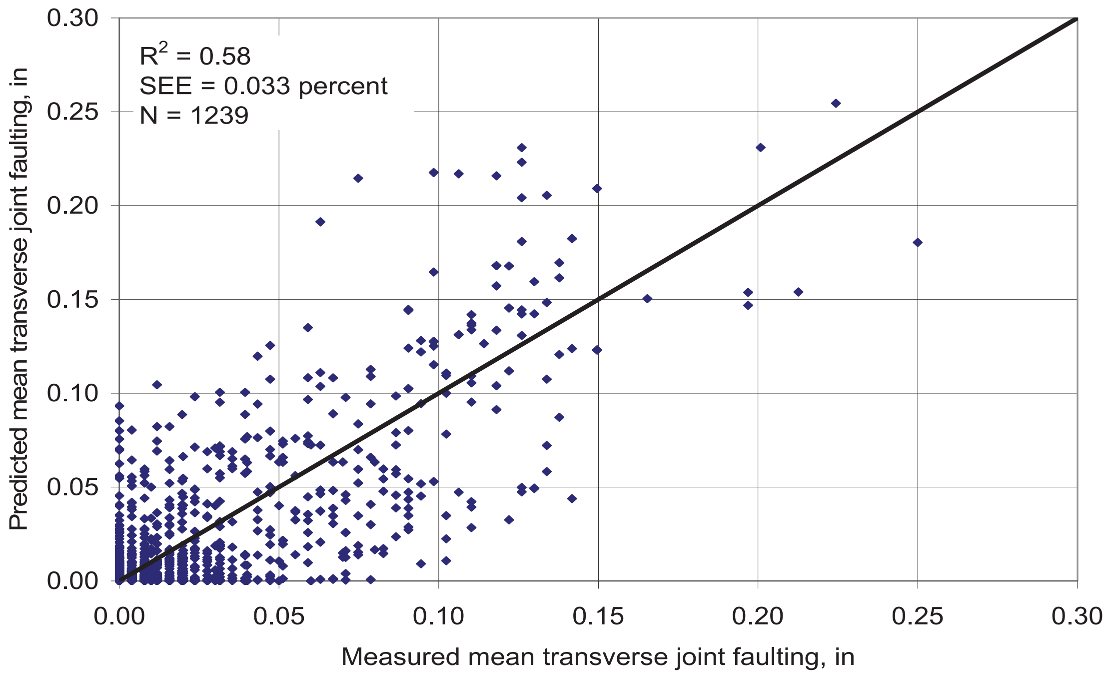

Figure 5-15. Comparison of Measured and Predicted Transverse Joint Faulting for New JPCP Resulting from Global Calibration Process

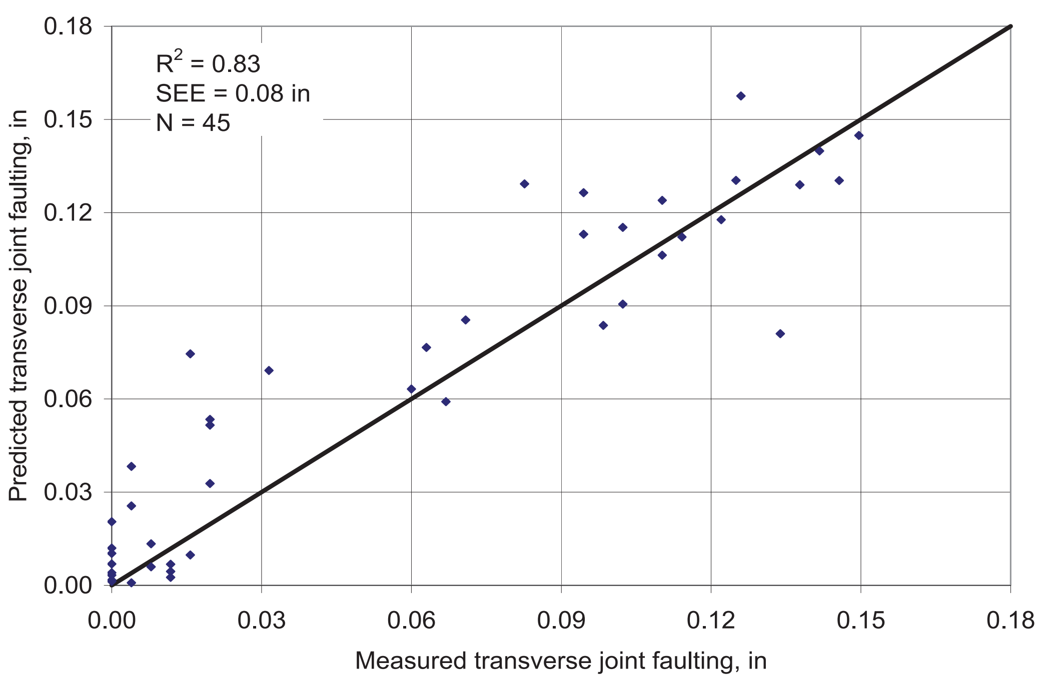

Figure 5-16. Comparison of Measured and Predicted Transverse Joint Faulting for Unbound JPCP Overlays Resulting from Global Calibration Process

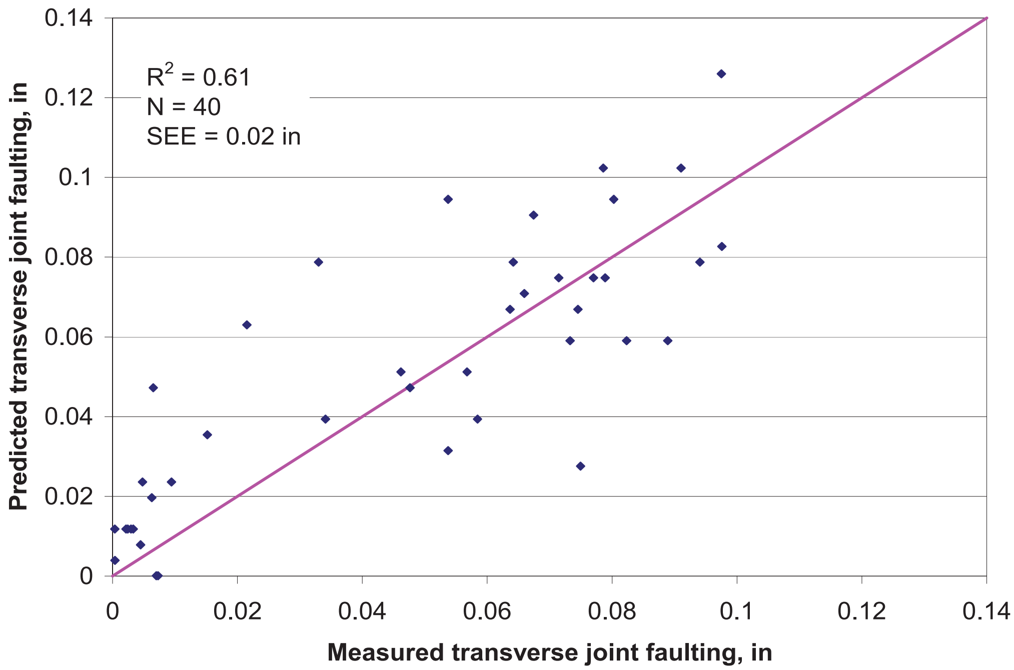

Figure 5-17. Comparison of Measured and Predicted Transverse Joint Faulting for Restored (Diamond Grinding) JPCP Resulting from Global Calibration Process

5.4.3 *CRCP Punchouts*

The following globally calibrated model predicts CRCP punchouts as a function of accumulated fatigue damage due to top-down stresses in the transverse direction:

$$PO = \frac{C_3}{1 + C_4\left(DI_{PO}\right)^{C_5}} \tag{5-32}$$

where:

PO = Total predicted number of medium and high severity punchouts per mile

DI_{PO} = Accumulated fatigue damage (due to slab bending in the transverse direction) at the end of y^{th} year

C_3, C_4, C_5 = Calibration constants (107.73, 2.475, and –0.785, respectively)

Subsection 11.2.3, CRCP Design, identifies the more important factors that affect the number of punchouts and crack spacing, which determine the overall performance of CRCP. The mean crack spacing for the selected trial design and time of construction is calculated in accordance with Equation 5-33.

$$\overline{L} = \frac{\left(f_t - \sigma_{env}\right)}{\frac{f}{2} + \frac{U_m P_{steel}}{c_1 d_b}} \tag{5-33}$$

where:

$\overline{L}$ = Mean transverse crack spacing, in.

f_t = Concrete indirect tensile strength, psi
f = Base friction coefficient
U_m = Peak bond stress, psi
P_{steel} = Percent longitudinal steel
d_b = Reinforcing steel bar diameter, in.
c_1 = First bond stress coefficient
σ_{env} = Tensile stress in the PCC due to environmental curling, psi

The environmental tensile stress in the PCC from the slab curing is calculated in accordance with Equation 5-34:

$$\sigma_{env} = B_{curl}\sigma_o\left(1 - \frac{2D_{steel}}{h_{PCC}}\right) \tag{5-34}$$

where:
H_{PCC} = Slab thickness, in.
D_{steel} = Depth to steel layer, in.
B_{curl} = Bradbury's curling/warping stress coefficient
σ_0 = Westergaard's nominal stress factor based on PCC modulus, Poisson's ratio, unrestrained curling, and warping strain

The damage accumulated at the critical point on top of the slab is calculated for each time increment of the design life. Damage is calculated in the following manner:

- For the given time increment, calculate crack width at the level of steel as a function of drying shrinkage, thermal contraction, and the restraint from reinforcing steel and base friction:

$$cw = Max\left[L\left(\varepsilon_{shr} + \alpha_{PCC}\Delta T_{\varsigma} - \frac{c_2 f_{\sigma long}}{E_{PCC}}\right)(C_c)1000\right] \tag{5-35}$$

where:
cw = Average crack width at the depth of the steel, mils
L = Mean crack spacing based on design crack distribution, in.
ε_{shr} = Unrestrained concrete drying shrinkage at steel depth, $\times 10^{-6}$
α_{PCC} = PCC coefficient of thermal expansion, /°F
ΔT_{ζ} = Drop in PCC temperature from the concrete set temperature at the depth of the steel for construction month, °F
c_2 = Second bond stress coefficient
$f_{\sigma ong}$ = Maximum longitudinal tensile stress in PCC at steel level, psi
E_{PCC} = PCC elastic modulus, psi
C_C = Local calibration constant (C_C = 1 for the global calibration)

- For the given time increment, calculate shear capacity, crack stiffness, and LTE across transverse cracks. LTE is determined as:

$$LTE_{TOT} = 100 * \left\{ 1 - \left[1 - \frac{1}{1 + \log^{-1} \dfrac{0.214 - 0.183\dfrac{a}{l} - \log(J_c) - r_d}{1.18}} \right] \left(1 - \frac{LTE_{Base}}{100} \right) \right\} \tag{5-36}$$

where:

LTE_{TOT} = Total crack LTE due to aggregate interlock, steel reinforcement, and base support, %
l = Radius of relative stiffness computed for time increment i, in.
a = Radius for a loaded area, in.
r_d = Residual dowel-action factor to account for residual load transfer provided by the steel reinforcement = $2.5P_{steel} - 1.25$
LTE_{Base} = Base layer contribution to the LTE across transverse crack, % (Typical values were given in Table 5-6)
J_c = Joint stiffness on the transverse crack for current time increment
P_{steel} = Percent steel reinforcement

- The loss of support for the given time increment is calculated using the base erosion model. The loss of support is a function of base type, quality of base material, precipitation, and age.
- For each load level in each gear configuration or axle-load spectra, the tensile stress on top of slab is used to calculate the number of allowable load repetitions, $N_{i,j}$, due to this load level in this time increment as:

$$\log N_{i,j} = C_1 * \left(\frac{M_{Ri}}{\sigma_{i,j}} \right)^{C_2} - 1 \tag{5-37}$$

where:

M_{Ri} = PCC modulus of rupture at age i, psi
$\sigma_{i,j}$ = Applied stress at time increment i due to load magnitude j, psi
$C_{1,2}$ = Calibration constants (C_1 = 2.0 and C_2 = 1.22)

- The loss in shear capacity and loss in load transfer is calculated at the end of the time increment in order to estimate these parameters for the next time increment. The crack LTE is output monthly for evaluation. A minimum of 90–95 percent is considered good LTE over the design period.

The critical stress at the top of the slab that is transverse and located near a transverse crack was found to be 40–60 in. from the edge (48 in. was used, since this was often the critical location). A crack spacing of 2 ft was used as the critical width after observations that a very high percentage of punchouts were 2 ft or less. This stress is calculated using the neural net models, which are a function of slab thickness, traffic offset from edge, PCC properties, base course properties and thickness, subgrade stiffness, equivalent temperature gradient, and other factors.

Fatigue damage, *FD*, due to all wheel loads in all time increments is calculated (according to Miner's damage hypothesis) by summing the damage over design life in accordance with Equation 5-22a. Once damage is estimated using Equation 5-22a, the corresponding punchouts are computed using the globally calibrated Equation 5-32.

A plot of measured versus predicted CRCP punchouts and statistics from the global calibration is shown in Figure 5-18. The standard error for the CRCP punchouts prediction model is shown in Equation 5-38.

$$s_{e(PO)} = 2.208(PO)^{0.5316} \tag{5-38}$$

where:

PO = Predicted mean medium and high severity punchouts, no./mile

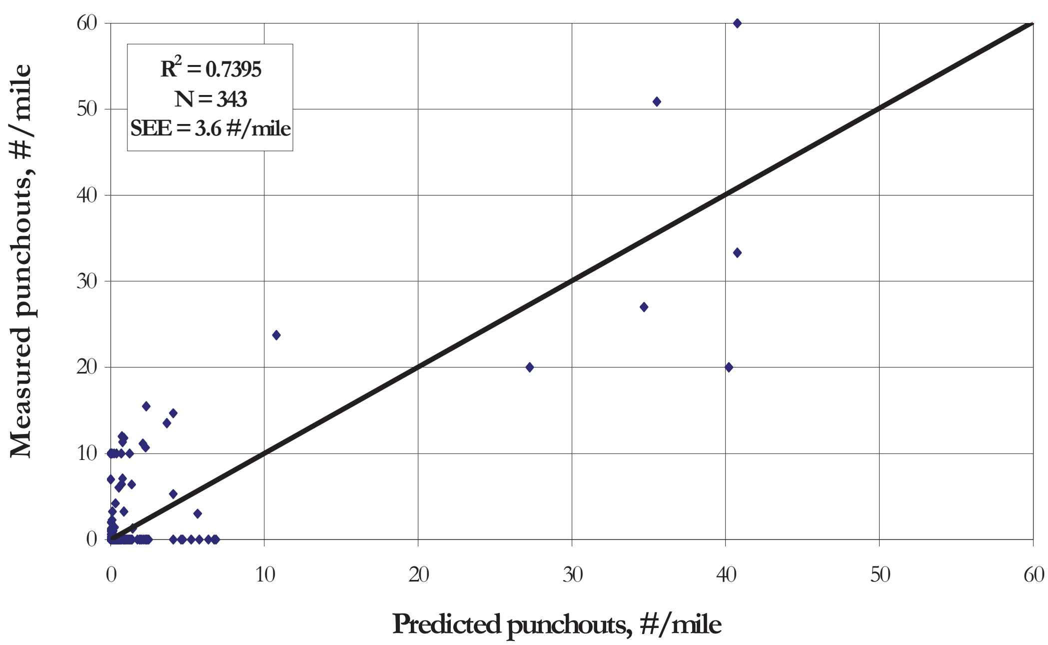

Figure 5-18. Comparison of Measured and Predicted Punchouts for New CRCP Resulting from Global Calibration Process

5.4.4 Longitudinal Slab Cracking—SJPCP on Flexible Pavements

Bottom-up longitudinal fatigue cracking in the wheel paths is predicted as the primary structural distress in accordance with the procedure developed by Li and Vanderbossche (*17*). Critical bending stresses occur when the truck axle approaches the transverse joint of the slabs in both wheel paths. The wheel paths occur between the longitudinal joints (which are typically spaced from

5–8 ft depending on lane width), as illustrated in Figure 5-19. Similar to conventional JPCP design, calculation of critical stresses was done using neural nets (for speed) that require the slab and lower layer to be combined into an "equivalent slab" thickness based on equivalent stresses (load and temperature/moisture gradients) and contact friction between slab and base. This is done monthly as these parameters change over time.

A critical tensile bending stress occurs at the bottom of the slab under the wheel load, which increases when there is a high positive temperature gradient through the slab (the top of the slab is warmer than the bottom of the slab). Repeated loadings of heavy axles under those conditions result in fatigue damage along the bottom transverse joint of the slab (the point of maximum fatigue damage is computed), which eventually results in a longitudinal crack that propagates to the surface of the slab and along the slab. Bottom-up longitudinal cracking is calculated as a percent of the total number of slabs in the wheel paths, which is the output performance criteria used for structural design. This distress is predicted using the following globally calibrated Equation 5-39 for bottom-up longitudinal fatigue cracking:

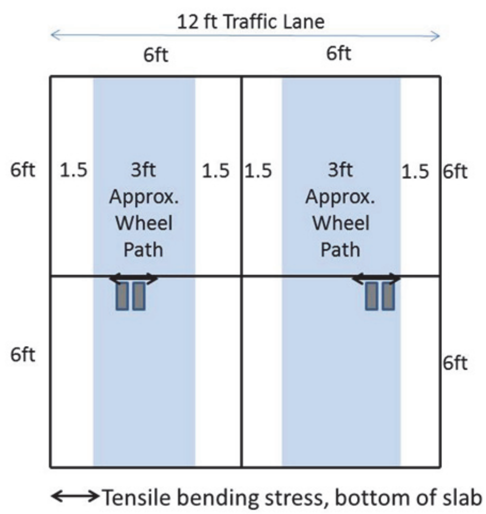

Figure 5-19. Illustration of Proper Location of Longitudinal Joints to Avoid Overlap with Truck Wheel Paths (to Avoid Corner Cracking) and the Resulting Critical Bending Stresses at Bottom of Slab That Are Considered to Limit Longitudinal Fatigue Cracking

$$LCRK = \frac{1}{1 + C_4 \left(DI_F \right)^{C_5}} \tag{5-39}$$

where:

$LCRK$ = Predicted amount of bottom-up longitudinal fatigue cracking, %

DI_F = Fatigue damage calculated using the procedure described in this section (fraction from 0 to >1) at the most critical point along the transverse joint

C_4, C_5 = Global calibration constants (C_4 = 0.40 and C_5 = −2.21)

The fatigue damage calculation is a process of summing damage from each damage increment at several critical points across the bottom of the slab along the transverse joint. The general expression for fatigue damage accumulation considering all critical factors for SJPCP longitudinal cracking is Equation 5-40 and referred to as Miner's hypothesis:

$$DI_F = \sum \frac{n_{i,j,k,l,m,n,o}}{N_{i,j,k,l,m,n,o}} \tag{5-40}$$

where:

DI_F = Total fatigue damage (bottom-up)
$n_{i,j,k,\ldots}$ = Applied number of load applications at condition *i, j, k, l, m, n*
$N_{i,j,k,\ldots}$ = Allowable number of load applications at condition *i, j, k, l, m, n*
i = Age (accounts for change in PCC modulus of rupture and elasticity, slab/AC contact friction)
j = Month (accounts for change in AC dynamic modulus and dynamic subgrade K-Value)
k = Axle type (single, tandem, and tridem for bottom-up cracking)
l = Load level (incremental load for each axle type)
m = Equivalent temperature difference between top and bottom PCC surfaces
n = Traffic offset path (normal distribution)
o = Hourly truck traffic fraction

The applied number of load applications ($n_{i,j,k,l,m,n}$) is the actual number of axle type, *k*, of load level, *l*, that passed through traffic pattern, *n*, under each condition *i*, *j*, and *m* (age, season, and temperature difference). The allowable number of load applications (to cracking $N_{i,j,k,l,m,n}$) is the number of load cycles at which fatigue cracking is expected on average and is a function of the applied stress and PCC strength. The allowable number of load applications ($N_{i,j,k,l,m,n}$) to cracking is determined using Equation 5-41 and applied to the PCC field fatigue Equation 5-40 to calculate the DI:

$$\log\left(N_{i,j,k,l,m,n}\right) = C_1 \cdot \left(\frac{MR_i}{\sigma_{i,j,k,l,m,n}}\right)^{C_2} - 0.4371 \tag{5-41}$$

where:

$N_{i,j,k,\ldots}$ = Allowable number of load applications at condition *i, j, k, l, m, n*
MR_i = PCC modulus of rupture at age *i*, psi
$\sigma_{i,j,k,\ldots}$ = Applied stress at condition *i, j, k, l, m, n*
C_1 = Calibration constant, 2.0
C_2 = Calibration constant, 1.22

A plot of measured longitudinal cracking versus the computed fatigue damage at the bottom of the PCC slab is shown in Figure 5-20. This plot follows the typical S-shaped curve and is termed the transfer function between slab longitudinal fatigue cracking and cumulative fatigue damage at the bottom of the slab.

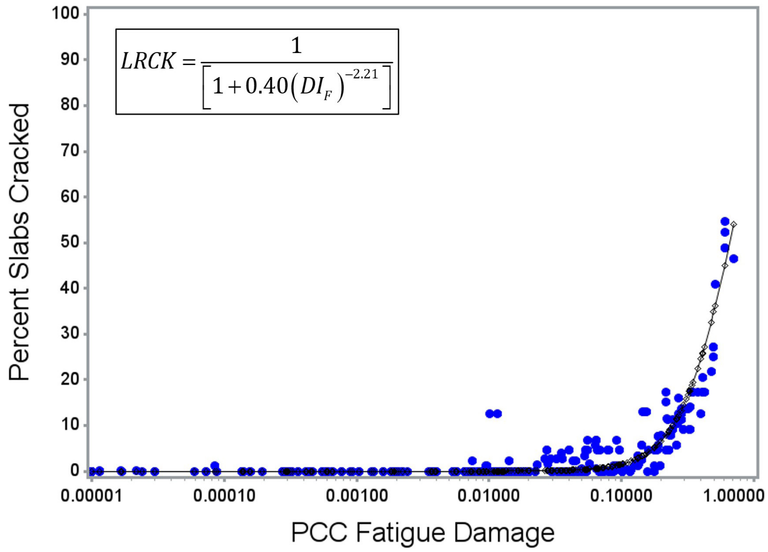

Figure 5-20. Measured Longitudinal Fatigue Cracking (LCRK) versus PCC Fatigue Damage (DIF) at Bottom of PCC Slab

A plot of measured versus predicted longitudinal cracking and the statistics resulting from the global calibration process is shown in Figure 5-21. Statistical hypothesis testing at the 0.05 significance level for the slope of the line (equal to 1.0), intercept (equal to 0), and for prediction bias (either over or under prediction) were not significant.

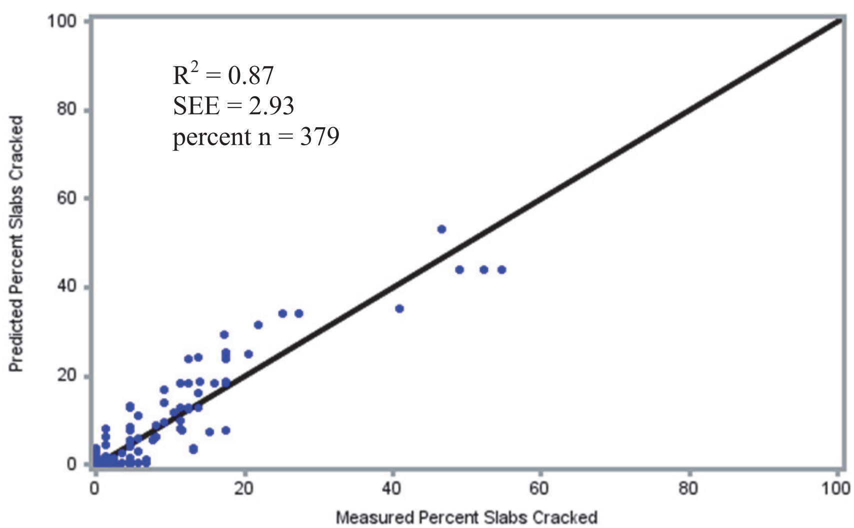

Figure 5-21. Comparison of Measured and Predicted Percentage SJPCP Overlay Slabs Longitudinally Cracked Resulting from Global Calibration Process

The standard error (or standard deviation of the residual error) for the percentage of slabs longitudinally cracked prediction global equation is shown in Equation 5-42.

$$s_{e(LCRACK)} = 3.5522 * LCRACK^{0.4315} + 0.5000 \tag{5-42}$$

where:

$LCRACK$ = Predicted longitudinal fatigue cracking based on mean inputs (corresponding to 50% reliability), percentage of slabs

$s_{e(LCRACK)}$ = Standard error of the estimate of longitudinal fatigue cracking at the predicted level of mean longitudinal cracking

5.4.5 *Smoothness—JPCP*

In AASHTOWare Pavement ME Design, smoothness is predicted as a function of the initial as-constructed profile of the pavement and any change in the longitudinal profile over time and traffic due to distresses and foundation movements. The IRI model was calibrated and validated using LTPP field data to assure that it would produce valid results under a variety of climatic and field conditions. The following is the final calibrated model:

$$IRI = IRI_I + J1 * CRK + J2 * SPALL + J3 * TFAULT + J4 * SF \tag{5-43a}$$

where:

IRI = Predicted IRI, in./mi

IRI_I = Initial smoothness measured as IRI, in./mi

CRK = Percent slabs with transverse cracks (all severities)

$SPALL$ = Percentage of joints with spalling (medium and high severities)

$TFAULT$ = Total joint faulting cumulated per mi, in.

$J1$ = 0. 8203

$J2$ = 0.4417

$J3$ = 1.4929

$J4$ = 25.24

SF = Site factor

$$SF = AGE \ \left(1 + 0.5556 * FI\right) \ \left(1 + P_{200}\right) * 10^{-6} \tag{5-43b}$$

where:

AGE = Pavement age, yr

FI = Freezing index, °F-days

P_{200} = Percent subgrade material passing No. 200 sieve

The transverse cracking and faulting are obtained using the models described earlier. The transverse joint spalling is determined in accordance with Equation 5-43c, which was calibrated using LTPP and other data.

$$SPALL = \left[\frac{AGE}{AGE + 0.01}\right]\left[\frac{100}{1 + 1.005^{(-12 * AGE + SCF)}}\right] \tag{5-43c}$$

where:

$SPALL$ = Percentage joints spalled (medium- and high-severities)

AGE = Pavement age since construction, yr
SCF = Scaling factor based on site, design, and climate

$$\begin{aligned} SCF = {} & -1400 + 350 \cdot AC_{PCC} \cdot (0.5 + PREFORM) + 43.4 f_c'^{\,0\ 4} \\ & - 0.2 \left(FT_{cycle} \cdot AGE \right) + 43\, H_{PCC} - 536\, WC_{PCC} \end{aligned} \tag{5-43d}$$

AC_{PCC} = PCC air content, %
AGE = Time since construction, yr
$PREFORM$ = 1 if preformed sealant is present; 0 if not
f'_c = PCC compressive strength, psi
FT_{cycle} = Average annual number of freeze-thaw cycles
H_{PCC} = PCC slab thickness, in.
WC_{PCC} = PCC water/cement ratio

Model Statistics for Equation 5-43d are listed below:
R^2 = 78 %
SEE = 6.8 %
N = 179

A plot of measured versus predicted IRI values (smoothness) for new JPCP and the statistics from the global calibration is shown in Figure 5-22. The standard error for the initial JPCP IRI is 5.4 (in./mi). The equation for the standard error of predicted mean JPCP is shown in Equation 5-44.

$$s_{eJCPC\_IRI\_model} = 29.03 \ln(IRI) - 103.8 \tag{5-44}$$

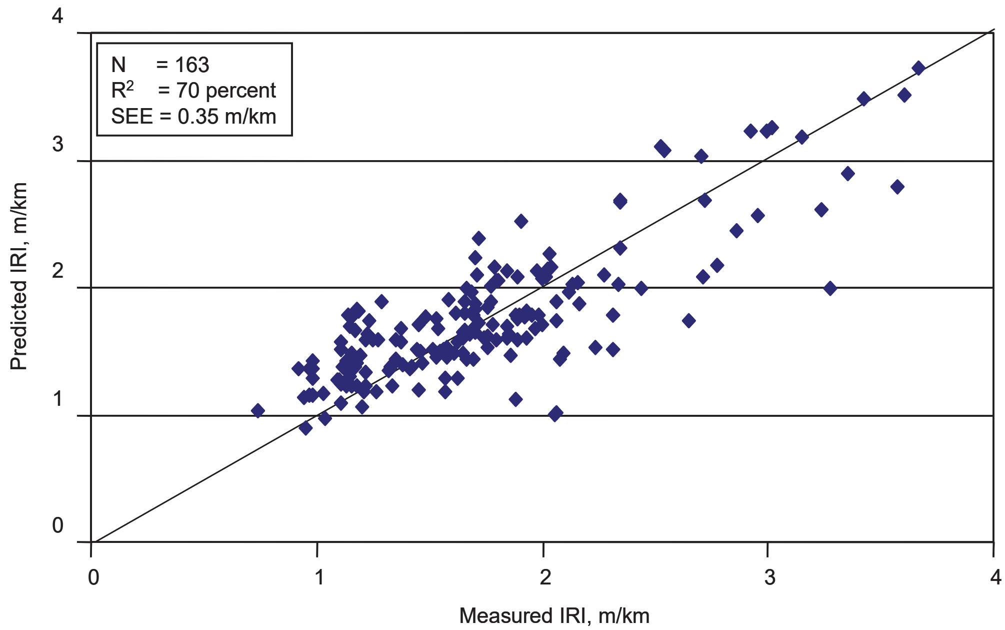

Figure 5-22. Comparison of Measured and Predicted IRI Values for New JPCP Resulting from Global Calibration Process

5.4.6 *Smoothness—CRCP*

Smoothness change in CRCP is the result of a combination of the initial as-constructed profile of the pavement and any change in the longitudinal profile over time and traffic due to the development of distresses and foundation movements. Key distresses affecting the IRI for CRCP include punchouts. The global IRI model for CRCP is given as follows:

$$IRI = IRI_I + C_1 \cdot PO + C_2 \cdot SF \tag{5-45a}$$

where:

IRI_I = Initial IRI, in./mi
PO = Number of medium and high severity punchouts/mi
C_1 = 3.15
C_2 = 28.35
SF = Site factor

$$SF = AGE \cdot (1 + 0.556FI) \cdot (1 + P_{200}) * 10^{-6} \tag{5-45b}$$

where:

AGE = Pavement age, yr
FI = Freezing index, °F days
P_{200} = Percent subgrade material passing No. 200 sieve

A plot of measured versus predicted IRI values for new CRCP and the statistics from the global calibration process is shown in Figure 5-22. The standard error for the initial CRCP

IRI is 5.4 (in./mi). The equation for the standard error of predicted mean CRCP is shown in Equation 5-44.

$$s_{eCRCP\_IRI\_model} = 7.08\ln(IRI) - 11 \qquad (5\text{-}46)$$

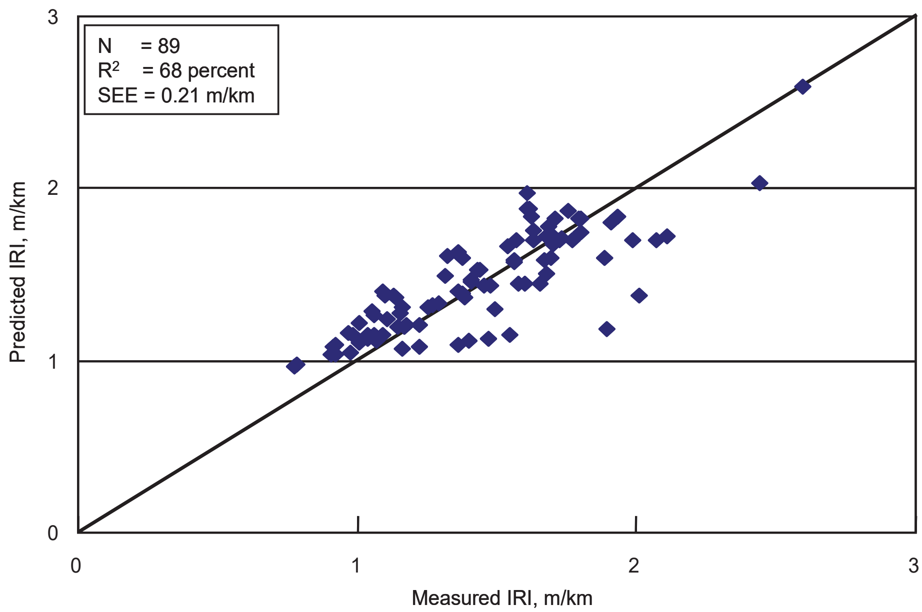

Figure 5-23. Comparison of Measured and Predicted IRI Values for New CRCP Resulting from Global Calibration Process

This page intentionally left blank.

Table 9-8. Models Relating Material Index and Strength Properties to M_r **(21)**

Strength/ Index Property	Model	Comments	Test Standard
CBR	$M_r = 2555(CBR)^{0.64}$ M_r, psi	CBR = California Bearing Ratio, %	AASHTO T 193, "The California Bearing Ratio"
R-value	$M_r = 1155 + 555R$ M_r, psi	R = R-value	AASHTO T 190, "Resistance R-Value and Expansion Pressure of Compacted Soils"
AASHTO layer coefficient	$M_r = 30{,}000\left(\frac{a_i}{0.14}\right)$ M_r, psi	a_i = AASHTO layer coefficient	*AASHTO Guide for the Design of Pavement Structures*
PI and gradation*	$CBR = \frac{75}{1+0.278\left(P_{200}PI\right)}$	P_{200} = percent passing No. 200 sieve size PI = plasticity index, %	AASHTO T 27, "Sieve Analysis of Coarse and Fine-Aggregates" AASHTO T 90, "Determining the Plastic Limit and Plasticity Index of Soils"
DCP*	$CBR = \frac{292}{DCP^{1.12}}$	CBR = California Bearing Ratio, % DCP = DCP index, mm/blow	ASTM D6951, "Standard Test Method for Use of the Dynamic Cone Penetrometer in Shallow Pavement Applications"

* Estimates of CBR are used to estimate M_r.

Interface Friction between Bound Layers

Layer interface friction is an input parameter to the AASHTOWare PMED, but is difficult to define and measure. Cores and visual surveys are used to determine if debonding exists along the project. Slippage cracks and two adjacent layers separating during the coring process may be a result of low interface friction between two AC layers. If these conditions are found to exist along a project, the designer could consider assuming no bond or a low interface friction during the rehabilitation design using the AASHTOWare PMED software, if those layers are to remain in place and not be milled or removed.

All of the global calibration efforts for flexible pavements, however, were completed assuming full friction between all layers—an interface friction value of 1.0 in the AASHTOWare PMED software. This value could be used unless debonding is found. Interface friction values less than 1.0 will increase rutting and cracking of the AC layers. The decrease in rutting and cracking of AC is minimal until the condition of full bond, a value of 1.0, is used. Thus, friction can be defined for just two conditions without significantly affecting the accuracy of the answer—fully bonded (a value of 1.0) or no bond (a value of 0). It should be noted that incomplete bonding is a condition that should be limited and that the use of milling down to a stable layer is recommended in practice.

JPCP allows the user to define the PCC-base contact friction with a simple true/false statement. A statement of false designates no contact friction. A statement of true designates no slippage between layers and requires the user to input "Months until friction loss." Calibration results for new or reconstructed JPCP showed that full contact friction existed over the life of the pavements for all base types, with the exception of CTB or lean concrete where extraordinary efforts were made to debond the layers. For this situation, the months of full contact friction were reduced to a range of 0–100 years, with a default value equal to the design life, to match the cracking exhibited. For new and reconstructed PCC designs, full friction should be assumed, unless debonding techniques are specified and confirmed through historical pavement construction records and defaults to 20 years, based on design life.

For rehabilitation of JPCP (CPR and overlays), full contact friction is input over the rehabilitation design life when cores through the base course show that an interface bond exists. Otherwise, the two layers are considered to have zero friction over the design life.

Edge Drains

If the existing pavement has subsurface drains that remain in place, the outlets need to be found and inspected. Mini-cameras are used to inspect the edge drains and lateral lines to verify that they are free-flowing and not restricting the removal of water from the pavement structure.

9.2.8 Laboratory Tests for Materials Characterization of Existing Pavements

Table 9-6 provided a listing of the materials properties that must be measured to determine the inputs to the AASHTOWare PMED and to specify the condition of the existing pavement layers. Chapter 10 includes details on the testing of different pavement layers that is required in support of the MEPDG.

It is recommended that a sufficient laboratory test program to estimate the material properties of each layer is established as these are required inputs in accordance with the MEPDG. The following section lists the type of samples needed for measuring the properties of the in-place layers (refer to Table 9-5).

AC Mixtures and Layers

- **Volumetric Properties** (air voids, asphalt content, gradation): Air voids (bulk specific and maximum theoretical specific gravities) of existing layers are obtained from as-built project records and used as input for Levels 1 and 2 (Table 9-2). The average effective asphalt content by volume and gradation measured during construction are used for the rehabilitation design. Selected cores recovered from the project are used to measure these properties whenever this volumetric data is unavailable from construction records. Samples recovered from 6-in.-diameter cores are used to ensure a sufficient amount of material for gradation tests. The ignition oven is used to measure the asphalt content (in accordance with AASHTO T 308 or an equivalent procedure) and then the gradation on their unique needs and testing capabilities. The following provides more detailed discussion on determining the volumetric properties that are used to estimate these input parameters for new AC mixtures.

- **Air Voids (AASHTO T 269),** V_a**:** The air voids at construction need to represent the average, in-place air voids expected after the AC has been compacted with the rollers, but prior to opening the roadway to truck traffic. This value will be unavailable during structural design because it has yet to be produced. It is recommended that this value be obtained from previous construction records for similar mixtures or the designer could enter the target value from the project specifications.
- **Bulk Specific Gravity of the Combined Aggregate Blend (AASHTO T 84 and T 85),** G_{sb}**:** This value is dependent on the type of aggregates used in the AC and gradation. Most agencies will have an expected range of this value from previous mixture designs for the type of aggregates used, their source, and combined gradation (type of mixture dependent) specified for the project.
- **Maximum Specific Gravity of Mixture (AASHTO T 209),** G_{mm}**:** This value is dependent on the type of aggregate, gradation, and asphalt content used in the AC. Most agencies will have an expected range of this value from previous mixture designs using the aggregate source and gradation (type of mixture) specified for the project. The maximum specific gravity can be calculated from the component properties if no historical information exists for the AC mixture specified for the project.
- **Voids in Mineral Aggregate,** VMA**:** VMA is an input for thermal cracking predictions and determination of other volumetric properties. The mixture VMA needs to represent is the condition of the mixture after it has been compacted with the rollers, but prior to opening the roadway to truck traffic. This value will be unavailable during structural design because it has yet to be produced and placed. It is recommended that the value be calculated from other volumetric properties that are obtained from construction records for similar type mixtures, aggregate sources, and gradations.
- **Effective Asphalt Content by Volume,** V_{be}**:** The effective asphalt content by volume needs to represent the in-place asphalt content, after the mix has been placed by the paver. This value will be unavailable during structural design because it has yet to be produced. It is recommended that the value be calculated from the other volumetric properties, as shown in Table 10-3.

Table 10-3. Recommended Input Parameters and Values; Limited or No Testing Capabilities for AC (Input Levels 2 and/or 3)

Measured Property	Input Levels 2 or 3
Dynamic modulus, E_{HMA} (new AC)	• No dynamic modulus, E_{AC}, laboratory testing required. • Use MEPDG E_{AC} predictive equation. Inputs are gradation, asphalt viscosity, loading frequency, air void content, and effective bitumen content by volume. Input variables may be obtained through testing of lab prepared mix samples or from agency historical records. • Use typical *Ai-VTS-* values based on asphalt binder grade (PG, viscosity, or penetration grades).
Dynamic modulus, E_{HMA} (existing AC layer)	• No dynamic modulus, E_{AC}, laboratory testing required. • Use MEPDG E_{AC} predictive equation. Inputs are gradation, bitumen viscosity, loading frequency, air void content, and effective bitumen content by volume. Input variables may be obtained through testing of extracted cores or from agency historical records. • Use typical *Ai-VTS-* values based on asphalt binder grade (PG, viscosity, or penetration grades). • Determine existing pavement condition rating (excellent, good, fair, poor, or very poor).
Tensile strength, *TS* (new AC surface; not required for existing AC layers)	Use MEPDG regression equation: $TS(\text{psi}) = 7416.712 - 114.016*Va - 0.304*Va^2 - 122.592*VFA + 0.704*VFA^2 + 405.71*\log 10(Pen77) - 2039.296*\log 10(A)$ where: *TS* = Indirect tensile strength at 14°F, psi *Va* = HMA air voids, as-constructed, % *VFA* = Voids filled with asphalt, as-constructed, % *Pen77* = Asphalt penetration at 77°F, mm/10 *A* = Asphalt viscosity-temperature susceptibility intercept Input variables may be obtained through testing of lab prepared mix samples, extracted cores (for existing pavements), or from agency historical records.

Continued on next page.

Table 10-3. Recommended Input Parameters and Values; Limited or No Testing Capabilities for AC (Input Levels 2 and/or 3), *continued*

Measured Property	Input Levels 2 or 3
Creep compliance, $D(t)$ (new AC surface; not required for existing AC layers)	Use MEPDG regression equation: $$D(t) = D_1 * t^m$$ $$\log(D_1) = -8.524 + 0.01306 * T + 0.7957 * \log10(Va) + 2.0103 * \log10(VFA) - 1.923 * \log10(A)$$ $$m = 1.1628 - 0.00185 * T - 0.04596 * Va - 0.01126 * VFA + 0.00247 * Pen77 + 0.001683 * T * Pen77^{0.4605}$$ where: t = Time, months T = Temperature at which creep compliance is measured, °F Va = AC air voids, as-constructed, % VFA = Voids filled with asphalt, as-constructed, % $Pen77$ = Asphalt penetration at 77°F, mm/10 A = Asphalt viscosity-temperature susceptibility intercept Input variables may be obtained through testing of lab prepared mix samples, extracted cores (for existing pavements), or from agency historical records.
Air voids	Use as-constructed mix type specific values available from previous construction records.
Effective volumetric asphalt content	Use as-constructed mix type specific values available from previous construction records. The percent asphalt content by weight is typically reported in mixture design and construction records. (The effective asphalt content by volume is equal to the VMA minus the air voids.)
Total unit weight	Use as-constructed mix type specific values available from previous construction records.

**Note*: AASHTOWare PMED software computes input Levels 2 and 3 dynamic modulus, tensile strength, creep compliance, etc. internally once; all the required input variables required by the various equation are provided.

Continued on next page.

Table 10-3. Recommended Input Parameters and Values; Limited or No Testing Capabilities for AC (Input Levels 2 and/or 3), *continued*

<table>
<tr><th>Measured Property</th><th>Recommended Level 3 Input</th></tr>
<tr><td>Poisson's ratio</td><td>Use a predictive equation based on temperature included in the MEPDG for new AC mixtures and the typical values listed below for the existing AC layers:
<table>
<tr><th>Reference Temperature °F</th><th>Dense-Graded AC (Level 3)
$\mu_{typical}$</th><th>Open-Graded AC (Level 3)
$\mu_{typical}$</th></tr>
<tr><td>< 0°F</td><td>0.15</td><td>0.35</td></tr>
<tr><td>0–40°F</td><td>0.20</td><td>0.35</td></tr>
<tr><td>40–70°F</td><td>0.25</td><td>0.40</td></tr>
<tr><td>70–100°F</td><td>0.35</td><td>0.40</td></tr>
<tr><td>100–130°F</td><td>0.45</td><td>0.45</td></tr>
<tr><td>>130°F</td><td>0.48</td><td>0.45</td></tr>
</table>
</td></tr>
<tr><td>Surface shortwave absorptivity</td><td>Use AASHTOWare Pavement ME Design default of 0.85.</td></tr>
<tr><td>Thermal conductivity</td><td>Typical values for asphalt concrete range from 0.244–2.0 Btu/(ft)(hr)(°F). Use the default value set in the program—1.25 Btu/(ft)(hr)(°F).</td></tr>
<tr><td>Heat capacity</td><td>Typical values for asphalt concrete range from 0.1–0.50 Btu/(lb)(°F). Use the default value set in the program—0.28 BTU/lb.-°F</td></tr>
<tr><td>Coefficient of thermal contraction</td><td>Use the MEPDG predictive equation shown below:
$$L_{MIX} = \frac{VMA * B_{ac} + V_{AGG} * B_{AGG}}{3 * V_{TOTAL}}$$
where:
L_{MIX} = Linear coefficient of thermal contraction of the AC mixture (1/°C)
B_{ac} = Volumetric coefficient of thermal contraction of the asphalt cement in the solid state (1/°C)
B_{AGG} = Volumetric coefficient of thermal contraction of the aggregate (1/°C)
VMA = Volume of voids in the mineral aggregate, % (equals percent volume of air voids plus percent volume of asphalt cement, minus percent volume of absorbed asphalt cement)
V_{AGG} = Volume of aggregate in the mixture, %
V_{TOTAL} = 100%</td></tr>
</table>

Continued on next page.

Table 10-4. PCC Material Input Level 1 Parameters and Test Protocols for New and Existing PCC, *continued*

Design Type	Measured Property	Source of Data		Recommended Test Protocol and/or Data Source
		Test	Estimate	
Existing intact and fractured PCC	Elastic modulus	X		ASTM C469 (extracted cores) AASHTO T 256 (non-destructive deflection testing)
	Poisson's ratio	X		ASTM C469 (extracted cores)
	Flexural strength	X		AASHTO T 97 (extracted cores)
	Unit weight	X		AASHTO T 121 (extracted cores)
	Surface shortwave absorptivity		X	National test protocol not available. Use AASHTOWare Pavement ME Design defaults
	Thermal conductivity	X		ASTM E1952 (extracted cores)
	Heat capacity	X		ASTM D2766 (extracted cores)

Table 10-5. Recommended Input Parameters and Values; Limited or No Test Capabilities for PCC Materials (Input Levels 2 or 3)

<table>
<tr><th>Measured Property</th><th>Recommended Input Levels 2 and 3</th></tr>
<tr><td>New PCC elastic modulus and flexural strength</td><td>

28-day flexural strength and 28-day PCC elastic modulus, or
28-day compressive strength and 28-day PCC elastic modulus, or
28-day flexural strength only, or
28-day compressive strength only

</td></tr>
<tr><td>Existing intact PCC elastic modulus</td><td>Based on the pavement condition, select typical modulus values from the range of values given below:
<table>
<tr><th>Qualitative Description of Pavement Condition</th><th>Typical Modulus Ranges, psi</th></tr>
<tr><td>Adequate</td><td>3–4 × 10^6</td></tr>
<tr><td>Marginal</td><td>1–3 × 10^6</td></tr>
<tr><td>Inadequate</td><td>0.3–1 × 10^6</td></tr>
</table>
</td></tr>
<tr><td>Existing fractured PCC elastic modulus</td><td>The three common methods of fracturing PCC slabs include crack and seat, break and seat, and rubblization. In terms of materials characterization, cracked and seated or broken and seated PCC layers are considered a separate category from rubblized layers. At Level 3, typical modulus values may be adopted for design (see below):
<table>
<tr><th>Fractured PCC Layer Type</th><th>Typical Modulus Ranges, psi</th></tr>
<tr><td>Crack and Seat or
Break and Seat</td><td>150,00–1,000,000</td></tr>
<tr><td>Rubblized</td><td>50,000–150,000</td></tr>
</table>
</td></tr>
</table>

Continued on next page.

Table 10-5. Recommended Input Parameters and Values; Limited or No Test Capabilities for PCC Materials (Input Levels 2 or 3), *continued*

<table>
<tr><th>Measured Property</th><th>Recommended Input Levels 2 and 3</th></tr>
<tr><td>Poisson's ratio</td><td>Poisson's ratio for new PCC typically ranges between 0.10 and 0.21, with a value of 0.20 the default value assumed for PCC design. See below for typical Poisson's ratio values for PCC materials.
<table>
<tr><th>PCC Materials</th><th>Input Level 3 μtypical</th></tr>
<tr><td>PCC Slabs (newly constructed or existing)</td><td>0.20</td></tr>
<tr><td>Fractured Slab:
Crack/Seat
Break/Seat
Rubblized</td><td>
0.20
0.20
0.30</td></tr>
</table></td></tr>
<tr><td>Unit weight</td><td>Select agency historical data or from the typical range for normal weight concrete: 140–160 lb/ft^3</td></tr>
<tr><td>Coefficient of thermal expansion</td><td>Select agency historical values or typical values based on PCC coarse aggregate type.
<table>
<tr><th>Aggregates Type</th><th>Coefficient of Thermal Expansion (10^{-6}/°F)</th></tr>
<tr><td>Andesite</td><td>4.3</td></tr>
<tr><td>Basalt</td><td>4.3</td></tr>
<tr><td>Diabase</td><td>4.6</td></tr>
<tr><td>Gabbro</td><td>4.4</td></tr>
<tr><td>Granite</td><td>4.7</td></tr>
<tr><td>Schist</td><td>4.4</td></tr>
<tr><td>Dolomite</td><td>5.0</td></tr>
<tr><td>Limestone</td><td>4.3</td></tr>
<tr><td>Quartzite</td><td>5.2</td></tr>
<tr><td>Sandstone</td><td>5.3</td></tr>
<tr><td>Expanded shale</td><td>4.5</td></tr>
</table>
Where coarse aggregate type is unknown, use MEPDG default value of 4.4×10^{-6}/°F</td></tr>
<tr><td>Surface shortwave absorptivity</td><td>Use the MEPDG default value of 0.85</td></tr>
<tr><td>Thermal conductivity</td><td>Typical values for PCC range from 0.2–2.0 Btu/(ft)(hr)(°F). Use the MEPDG default value—1.25 Btu/(ft)(hr)(°F).</td></tr>
<tr><td>Heat capacity</td><td>Typical values for PCC range from 0.1–0.50 Btu/(lb)(°F). Use the MEPDG default value—0.28 BTU/lb.-°F.</td></tr>
</table>

Continued on next page.

Table 10-5. Recommended Input Parameters and Values; Limited or No Test Capabilities for PCC Materials (Input Levels 2 or 3), *continued*

Measured Property	Recommended Input Levels 2 and 3
PCC set temperature	Zero stress temperature, T_z, can be input directly or can be estimated from monthly ambient temperature and cement content using the equation shown below: $T_z = (C_C*0.59328*H*0.5*1000*1.8/(1.1*2400) + MMT)$ where: T_z = PCC set temperature (allowable range: 70–212°F) C_C = Cementitious content, lb/yd^3 $H = -0.0787+0.007*MMT-0.00003*MMT^2$ MMT = Mean monthly temperature for month of construction, °F An illustration of the zero stress temperatures for different mean monthly temperatures and different cement contents in the PCC mix design is presented below:

Mean Monthly Temperature, °F	*H*	Cement Content, lbs/cy 400	500	600	700
40	0.1533	52	56	59	62
50	0.1963	66	70	74	78
60	0.2333	79	84	88	93
70	0.2643	91	97	102	107
80	0.2893	103	109	115	121
90	0.3083	115	121	127	134
100	0.3213	126	132	139	145

Measured Property	Recommended Level 3 Input
Cement type	Estimate based on agency practices.
Cementitious material content	Estimate based on agency practices.
Water to cement ratio	Estimate based on agency practices.
Aggregate type	Estimate based on agency practices.
Curing method	Estimate based on agency practices.
Ultimate shrinkage	Estimate using MEPDG prediction equation.
Reversible shrinkage	Use MEPDG global default of 50 percent unless more accurate information is available.
Time to develop 50 percent of ultimate shrinkage	Use MEPDG global default of 35 days unless more accurate information is available.

Note: Project specific testing is not required at Level 3. Historical agencies test values assembled from past construction with tests conducted using the list protocols.

Table 10-6. Chemically Stabilized Materials Input Level 1 Requirements and Test Protocols for New and Existing Chemically Stabilized Materials

Design Type	Material Type	Measured Property	Source of Data		Recommended Test Protocol and/or Data Source
			Test	Estimate	
New	Lean concrete and cement-treated aggregate	Elastic modulus	X		ASTM C469
		Flexural strength (only required when used in AC pavement design)	X		AASHTO T 97
	Lime-cement-fly ash stabilized material	Resilient modulus		X	No test protocols available. Estimate using Levels 2 and 3.
	Soil cement	Resilient modulus	X		Mixture Design and Testing Protocol (MDTP) in conjunction with AASHTO T 307
	Lime stabilized soil	Resilient modulus	X		Mixture Design and Testing Protocol (MDTP) in conjunction with AASHTO T 307
	All	Unit weight		X	No testing required. Estimate using Levels 2 and 3.
		Poisson's ratio		X	No testing required. Estimate using Levels 2 and 3.
		Thermal conductivity	X		ASTM E1952
		Heat capacity	X		ASTM D2766
		Surface short wave absorptivity		X	No test protocols available. Estimate using Levels 2 and 3.
Existing	All	FWD backcalculated modulus	X		AASHTO T 256 & ASTM D5858 (see Section 9.3.4)
		LTE Transverse Cracks	X		AASHTO T 256 & ASTM D5858 (see Section 9.3.4)
	All	Unit weight		X	No testing required. Estimate using Levels 2 and 3.
		Poisson's ratio		X	No testing required. Estimate using Levels 2 and 3.
		Thermal conductivity	X		ASTM E1952 (cores)
		Heat capacity	X		ASTM D2766 (cores)
		Surface short wave absorptivity		X	No test protocols available. Estimate using Levels 2 and 3.

Table 10-7. Recommended Input Levels 2 and 3 Parameters and Values for Chemically Stabilized Material Properties

<table>
<tr><th>Required Input</th><th>Recommended Input Level</th></tr>
<tr><td>Elastic/
resilient modulus</td><td>Use unconfined compressive strength (f'_c or q_u) in psi of lab samples or extracted cores converted into elastic/resilient modulus by the following:
<table>
<tr><th>Material</th><th>Relationship for Modulus</th><th>Test Method</th></tr>
<tr><td>Lean concrete and cement treated aggregate</td><td>$E = 57000(f'_c)^{0.5}$</td><td>AASHTO T 22</td></tr>
<tr><td>Open graded cement stabilized aggregate</td><td>Use input Level 3</td><td>None</td></tr>
<tr><td>Lime-cement-fly ash</td><td>$E = 500 + q_u$</td><td>ASTM C593</td></tr>
<tr><td>Soil cement</td><td>$E = 1200(q_u)$</td><td>ASTM D1633</td></tr>
<tr><td>Lime stabilized soil</td><td>$M_r = 0.124(q_u) + 9.98$</td><td>ASTM D5102</td></tr>
</table>
or
Select typical E and M_r values in psi as follows:
<table>
<tr><td>Lean concrete, E</td><td>2,000,000</td></tr>
<tr><td>Cement stabilized aggregate, E</td><td>1,000,000</td></tr>
<tr><td>Open graded cement stabilized aggregate, E</td><td>750,000</td></tr>
<tr><td>Soil cement</td><td>500,000</td></tr>
<tr><td>Lime-cement-fly ash, E</td><td>1,500,000</td></tr>
<tr><td>Lime stabilized soil, M_r</td><td>45,000</td></tr>
</table></td></tr>
<tr><td>Flexural strength
(only required for flexible pavements)</td><td>Use 20 percent of compressive strength of lab samples or extracted cores as an estimate of the flexural strength for all chemically stabilized materials, or select typical M_r values in psi as follows:
<table>
<tr><td>Chemically stabilized material placed under flexible pavement (base)</td><td>750</td></tr>
<tr><td>Chemically stabilized material used as subbase, select material, or subgrade under flexible pavement</td><td>250</td></tr>
</table></td></tr>
<tr><td>Poisson's ratio</td><td>Select typical Poisson's ratio values as follows:
<table>
<tr><td>Lean concrete and cement stabilized aggregate</td><td>0.1–0.2</td></tr>
<tr><td>Soil cement</td><td>0.15–0.35</td></tr>
<tr><td>Lime-fly ash materials</td><td>0.1–0.15</td></tr>
<tr><td>Lime stabilized soil</td><td>0.15–0.2</td></tr>
</table></td></tr>
<tr><td>Unit weight</td><td>Use the MEPDG default value of 150 pcf.</td></tr>
<tr><td>Thermal conductivity</td><td>Use the MEPDG default value of 1.25 BTU/h-ft-°F.</td></tr>
<tr><td>Heat capacity</td><td>Use the MEPDG default value of 0.28 BTU/lb-°F.</td></tr>
</table>

10.5 Unbound Aggregate Base Materials and Engineered Embankments

Similar to AC and PCC, physical and engineering properties are required for the unbound pavement layers and foundation. The physical properties include dry density, moisture content, and classification properties, while the engineering property includes the resilient modulus. Designers must be aware that the resilient modulus values have to be determined at the optimum moisture content and maximum dry density, thus ensuring the unbound layers are representative of conditions when the pavement is opened to truck traffic.

For new alignments or new designs, the MEPDG default resilient modulus values (input Level 3) may be used, the modulus may be estimated from other properties of the material (input Level 2), or the modulus may be measured in the laboratory (input Level 1). For rehabilitation or reconstruction designs, the resilient modulus of each unbound layer and embankment is backcalculated from deflection basin data or estimated from DCP or CBR tests. If the resilient modulus values are determined by backcalculating elastic layer modulus values from deflection basin tests, those values need to be adjusted to laboratory conditions (*31, 32*). Table 10-8 lists the values recommended in those design pamphlets. If the resilient modulus values are estimated from the DCP or other tests, those values may be used as inputs to the MEPDG, but should be checked based on local material correlations and adjusted to laboratory conditions, if necessary. The DCP test is performed in accordance with ASTM D6951 or an equivalent procedure. For compatibility, the dry density and water content should be representative of the condition of the soil in determining the resilient modulus.

Table 10-8. C-Values to Convert the Calculated Layer Modulus Values to an Equivalent Resilient Modulus Measured in the Laboratory

Layer Type	Location	C-Value or M_r/EFWD Ratio
Aggregate Base/ Subbase	Between a stabilized and AC layer	1.43
	Below a PCC layer	1.32
	Below an AC layer	0.62
Subgrade-Embankment	Below a stabilized subgrade/embankment	0.75
	Below an AC or PCC layer	0.52
	Below an unbound aggregate base	0.35

Table 10-9 summarizes the input Level 1 parameters required for the unbound aggregate base, subbase, embankment, and subgrade soil material types listed in Table 10-1. The recommended test protocols are also listed in Table 10-9. Although input Level 1 is preferred for pavement design, most agencies are not equipped with the testing facilities required to characterize the paving materials. Thus, for the more likely situation where agencies have only limited or no testing capability for characterizing unbound aggregate base, subbase, embankment, and subgrade soil materials, input Levels 2 and 3 are recommended, which are provided in Table 10-10. For most analyses, it is permissible for designers to use a combination of Levels 1, 2, and 3 material inputs based on their unique needs and testing capabilities.

Table 10-9. Unbound Aggregate Base, Subbase, Embankment, and Subgrade Soil Input Level 1 Material Requirements and Test Protocols for New and Existing Materials

Design Type	Measured Property	Source of Data		Recommended Test Protocol and/or Data Source
		Test	Estimate	
New (lab samples) and existing (extracted materials)	Two Options: Regression coefficients k_1, k_2, and k_3 for the generalized constitutive model that defines resilient modulus as a function of stress state and regressed from laboratory resilient modulus tests. Determine the average design resilient modulus for the expected in-place stress state from laboratory resilient modulus tests.	X		AASHTO T 307 or NCHRP 1-28A The MEPDG generalized model is as follows: $M_r = k_1 p_a \left(\frac{\theta}{P_a}\right)^{k_2} \left(\frac{\tau_{oct}}{P_a} + 1\right)^{k_3}$ where: M_r = resilient modulus, psi θ = bulk stress $= \sigma_1 + \sigma_2 + \sigma_3$ σ_1 = major principal stress σ_2 = intermediate principal stress σ_3 = minor principal stress confining pressure τ_{oct} = octahedral shear stress $= \frac{1}{3}\sqrt{(\sigma_1 - \sigma_2)^2 + (\sigma_1 - \sigma_3)^2 + (\sigma_2 - \sigma_3)^2}$ P_a = normalizing stress k_1, k_2, k_3 = regression constants
	Poisson's ratio		X	No national test standard, use MEPDG default values
	Maximum dry density	X		AASHTO T 180
	Optimum moisture content	X		AASHTO T 180
	Gradation	X		AASHTO T 88
	Specific gravity	X		AASHTO T 100
	Saturated hydraulic conductivity	X		AASHTO T 215
	Soil water characteristic curve parameters	X		Pressure plate (AASHTO T 99), *or* Filter paper (AASHTO T 180), *or* Tempe cell (AASHTO T 100)
Existing material to be left in place	FWD backcalculated modulus	X		AASHTO T 256 and ASTM D5858
	Poisson's ratio		X	No national test standard, use MEPDG default values

Table 10-10. Recommended Levels 2 and 3 Input Parameters and Values for Unbound Aggregate Base, Subbase, Embankment, and Subgrade Soil Material Properties

<table>
<tr><th>Required Input</th><th>Recommended Input Level</th></tr>
<tr><td>Resilient modulus</td><td>Use Level 3 inputs based on the unbound aggregate base, subbase, embankment, and subgrade soil material AASHTO Soil Classification. AASHTO Soil Class is determined using the material gradation, plasticity index, and liquid limit.
<table>
<tr><th rowspan="2">AASHTO Soil Classification</th><th colspan="3">Recommended Resilient Modulus at Optimum Moisture (AASHTO T 180), psi</th></tr>
<tr><th>Base/Subbase for Flexible and Rigid Pavements</th><th>Embankment and Subgrade for Flexible Pavements</th><th>Embankment and Subgrade for Rigid Pavements</th></tr>
<tr><td>A-1-a</td><td>40,000</td><td>29,500</td><td>18,000</td></tr>
<tr><td>A-1-b</td><td>38,000</td><td>26,500</td><td>18,000</td></tr>
<tr><td>A-2-4</td><td>N/A</td><td>24,500</td><td>16,500</td></tr>
<tr><td>A-2-5</td><td>N/A</td><td>21,500</td><td>16,000</td></tr>
<tr><td>A-2-6</td><td>N/A</td><td>21,000</td><td>16,000</td></tr>
<tr><td>A-2-7</td><td>N/A</td><td>20,500</td><td>16,000</td></tr>
<tr><td>A-3</td><td>N/A</td><td>16,500</td><td>16,000</td></tr>
<tr><td>A-4</td><td>N/A</td><td>16,500</td><td>15,000</td></tr>
<tr><td>A-5</td><td>N/A</td><td>15,500</td><td>8,000</td></tr>
<tr><td>A-6</td><td>N/A</td><td>14,500</td><td>14,000</td></tr>
<tr><td>A-7-5</td><td>N/A</td><td>13,000</td><td>10,000</td></tr>
<tr><td>A-7-6</td><td>N/A</td><td>11,500</td><td>13,000</td></tr>
</table>
Note: (1) The resilient modulus is converted to a k-value within the software when evaluating rigid pavements. (2) The resilient modulus values at the time of construction for the same AASHTO soil classification are different under flexible and rigid pavements because the stress-state under these pavements is different. Soils are stress dependent and the resilient modulus will change with changing stress-state (refer to Table 10-9). The above default values can be used assuming the soils are at the maximum dry density and optimum water content as defined from AASHTO T 180. (3) Only A-1-a and A-1-b soils are used as base courses.</td></tr>
<tr><td>Maximum dry density</td><td rowspan="4">Estimate using the following inputs: gradation, plasticity index, and liquid limit.</td></tr>
<tr><td>Optimum moisture content</td></tr>
<tr><td>Specific gravity</td></tr>
<tr><td>Saturated hydraulic conductivity</td></tr>
<tr><td>Soil water characteristic curve parameters</td><td>Select based on aggregate/subgrade material class.</td></tr>
</table>

AASHTOWare PMED software and is intended to indicate the amount of damage removed from the existing surface prior to the placement of a new overlay. The thickness of the existing AC layers represented in the MEPDG is the thickness of the AC layers measured from cores, minus the depth of milling.

In-place recycling may be an option for reconstruction in those cases where an AC overlay is not feasible due to the extent of repair required to provide uniform support conditions. Recent equipment advances allow for the recycling of pavements in place to a depth of 8–12 in. If the in-place recycling process includes all of the existing AC layers (defined as pulverization), it could be treated as a new flexible pavement design strategy. The pulverized layer may be treated as a granular layer if not stabilized or a stabilized layer if asphalt emulsion or some other type of stabilizer is added prior to compaction.

Agencies have used a wide range of materials and techniques as part of a rehabilitation design strategy to delay the occurrence of reflection cracks in AC overlays of existing pavements. These materials include paving fabrics, a stress-absorbing interlayer (SAMI), chip seals, a crack relief layer or mixture, a cushion course, and hot in-place recycling. Paving fabrics, thin layers, pavement preservation techniques, and other non-structural layers are not analyzed mechanistically in the AASHTOWare PMED software. Pavement preventive maintenance strategies are considered by resetting the surface distress or performance measures (faulting, rutting, IRI).

The fitting and user-defined cracking calibration parameters in the MEPDG reflection crack prediction equation are provided only for the AC overlay with paving fabrics (refer to Table 5-4 in Subsection 5.3.5). The fitting parameters were estimated from limited test sections with a narrow range of existing pavement conditions and in localized areas. Additional performance data are needed to determine the values for both the fitting and user-defined cracking calibration parameters for a more diverse range of conditions and materials.

In the interim, designers may use the default fitting or calibration parameters for predicting the amount of reflection cracks over time (see Chapter 5). Design strategies to delay the amount of reflection cracks could be based on local and historical experience, until a more diverse set of existing pavement conditions and reflection cracking mitigation techniques are available for different materials and structures.

12.2.5 Determination of Damaged Modulus of Bound Layers and Reduced Interface Friction

Deterioration in the existing pavement includes visible distress and damage not visible at the surface. Damage not visible at the surface must be detected by a combination of NDT and pavement investigations (cores and borings).

In the overlay analysis, the modulus of certain bound layers of the existing pavement is characterized by a damaged modulus representing the condition at the time of overlay placement. The modulus of chemically stabilized materials and AC is reduced due to traffic induced damage during the overlay period. The modulus reduction is not applied to JPCP and CRCP because these type pavements are modeled exactly as they exist. Cracks in these slabs are considered reflective transverse cracks through the AC overlay. Damage of AC is simulated in AASHTOWare Pavement ME Design as a modulus reduction of that layer.

Results from the pavement investigation need to identify any potential areas or layers with reduced or no interface friction. Reduced interface friction is usually characterized by slippage cracks and potholes. If this condition is found, the layers where the slippage cracks have occurred could be considered for removal, or the interface friction input parameter in the overlay design should be reduced to zero between those adjacent layers.

12.2.6 AC Overlay Options of Existing Pavements

Table 12-3 listed different repair strategies for existing AC and AC over PCC pavements with different surface conditions that have some type of structural-material deficiency.

AC Overlay of Existing Flexible and Semi-Rigid Pavements

An AC overlay is generally a feasible rehabilitation alternative for an existing flexible or semi-rigid pavement, except when the conditions of the existing pavement dictate substantial removal and replacement or in-place recycling of the existing pavement layers. Conditions where an AC overlay is considered unfeasible for existing flexible or semi-rigid pavements are listed below:

1. The amount of high-severity alligator cracking is so great that complete removal and replacement of the existing pavement surface layer is dictated.
2. Excessive structural rutting indicates that the existing materials lack sufficient stability to prevent rutting from reoccurring.
3. The existing stabilized base shows signs of serious deterioration and requires a large amount of repair to provide a uniform support for the AC overlay.
4. When the existing granular base must be removed and replaced due to infiltration and contamination of clay fines or soils, or saturation of the granular base with water due to inadequate drainage.
5. Stripping in existing AC layers dictates that those layers need to be removed and replaced.

In the MEPDG, the design procedure for AC overlays of existing AC surfaced pavements considers distresses developing in the overlay as well as the continuation of damage in the existing pavement structure. The overlay generally reduces the rate at which distresses develop in the existing pavement. The design procedure provides for the reflection of these distresses through the overlay layers when they become critical. The condition of the existing pavement also has a major effect on the development of damage in the new overlay layers.

AC Overlay of Intact PCC Slabs

An AC overlay is generally a feasible option for existing PCC and composite pavements provided reflection cracking is addressed during the overlay design. Conditions under which an AC overlay is considered unfeasible include:

- The amount of deteriorated slab cracking and joint spalling is so great that complete removal and replacement of the existing PCC pavement is dictated.
- Significant deterioration of the PCC slab has occurred due to severe durability problems.

The design procedure presented in the MEPDG considers distresses developing in the overlay as well as the continuation of damage in the PCC. For existing JPCP, the joints, existing cracks, and any new cracks that develop during the overlay period are reflected through the AC overlay using the ME-based fracture mechanics approach reflection cracking models (see Chapter 5). A primary design consideration for AC overlays of existing CRCP is to full-depth repair all working cracks and existing punchouts. Sufficient AC overlay is then provided to increase the structural section, keep the cracks sufficiently tight, and exhibit little loss of crack LTE over the design period. A sufficient AC overlay is also needed to reduce the critical top-of-slab tensile stress and fatigue damage that leads to punchouts.

AC Overlay of Fractured PCC Slabs

The design of an AC overlay of fractured PCC slabs is very similar to the design of a new flexible pavement structure. The primary design consideration is the estimation of an appropriate elastic modulus for the fractured slab layer. One method to estimate the elastic modulus of the fractured PCC pavement condition is to backcalculate the modulus from deflection basins measured on previous projects (refer to Chapter 9). The three methods referred to as fractured PCC slabs are defined below:

- **Rubblization:** Fracturing the slab into pieces less than 12 in. and reducing the slab to a high-strength granular base. Used on all types of PCC pavements with extensive deterioration (severe mid-slab cracks, faulting, spalling at cracks and joints, D-cracking, etc.).
- **Crack and Seat:** Fracturing the JPCP slabs into pieces typically 1–3 ft in size.
- **Break and Seat:** Fracturing the JRCP slabs to rupture the reinforcing steel across each crack or break its bond with the concrete.

12.2.7 AC Overlays of Existing AC Pavements, Including Semi-Rigid Pavements

AC overlays of flexible and semi-rigid pavements may be used to restore surface profile or provide structural strength to the existing pavement. The trial overlay and pre-overlay treatments need to be selected considering the condition of the existing pavement, foundation, and future traffic levels. The AC overlay may consist of up to four layers, including three asphalt layers and one layer of an unbound aggregate (sandwich section) or chemically stabilized layer.

The same distresses used for new flexible pavement designs are also used for rehabilitation designs of flexible and semi-rigid pavements (refer to Subsection 5.3). For overlaid pavements, the distress analysis includes considerations of distresses (cracking and rutting) originating in the AC overlay and the continuation of damage and rutting in the existing pavement layers. The total predicted distresses from the existing pavement layers and AC overlay are used to predict the IRI values over time (refer to Subsection 5.3).

Longitudinal and thermal cracking distresses in the AC overlay are predicted at the same locations as new pavement designs. Fatigue damage is evaluated at the bottom of the AC layer of the overlay using the alligator fatigue cracking model. Reflection cracking in the AC overlays is predicted by applying the ME-based fracture mechanics reflection cracking model, which is based on the length of transverse cracking and area of bottom-up fatigue cracking measured at the surface of the existing pavement.

The continuation of damage in the existing pavement depends on the composition of the existing pavement after accounting for the effect of pre-overlay treatments, such as milling or in-place recycling. Using the damaged layer concept, fatigue damage will continue to develop in the AC layers remaining in place in existing flexible and semi-rigid pavements. All pavement responses used to predict continued fatigue damage in the existing AC layers remaining in place are computed with the damaged modulus, which is determined using pavement evaluation data and the methods discussed in Chapter 9. The pavement responses used to predict the fatigue damage of the AC overlay use the undamaged modulus of that layer.

Plastic deformations in all AC and unbound layers are included when predicting rutting for the rehabilitated pavement. As discussed in Chapter 5, rutting in the existing pavement layers will continue to accumulate, but at a lower rate than new materials due to the strain-hardening effect of past truck traffic and time.

12.2.8 AC Overlays of Existing Intact PCC Pavements, Including Composite Pavements (One or More AC overlays of Existing JPCP and CRCP)

The transverse joints and cracks of the underlying JPCP will reflect through the HMA overlay, depending on several factors. The ME-based reflection cracking transfer function included in the MEPDG may be calibrated to local conditions prior to use of the software (refer to Subsection 5.3). The transfer function has been globally calibrated. The global calibration model coefficients are included in Tables 5-4 and 5-5.

It is recommended that reflection cracking mitigation be considered outside of the MEPDG by means such as fabrics and grids or saw and sealing of the AC overlay above joints. The MEPDG considers reflection cracking treatments of fabrics and other interlayers, but the test sections used in the global calibration process did not show a statistical difference in performance (refer to Subsection 5.3).

For CRCP, there is no reflection cracking of transverse joints. The design procedure assumes that all medium and high severity punchouts will be repaired with full depth reinforced concrete repairs.

Table 12-13. Recommendations for Modifying Trial Design to Reduce Distress/Smoothness for JPCP Rehabilitation Design, *continued*

Distress Type	Recommended Modifications to Design
Faulting *(continued)*	• **Decrease joint spacing.** This is applicable to JPCP overlays over existing flexible pavements and unbonded JPCP overlays. Shorter joint spacing generally results in smaller joint openings, making aggregate interlock more effective and increasing joint LTE. • **Erodibility of separator layer.** This is mostly only applicable to unbonded JPCP overlays. It may be applicable to the leveling course placed during the construction of JPCP overlays of existing flexible pavements. Specifying a non-erodible AC material or a geotextile as the separator reduces the potential for base/underlying layer erosion and, consequently, faulting.
Transverse cracking	• **Increase slab thickness.** This is only applicable to JPCP overlays. Thickening the overlay slab is an effective way to decrease critical bending stresses both from truck axle loads and from temperature differences in the slab. Field studies have shown that thickening the slab can reduce transverse cracking significantly. At some thickness, however, a point of diminishing returns is reached and fatigue cracking does not decrease significantly. • **Decrease joint spacing.** This is only applicable to JPCP overlays. A shorter joint spacing results in lower curling stresses in the slab. This effect is very significant, even over the normal range of joint spacing for JPCP, and should be considered a critical design feature. • **Increase PCC strength (and concurrent change in PCC elastic modulus and CTE).** This is applicable only to JPCP overlays. By increasing the PCC strength, the modulus of elasticity also increases, thereby reducing its effect. The increase in modulus of elasticity will actually increase the critical bending stresses in the slab. There is probably an optimum PCC flexural strength for a given project that provides the most protection against fatigue damage. • **Widen the traffic lane slab by 2 ft.** This is applicable to rehabilitation with overlays. Widening the slab effectively moves the wheel load away from the longitudinal free edge of the slab and greatly reduces the critical bending stress and potential for transverse cracking.

Continued on next page.

Table 12-13. Recommendations for Modifying Trial Design to Reduce Distress/Smoothness for JPCP Rehabilitation Design, *continued*

Distress Type	Recommended Modifications to Design
Transverse cracking (*continued*)	• **Add a tied PCC shoulder (monolithically placed with the traffic lane).** This is applicable to rehabilitation with or without overlays. The use of a monolithically placed tied-PCC shoulder that has the properly sized tie-bars is generally an effective way to reduce edge bending stress and reduce transverse cracking. A PCC shoulder that is placed after the traffic lane does not generally produce high LTE and significantly reduced bending stresses over the design period.
Longitudinal Fatigue Cracking	• Increase slab thickness (8 in. maximum) • Increase existing AC layer thickness • Increase PCC strength (and concurrent change in PCC elastic modulus and CTE) • Tied PCC shoulder
Smoothness	• **Build smoother pavements initially and minimize distress.** The smoothness prediction model shows that smoothness loss occurs mostly from the development of distresses such as cracking, faulting, and spalling. Minimizing or eliminating such distresses by modifying trial design properties that influence the distresses would result in a smoother pavement. Hence, all of the modifications discussed in previous sections (for cracking and faulting) are applicable to improving smoothness.

12.3.5 CRCP Rehabilitation Design

A brief description of the CRCP rehabilitation designs options is described in this section.

- **Unbonded CRCP overlay of existing rigid pavement:** Unbonded CRCP (≥7 in. thick) placed on existing intact concrete pavement (JPCP, JRCP, or CRCP), existing composite pavement, or fractured PCC pavement. Unbonded overlays must have a separator layer similar to that described for unbonded JPCP overlays (see paragraph 12.3.3).
- **Bonded PCC overlay of existing CRCP:** Bonded PCC overlays over existing CRCP involve the placement of a thin concrete layer atop the prepared existing CRCP to form a permanent monolithic CRC section.
- **CRCP overlay of existing flexible pavement:** Conventional CRCP overlays (>7 in. thick) can be applied to existing flexible pavements. When subjected to axle loads, the CRCP overlaid flexible pavement behaves similarly to a new CRCP with an asphalt base course.

Design Considerations

- **Performance criteria:** Performance indicators used for CRCP rehabilitation design are crack width, LTE, punchouts, and smoothness.
- **Design reliability:** Handled in the same manner as new designs (see Chapter 7).
- **Factors that affect distress:** A detailed description of the factors that affect the performance indicators to CRCP rehabilitation design are presented in Table 12-14. By selecting the appropriate values of these factors, designers may reduce specific distress and improve overall pavement performance.

Trial Rehabilitation with CRCP Designs

The rehabilitation design process described under Subsection 12.3.3 for JPCP rehabilitation design is valid for CRCP as well. The performance prediction models for new CRCP are also valid for CRCP overlays. Further, as with JPCP rehabilitation, selecting the appropriate design features for the rehabilitated CRCP is key to achieving a successful design. For most rehabilitated CRCP design situations, the pavement design features are a combination of the existing design features and new features introduced as part of rehabilitation. Guidance on how to select the appropriate design features is presented in Table 12-15.

Design Modifications to Reduce Distress for CRCP Overlays

Crack width, longitudinal reinforcement percentage, slab thickness, and support conditions are the primary factors affecting CRCP performance and punchout development. Hence, modifying the factors that influence them is the most effective manner of reducing punchouts and smoothness loss. Crack spacing cannot be modified for bonded PCC over existing CRCP.

Table 12-14. Summary of Factors that Influence Rehabilitated CRCP Distress and Smoothness

Parameter	Comment
Transverse crack width and spacing	Transverse crack width is very critical to CRCP performance. It plays a dominant role in controlling the degree of load transfer capacity provided at the transverse cracks. It is strongly influenced by the reinforcement content, PCC shrinkage, construction PCC set temperature, and PCC CTE. Smaller crack widths increase the capacity of the crack for transferring repeated shear stresses (caused by heavy axle loads) between adjacent slab segments over the long term. Wider cracks exhibit lower LTE over time and traffic, which results in increased load-related critical tensile stresses at the top of the slab, followed by increased fatigue damage and punchouts. A maximum crack width of 0.02 in. over the design life is recommended.
Transverse crack LTE	The LTE of transverse cracks is a critical factor in controlling the development of punchout related longitudinal cracking. Maintaining a load transfer of 95 percent or greater (through aggregate interlock over the CRC overlay design life) will limit the development of punchout distress. This is accomplished by limiting crack width over the entire year, especially the cold months.

Continued on next page.

Table 12-14. Summary of Factors that Influence Rehabilitated CRCP Distress and Smoothness, *continued*

Parameter	Comment
Lane to shoulder longitudinal joint load transfer	The load transfer of the lane to shoulder joint affects the magnitude of the tensile bending stress at the top of the slab (between the wheel loads in a transverse direction). It is a critical pavement response parameter that controls the development of longitudinal cracking between adjacent transverse cracks and, consequently, the development of punchouts. The use of design features that could provide and maintain adequate edge support throughout the pavement rehabilitation design life is therefore key to adequate performance.
Overlay CRC thickness	From the standpoint of slab stiffness, this is an important design feature that has a very significant influence on performance. Note that for bonded PCC over existing CRCP, the equivalent stiffness of the overlay and existing PCC layer is used in analysis. In general, as the slab thickness of a CRC overlay increases, the capacity to resist critical bending stress increases, as does the slab's capability to transfer load across the transverse cracks. Consequently, the rate of development of punchouts decreases and smoothness loss is reduced.
Amount of longitudinal reinforcement and depth of reinforcement	Longitudinal steel reinforcement is an important design parameter because it is used to control the opening of the transverse cracks for unbonded CRCP overlays and CRCP overlays over existing flexible pavement. Also, the depth at which longitudinal reinforcement is placed below the surface greatly affects crack width. It is recommended that longitudinal steel reinforcement be placed above mid-depth in the slab. For bonded PCC over existing CRCP, the amount of reinforcement entered into the models is the same as that of the existing CRCP because cracks are already formed and no reinforcement is placed in the overlay PCC. Depth of the steel reinforcement is equal to the depth to the reinforcement in the existing CRCP (ignore the overlay PCC thickness because cracks are already formed through the slabs).
Slab width	Slab width has typically been synonymous with lane width (usually 12 ft). Widened lanes are typically 13–14 ft. Field and analytical studies have shown that the wider slab keeps truck axles away from the free edge, greatly reducing tensile bending stresses (in the transverse direction) at the top slab surface and deflections at the lane-shoulder joint. This has a significant effect on reducing the occurrence of edge punchouts. This design procedure does not directly address CRCP with widened slabs but can be approximately modeled by shifting the mean lateral load position by the width of slab widening.

Table 12-15. Guidance on How to Select the Appropriate Design Features for Rehabilitated CRCP Design.

Type of CRCP Rehabilitation	Specific Rehabilitation Treatments	Recommendation on Selecting Design Feature
Unbonded CRCP overlay	Interlayer placement	An adequate asphalt separator layer is very important for a CRCP overlay, because it ensures that no working joints or cracks in the existing pavement will reflect upward through the CRCP. This normally requires 1 in. of AC, but if joints with poor LTE exist, a thicker AC layer may be necessary. The AC separator layer should have normal contact friction with the CRCP overlay and the existing PCC layer in order to improve the structural capacity of the pavement. Erodibility of the separation layer is calculated based upon properties of the AC separation layer. (This utilizes percent asphalt by volume.
Unbonded CRCP overlay *(continued)*	Interlayer placement ***(continued)***	If this separation layer is permeable with a typically very low asphalt content, the designer must adjust the percent asphalt to a value of 11 percent.)
	Exiting PCC condition	The existing PCC overall condition must be considered when selecting the appropriate layer elastic modulus. This is done by adjusting backcalculated or lab-tested estimates of elastic modulus with a damage factor determined by existing CRCP visual condition.
	CRCP overlay	Selection of design features for the CRCP overlay (including shoulder type and slab width) is similar to that outlined for new/reconstruction design in Chapter 10.
Bonded PCC overlay on CRCP	PCC bonded overlay	The existing CRCP surface must be prepared and a new PCC overlay bonded on top. The only joint that needs sawing is the longitudinal lane-to-lane joint, which should be sawed completely through, plus 0.5 in. This bonded PCC design is unusual but has performed well in a number of projects in Texas and elsewhere. Design input features must reflect the condition of the existing CRCP.
CRCP overlay over existing flexible pavement	CRCP overlay	Selection of design features for the CRCP overlay (including shoulder type and slab width) is similar to that outlined for new or reconstructed design in Chapter 10. Condition of existing flexible pavement is rated as Excellent, Good, Fair, Poor, or Very Poor, as described in Table 12-10. These ratings will result in adjustments to the dynamic modulus, E_{AC}, of the existing AC layer that now becomes the base course. The lower the rating the larger the downward adjustment of E^* of the existing AC layer.

- **Increase overlay slab thickness.** An increase in CRCP slab thickness will reduce punchouts based on a decrease in critical tensile fatigue stresses at the top of the slab and an increase in crack shear capability. There is also a greater tolerance to maintain a high load transfer capability at the same crack width, allowing for reduced tensile stress at top of the slab.
- **Increase percent longitudinal reinforcement in overlay.** Even though an increase in steel content will reduce crack spacing, it has been shown to greatly reduce punchouts overall due to narrower cracks widths.
- **Reduce the PCC set temperature** (when PCC sets) through improved curing procedure (water curing). The higher the PCC set temperature, the wider the crack openings at lower temperatures.
- **Reduce the depth of reinforcement in overlay.** This is applicable only to unbonded CRCP overlay and CRCP over existing flexible pavement. Placement of steel closer to the pavement surface reduces punchouts by keeping cracks tighter. (However, to avoid construction problems and limit infiltration of chlorides, do not place closer than 3.5 in. from the surface.)
- **Increase PCC tensile strength.** Increasing the CRCP tensile strength decreases the fatigue damage and, consequently, punchouts. However, it must be noted that there is a corresponding increase in PCC elastic modulus that increases the magnitude of stresses generated within the PCC, somewhat reducing the benefit of increased tensile strength.
- **Reduce the coefficient of thermal expansion of overlay PCC.** Use of a lower thermal coefficient of expansion concrete will reduce crack width opening for the same crack spacing.
- **Increase AC separator layer thickness.** The thicker the separator layer, the less sensitive the overlay is to deterioration in the existing pavement. For badly deteriorated existing pavements, thick (≥ 3 in. thick) AC separator layers are recommended for CRCP overlays.
- **Reduction in PCC shrinkage.** Reducing the cement content and improved curing are two ways to reduce ultimate shrinkage.

12.3.6 Additional Considerations for Rehabilitation with PCC

There are several important considerations that need to be addressed as part of rehabilitation design to ensure adequate performance of the rehabilitation design throughout its design life. These issues include:

- Shoulder reconstruction
- Subdrainage improvement
- CPR/pre-overlay repairs
- Separator layer design (for unbonded JPCP/CRCP over existing rigid pavements)

- Joint design (for JPCP overlays)
- Reflection crack control (for bonded PCC over existing JCPC/CRCP)
- Bonding (for bonded PCC overlays over existing JPCP/CRCP)
- Guidelines for the addition of traffic lanes
- Guidelines for the widening of narrow traffic lanes

This page intentionally left blank.

Table 13-3. Guidance for Modifying AC Trial Designs to Satisfy Performance Criteria

Distress and IRI	Design Feature Revisions to Minimize or Eliminate Distress
Alligator cracking (bottom initiated)	• Increase the thickness of AC layers • For thicker AC layers (> 5 in.), increase the dynamic modulus • For thinner AC layers (< 3 in.), reduce the dynamic modulus • Revise the mixture design of the AC base layer (increase the percent crushed aggregate, use manufactured fines, increase the asphalt content, use a harder asphalt but ensure that the same percent compaction level is achieved along the roadway, use a polymer-modified asphalt, etc.) • Increase the density and reduce the air void of the AC base layer • Increase the resilient modulus of the aggregate base (increase density, reduce plasticity, reduce amount of fines, etc.)
Thermal transverse cracking	• Use softer asphalt in the surface layer • Reduce the creep compliance of the AC surface mixture • Increase the indirect tensile strength of the AC surface mixture • Increase the asphalt content of the surface mixture
Rutting in AC	• Increase the dynamic modulus of the AC layers • Use a polymer-modified asphalt in the layers near the surface • Increase the amount of crushed aggregate • Increase the amount of manufactured fines in the AC mixtures • Reduce the asphalt content in the AC layers
Rutting in unbound layers and subgrade	• Increase the resilient modulus of the aggregate base and increase the density of the aggregate base • Stabilize the upper foundation layer for weak, frost-susceptible, or swelling soils, and use thicker granular layers • Place a layer of select embankment material with adequate compaction • Increase the AC thickness
IRI AC	• Require more stringent smoothness criteria and greater incentives (building the pavement smoother at the beginning) • Improve the foundation and use thicker layers of non-frost-susceptible materials • Stabilize any expansive soils • Place a subsurface drainage system to remove groundwater

Continued on next page.

Table 13-3. Guidance for Modifying AC Trial Designs to Satisfy Performance Criteria, *continued*

Distress and IRI	Design Feature Revisions to Minimize or Eliminate Distress
Longitudinal fatigue cracking (surface initiated)	*Note*: It is recommended to not use the surface-initiated crack prediction equation as a design criterion until the critical pavement response parameter and prediction methodology has been verified. Refer to Chapter 3. The cumulative damage and longitudinal cracking transfer function (Equations 5-5 and 5-8) should be used with caution when making design decisions (in terms of longitudinal cracking, or top-down cracking) regarding the adequacy of a trial design. • Reduce the dynamic modulus of the AC surface course • Increase AC thickness • Use softer asphalt in the surface layer • Use a polymer-modified asphalt in the surface layer; AASHTOWare Pavement ME Design does not adequately address the benefit of PMA mixtures
Reflection cracking	• Increase AC overlay thickness • Increase the modulus of the AC overlay

Note: Index page numbers are based on the original third edition; they have not been updated to reflect any supplement or errata repagination.

Index

A

AADTT (Annual Daily Truck Traffic) 95
AASHTOWare Pavement ME Design. *See* AASHTOWare PMED
AASHTOWare PMED 1, 20, 36
  axle-load distributions 97
  distress prediction 40
  inputs 217
  predicted performance values 220–222
  required inputs 6, 33
  supplemental information 219–220
  three-stage process 3
  TTC groups 100
absolute error 133
AC (asphalt concrete) 1. *See* asphalt concrete
accumulated damage 19
aggregate base 20
aggregate gradation 143
air voids 145
alkali silica reactivity (ASR) 27
alligator cracking 35, 46, 166, 220
  area, calculating 48
analysis 1
  interval 39
  of pavement evaluation data 130–137
  three-stage process 3
  trial design 7–9
Annual Daily Truck Traffic (AADTT) 95
annual modulus 165
AREA method 134
asphalt binder 12
asphalt classification 129
asphalt concrete (AC) 1
  design inputs 123
  differences, design 4
  existing pavements 185–186
  laboratory tests 128–129
  layers, number of 166
  leveling courses 192
  material property inputs 141–149
  milling 125
  overlays 22–23, 184
  pavement types 20–22
  performance indicators 18, 35–36
  pre-overlay treatment 182
  reflective cracks of 55
  rehabilitation 177–192
  test protocols 12
  trenching 125
  trial design, modifying 191, 223–224
  volumetric properties 128
asphalt content by volume 145
asphalt materials 140
asphalt shingles (RAS) 142
asphalt treated permeable base (ATPB) 28, 165, 166
ASR (alkali silica reactivity) 27
assessment, existing pavement 109–113
  checklist 111–113
  steps and activities 114
ATPB (asphalt treated permeable base) 28, 165, 166
Atterberg limits 159
axle-load
  configuration 99
  distribution 19, 96–98
  lateral wander 102
  spectra 33–34

B

backcalculation procedures 18, 132–133
base course 168
base erodibility 171
BCOA (Bonded Concrete Overlays of Asphalt pavements) 24
bedrock 140, 169
Best Fit method 134
Bonded Concrete Overlays of Asphalt pavements (BCOA) 24
borings 124
bottom-up cracking 35
  longitudinal 37, 77–80
  transverse 36
break and seat 185
bulk specific gravity 145

C

calibration
  coefficients 20
  factors 1, 31, 40
California bearing ratio (CBR) value 126. *See* CBR value
CAM (cement aggregate mixtures) 20
candidate repair treatments 181
CBR value 126
cement aggregate mixtures (CAM) 20, 28
cementitious materials 20
cement treated base (CTB) 20, 28
  fatigue cracks, calculating 50
classification, asphalt 129
climate 102–103
climatic effects 19
climatic loading 17

compacted embankment 164
composite pavements 20
Concrete Pavement Restoration (CPR) 85, 203, 208
condition assessment, existing pavements 109–113
  checklist 111–113
  steps and activities 114
condition survey 115
construction
  month 31, 85
  new 2
  staged 29
contact friction 169–170
continuously reinforced concrete pavement (CRCP) 18, 23
  analysis parameters 187–189
  design inputs 121
  distress factors 212, 213
  modifications 212
  overlays 24
  performance criteria, AC overlays 190
  predicted performance values 221–222
  punchouts 74–75
  rehabilitation 198, 212
  slab width 174
  smoothness 82, 226
  trial design 168
  trial design, modifying 191
conventional flexible pavements 20
cores 124
corner deflections 68
CPR (Concrete Pavement Restoration) 85, 203, 208
crack
  width 226
crack and seat 185
cracking
  asphalt concrete (AC) pavements 35
  comparison, measured and predicted 53–54
  existing slab 188
  load and non-load 29
  Portland cement concete (PCC) pavements 36
  spacing 172, 221
  width 173, 221
CRCP (continuously reinforced concrete pavement). *See* continuously reinforced concrete pavement
creep compliance 42, 129
  asphalt materials 143–144
criteria, performance indicator 6
CTB (cement treated base). *See* cement treated base
cumulative damage 1
  index 32, 47
curing time 86

D

damaged modulus 183
data collection, field 119
DCP (dynamic cone penetronmeter) testing 122, 126
D-cracking 27
deep strength flexible pavements 20
deflection basin tests 18, 116, 122
  spacing 123
deflections 1, 17
dense-graded base course 168
design 1
  direction, trucks in 95
  inputs, grouping 6
  lane, trucks in 95
  life 32, 85
  modifications, JPCP 207
  performance criteria 31–32, 87–88
  process, elements 17
  reliability 6, 32, 88–89
  three-stage process 3
design reliability 205, 212, 217
design strategy
  flexible pavements 20–23, 161–167
  overlay 21–22
  rigid pavement 23–26
  trial 6
destructive tests 18, 116, 124–128
  cores and borings 124
  edge drains 128
  in-place strength 126
  interface friction 127–128
  summary 125
deterioration 183
developing calibration factors 1
differential energy, cumulative 69
distress
  prediction models 27, 40
  reducing 191
  rehabilitated JPCP 205–206
  rehabilitating CRCP 212
  types and severity levels 131
Distress Identification Manual 118, 122
distribution factors, truck traffic 99
drainage systems 18, 23, 162, 164–165
dry density 159
dual tire spacing 27, 102
dynamic cone penetrometer (DCP) testing 122, 126. *See* DCP (dynamic cone penetronmeter) testing
dynamic modulus 19, 42, 129, 188, 200
  asphalt materials 143

E

early-age opening 29